BIOMATERIAL-BASED MODULATION OF DENDRITIC CELLS: ADHESION BASED MODULATION AND HIGHTHROUGHPUT PARTICLE VACCINE GENERATION, EVALUATION AND DELIVERY

By

ABHINAV P. ACHARYA

A DISSERTATION PRESENTED TO THE GRADUATE SCHOOL
OF THE UNIVERSITY OF FLORIDA IN PARTIAL FULFILLMENT
OF THE REQUIREMENTS FOR THE DEGREE OF
DOCTOR OF PHILOSOPHY

UNIVERSITY OF FLORIDA

2010

To my parents

ACKNOWLEDGMENTS

There are a lot of people who have guided and supported me throughout my Ph.D. and I would like to thank them. Firstly, I would like to thank Dr. Benjamin Keselowsky, who has been my mentor and guide for the past five years. I also thank my committee members, Dr. Laurie Gower, Dr. Christopher Batich, Dr. Eugene Goldberg, Dr Anthony Brennan, and Dr. Michael Clare-Salzler for their teachings, guidance and support. I have always been blessed with excellent teachers and mentors throughout my educational career and I would like to extend a special thanks to Dr. Henry Hess, Dr. William Ogle and Dr. Brain Sorg.

I thank all my colleagues in the Keselowsky group – Natalia Dolgova, Jerome Karpiak, Toral Zaveri, Jamal Lewis, Matt Carston and Matt Sines – for helping and supporting me in my work. I would like to specially thank Natalia for helping me with cell biology and being such a great friend. Furthermore, I would like to thank colleagues outside the lab, Ashutosh and Amit for driving me to deliver two most productive years of my Ph.D. work; Phil and Mamta for shaping my ideas, making the work enjoyable and for the memorable discussions over long lunches; Sewoon Choe for keeping me company in the lab through the long busy nights of research; Ying for being so nice and entertaining and introducing me to the hot pot; Chong, and Shan for keeping the research light and fun. Further, I would like to thank Jerome and Elona for their invaluable advice both outside and in the lab.

TABLE OF CONTENTS

page

LIST OF FIGURES

Abstract of Dissertation Presented to the Graduate School
of the University of Florida in Partial Fulfillment of the
Requirements for the Degree of Doctor of Philosophy

BIOMATERIAL-BASED MODULATION OF DENDRITIC CELLS: ADHESION BASED MODULATION AND HIGHTHROUGHPUT PARTICLE VACCINE GENERATION, EVALUATION AND DELIVERY

By

Abhinav P. Acharya

May 2010

Chair: Benjamin Keselowsky
Cochair: Laurie Gower
Major: Materials Science and Engineering

Modulation of immune-cell responses using biomaterials based cues is an exciting field of research that holds great potential to help solve disorders such as autoimmune diseases, cancer and infections. Medical devices used in numerous applications such as tissue-engineered constructs, combination products (e.g., drug-eluting stents) and therapeutic vaccines are excellent tools for modulating the immune system. Since dendritic cells (DCs) are the key regulators of the immune system, DCs can be targeted to generate a desired immune response. Dendritic cell functions can be altered using several different signals such as adhesion signaling, targeting extracellular/intracellular toll like receptors for activation and mechanical cues. Specifically, we are interested in modulating DC behavior using adhesion cues and delivery of agents that target extracellular and intracellular receptors.

Exogenously generated DCs have been suggested as a potential solution to diseases such as type 1 diabetes (T1D). Ex vivo expansion of cells require isolation from the patient and culturing them on tissue culture treated plates where they come in

contact with several different proteins. Adhesion of such cells on different extracellular matrix proteins can modulate cellular responses. While it is well-known that adsorbed proteins on biomaterials modulate inflammatory responses in vivo, modulation of dendritic cells (DCs), a key regulator of immune system, via adhesion-dependent signaling has only been begun to be characterized. Currently, DC-based immunotherapy approaches for diseases such as cancer and autoimmune diseases like type-I diabetes rely on ex vivo culture and expansion of patient-derived DCs onto tissue culture-treated polystyrene plates. The adhesive substrate provided for DCs in this ex vivo approach is typically tissue culture-treated polystyrene presenting serum proteins adsorbed from the culture media. We therefore chose to examine serum-coated tissue culture-treated polystyrene as a relevant benchmark to compare the effect of adhesion-dependent modulation of DC function when cultured on several of the extracellular matrix proteins. Furthermore, DCs isolated from non-obese diabetic mice and its background control of wild type mice were cultured on the extracellular matrix proteins and compared for optimal protein substrate for generating DC based vaccines. In addition to modulating DCs ex vivo, DCs can be targeted in vivo using particle-based vaccines. Currently there are scores of known antigenic epitopes and adjuvants, and numerous synthetic delivery systems accessible for formulation of vaccines. However, the lack of an efficient means to test immune cell responses to the abundant combinations available represents a significant blockade on the development of new vaccines. In order to overcome this barrier, we report fabrication of a new class of microarray consisting of antigen/adjuvant-loadable poly(D,L lactide-co-glycolide) microparticles (PLGA MPs), identified as a promising carrier for immunotherapeutics,

that are cultured with DCs. Furthermore, a technique was generated to manufacture scores of particle-based vaccines in a highthroughput manner. The intention is to utilize this high-throughput platform to optimize particle-based vaccines designed to target DCs in vivo for immune system-related disorders, such as autoimmune diseases, cancer and infection.

CHAPTER 1
INTRODUCTION

Active interaction of immune system with foreign body such as biomaterials provides an opportunity to rationally design medical devices incorporating synthetic and biological components that can generate desired immune responses. Dendritic cells (DCs) are the most efficient antigen presenting cells of the immune system that can generate an effective immune response. Hence targeting DCs to modulate the immune system is an attractive strategy. Implantable biomaterials, particle based targeting devices and biomaterials used to culture DCs are the available tools that can be modified to modulate DC-functions. Subsequently, these modified DCs can generate an effective and desired immune response. We are interested in generating biomaterials influenced vaccines – live DC vaccines and synthetic particle based vaccines targeting autoimmune diseases, cancer and infection.

Immunogenomic approaches, functional insight into pattern recognition receptors and progress in tolerance-inducing strategies, have aided in the rational design of vaccine strategies targeting antigen presenting cells, and in particular, dendritic cells (DCs) for different immune related disorders [1-6]. Specifically, type 1 diabetes (T1D) is an autoimmune disease characterized by T-cell mediated destruction of insulin-producing β-cells. The prevalence of T1D in US children is 1.7 to 2.5 cases per 1000 individuals, and the incidence is between 15 and 17 per 100,000/year. In the United States, 10,000 to 15,000 new cases of T1D are diagnosed each year. The associated cost of diabetes treatment and care in the US in 2002 was estimated at $132 billion [7]. Clinical trials are underway for generating immunotherapeutic solutions to T1D [8]. Notably, clinical safety studies are being pursued for the use of antisense

oligonucleotide-treated DCs down-regulating co-stimulatory molecules which have been shown to confer diabetes protection in NOD mice [9]. In this body of work, a systematic analysis of the interaction of exogenously generated DCs with several extracellular matrix proteins and their derivative was performed. The motivation for this research stems from the concept that adhesion of DCs to extracellular matrix proteins and their derivatives might induce modulation in their functions.

There are several limitations to cell-based vaccines, for e.g. dissemination of exogenously delivered DCs is inefficient and treatment involves isolation and storage of DCs over a period of time, which amounts to high treatment costs that will prohibit widespread application. An alternative strategy involves the development of a synthetic particle-encapsulated vaccine, or vaccine particle that can be easily administered with delivery of both prime & boost doses using time-release materials (in particular, poly lactide-co-glycolide, PLGA) [10-12]. Furthermore, a technique was developed to generate particle-based vaccines in a highthroughput format and characterize their effects on DC-functions using in situ high fidelity highthroughput microarrays. This work leverages the versatility and customizability of synthetic microparticles as vaccine carriers and develops new strategies for the high-throughput production and immunologic assessment of combinatorially-loaded and surface-modified synthetic vaccine particles.

Adhesion-Dependent Modulation of DC-Function

Interactions of DCs with biomaterials have been demonstrated to modulate DC functions. Ex vivo culture and expansion of DCs is an immunotherapeutic approach being pursued for treating diseases such as type 1 diabetes (**Figure 1-1**). Hence, it is important to study the modulation of DC-function before generation of DC-based

vaccines.

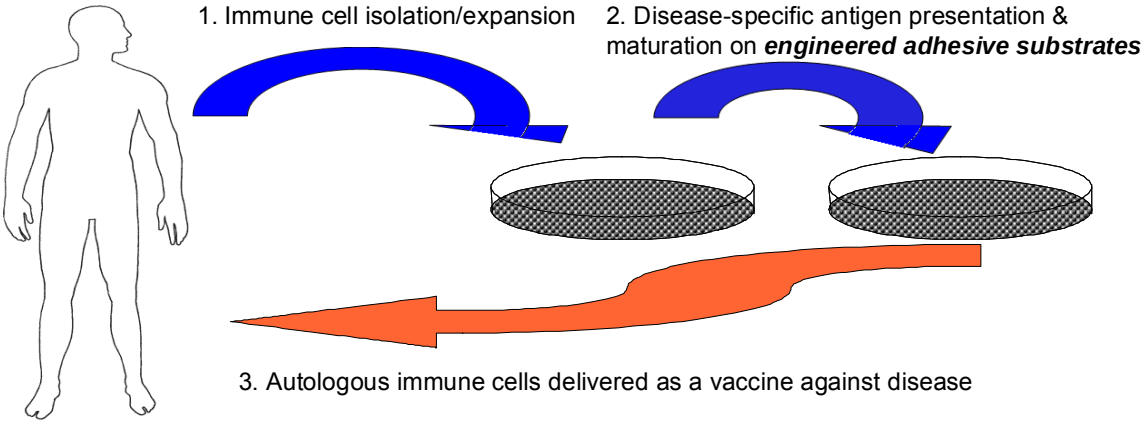

Figure 1-1. Schematic of immunotherapy approach with the introduction of engineered adhesive substrates to direct cell maturation that can be potential used for Diabetes Type I.

Activation of Dendritic Cells upon Adhesion – Type 1 Diabetes vs. Wild Type

Upon implantation, numerous proteins are quickly adsorbed onto biomaterials, including extracellular matrix proteins. Some of these (e.g., fibronectin, fibrinogen, vitronectin) have been shown to modulate inflammatory responses. DC adhesion to extracellular matrix proteins is therefore an important consideration in biomaterials. Additionally, DC adhesion to extracellular matrix proteins is of interest physiologically because DCs reside for much of their lifetime in connective tissues comprised largely of extracellular matrix proteins in both lymphoid and non-lymphoid organs, which may influence immune responses in the wake of injury, disease or tissue transplantation. However, despite its significance, modulation of innate and adaptive immune responses by DCs upon adhesion to extracellular matrix proteins has only been begun to be characterized.

DCs are critical for both immunity and tolerance and are involved in guiding innate and adaptive immune responses [13,14]. Dendritic cells act as sentinels,

constantly patrolling the body and presenting both self and non-self antigens to lymphocytes such as B-cells and T-cells [15,16]. Immature DCs (iDCs) mature/activate following interaction with pathogen associated molecular patterns or “danger signals” as well as self molecules (e.g. uric acid) [17-19]. DCs subsequently up-regulate antigen presenting molecules, co-stimulatory molecules, cytokines, and chemokine receptors. The latter mediate migration to secondary lymphoid tissues where they initiate adaptive immune responses and direct the development of T cell responses. DCs are the principal antigen-presenting cell involved in activation of naïve T-cells, as they provide three requisite signals: antigen presented in the context of major histocompatibility molecules (MHC), co-stimulatory molecules (e.g., CD80, CD86 and CD83), cytokines (e.g., interleukin-12; IL-12) and other factors that direct T cell functional development. Through these factors, DCs direct the differentiation of T-cells into different functional groups: interferon-γ (IFN-γ) producing effector Th1 cells IL-4/IL-5 –producing effector Th2 cells, TGF-β producing T-cells, and Th17 cells [20]. However, if DCs coming in contact with antigens remain in a resting or quiescent state, they are thought to promote tolerance through induction of regulatory T cells including CD4+/CD25+/FoxP3+ Treg and IL-10 producing Tr1 subtypes [21]. In addition, DCs activate natural killer (NK) cell and invariant NK T-cell responses as well as B-cell responses [22]. Dysregulation of DC function, therefore, can have enormous consequence and a role for DCs has been implicated in numerous pathologies such as type 1 diabetes, atherosclerosis, allergy and graft versus host disease [23,24]. Following trans-endothelial migration, DCs interact with tissue-specific extracellular matrix proteins present in connective tissues. The integrin family of cell-surface receptors is the primary receptor responsible for

mediating adhesion to extracellular matrix proteins, which has been shown to modulate numerous cell functions including proliferation and differentiation [25]. While it has been shown that DCs express multiple integrins, there are surprisingly few investigations into the effects of integrin binding to extracellular matrix proteins on DC maturation.

Interventional immunotherapies and tissue engineering constructs are being investigated as strategies to alleviate and/or ameliorate symptoms of type 1 diabetes (T1D). Tissue engineered constructs may incorporate scaffold components of both synthetic and biological origin, for e.g. extracellular matrix (ECM) proteins. Furthermore, upon implantation, numerous adhesive proteins adsorb onto synthetic constructs (e.g., vitronectin, fibrinogen, fibronectin) [26-31]. Adsorption of such proteins onto biomaterials might generate an unwanted immune response. The culture of DCs onto different ECM proteins might differentially modulate adaptive immune responses [32],[33]. Hence, it is important to investigate ECM proteins-mediated modulation of immune responses via DCs isolated from a type 1 diabetes mouse model.

Furthermore, interventional immunotherapies involve modulating DCs in vitro, where culture of ex vivo expanded DCs is performed in the presence of serum proteins which absorb onto culture substrates [34,35]. There is precedent that DCs present in a diabetic pathology themselves might be malfunctioning [36-39]. It has been reported that the non-obese diabetic (NOD) mice derived DCs have a defective maturation [40]. These defective DCs can potentially affect immune responses in the diabetic patient to tissue engineered constructs. Interestingly, ECM-protein fibronectin (FN) is up-regulated in targeted organs of diabetic angiopathy [41]. Additionally, it has been demonstrated that muscle capillary basement membrane containing numerous proteins namely,

laminin (LN) and collagen (COL) is abnormally enlarged in diabetic and pre-diabetic patients [42,43]. Thus, the up-regulated ECM-proteins might cause an increased migration and/or retention of antigen presenting cells in inflammatory-prone tissues. Furthermore, the adhesion of leukocytes to ECM-proteins that are up-regulated in pre-diabetic patients might initiate and propagate pro-inflammatory immune responses. Additionally, there is a potential for pathology-associated altered ECM-protein production in specific tissues to provide adhesion cues which may exacerbate pathogenesis. Dendritic cells can direct either pro-inflammatory or tolerogenic immune response [44] and defects in these functions may be linked to autoimmune disorders like T1D. Interestingly, adoptively transferred DCs presenting auto-reactive antigens induced acute autoimmune diabetes, thus suggesting a dominant role of DCs in inducing and propagating the disease [44,45]. Notably, immunotherapies such as selective activation of Th2 cell subset by DCs is one of the mechanisms that might induce antigen-specific tolerance, other mechanism that are worth investigating include DC-mediated induction of regulatory T-cells and IL-10 producing Tr1 cells, T-cell anergy and promotion of antigen-specific T-cell apoptosis [46,47]. Despite the growing interest in DC-based immunotherapies for T1D, there are very few studies to understand the effect of adhesive substrates on DC-maturation and adaptive immune responses.

In this work, we studied the effect of several adhesive substrates on activation and maturation of DCs derived from non-obese diabetic (NOD) mice and ability of such adhesive substrates to modulate an adaptive immune response via DCs. We are the first to report modulation of DC-responses to culture on adhesive substrates where the DCs were isolated from an animal predisposed toward T1D.

Integrin-Peptide Based Controlled Activation of Dendritic Cells

Growing use of biomaterials as targeted therapeutics and tissue constructs has generated the need to understand biomaterials induced immune responses and utilize the potential of biomaterials to modulate the immune system. Integrins are transmembrane cell-adhesion receptors comprised of two distinct subunits called α (alpha) and β (beta) with small cytoplasmic domains [48]. Several integrins are present on DCs that are involved in various cellular functions. Integrins can recognize different peptide sequences, for example, 8 of the known 24 heterodimeric integrins can recognize RGD peptide sequence and several of these are expressed by DCs. Peptides are short amino-acid polymeric chains present in the proteins providing special adhesion sites [49]. A short-peptide GRGDSPC (RGD) (glycine – arginine – glycine – asparatic acid – serine – praline – cystein) has been investigated extensively as an adhesion molecule for modulating cell function. The αV subunit of the integrins present on the cell surface has been shown to be co-localized with the RGD-peptide [50]. The RGD-peptide is present in several of the extracellular matrix proteins such as fibronectin and fibrinogen [51]. It has been demonstrated that modulation in cell-function is dependent on surface density of RGD [52]. Several studies have been done to modify the surface of a substrate to generate RGD-peptide gradients [53]. In this study, RGD peptide gradient developed by Gallant et al. were utilized to quantify the adhesion based activation of DCs, via major histocompatibility complex–II (MHC-II), CD86 cell surface molecule expression and intracellular IL (interleukin) -10 and IL-12p40 cytokine production. Furthermore, DC-expression of αV integrin was quantified. The DC surface molecules, MHC-II a stimulatory molecule that interacts with T-cell receptors and CD86

a co-stimulatory molecule that interacts with CD28 molecules on T-cells along with the soluble cytokines are the three signals required for directing T-cell-functions. Additionally, the level of expression of these signals generated by DCs, determine the type of immune response i.e. anti-inflammatory or pro-inflammatory. Furthermore, different stages of physiologically relevant DC-activation stages of immature, semi-mature and matured state have been observed. Hence, it is interesting to study the level of activation of DCs upon controlled presentation of such adhesive ligands. This study will help understand the extent of adhesion signaling required via biomaterials to generate effective immune responses and potentially modulate function of ex vivo cultured DCs in a highly controlled manner.

High-Throughput Production and Biological Evaluation of Antigen Presenting Cell-Directed Vaccine Particles

Advances in vaccine technologies promise solutions to some of today's most pressing medical problems including the induction of immune tolerance for applications toward autoimmune disease and organ transplantation. An attractive approach in vaccine technology involves the development of a synthetic particle-encapsulated vaccine, or vaccine particle that can be easily administered with simultaneous delivery of both prime & boost doses using time-release materials. This approach greatly simplifies issues related to manufacturing, storage and shipping, as biomaterial encapsulation provides vaccine stability and improved shelf-life. Furthermore, vaccine particles can be engineered to be multifunctional and modular. Features of particular interest are: control over phagocytosability, targeting to dendritic cells (DCs; a prime target cell for vaccines), and providing a depot for antigens, adjuvants, immunosuppressants, chemokines and growth factors. This system can thereby be

designed to attract DCs and precursors into a vaccination site, provide signals to drive differentiation into tolerogenic DCs, promote uptake of antigen and induce specific tolerance. However, the problem lies in the fact that although there are now scores of known antigenic epitopes and adjuvants, there has not emerged a systematic examination of the functional responses of immune cells in a combinatorial, high-throughput manner. The lack of an efficient means to produce and test numerous combinations of potential components represents a significant blockade on the development of new vaccines. In order to overcome this barrier, we are developing novel core technologies for high-throughput microparticle synthesis and evaluation.

High-throughput Microparticle Microarray for Dendritic Cell Targeted Vaccines

Immunotherapeutic strategies utilizing biomaterials involve modulation of immune responses by targeted delivery of immuno-modulatory molecules to leukocytes via a synthetic carrier. Microparticles (MPs), nanoparticles, micelles, vesicles, dendrimers and microchips have been all investigated as drug delivery vehicles designed to effect immunomodulation [54-59]. Of these, MPs fabricated using poly (d,l lactide-co-glycolide) (PLGA) have been the most investigated vehicle for delivering immunotherapeutics [60,61]. Poly (d,l lactide-co-glycolide) (PLGA), approved by the U.S. Food and Drug Administration (FDA) for biodegradable surgical sutures and drug delivery products, is degraded in the body via bulk erosion and hydrolysis. By altering the lactide/glycolide ratio, PLGA MPs can be designed to provide an initial burst of the encapsulated immuno-modulatory molecule followed by sustained release, permitting the design of a one-time drug administration with prime and boost doses [62]. Furthermore, PLGA MPs of appropriate size are phagocytosed efficiently by antigen presenting cells providing direct delivery of antigens for immune recognition [63]. Critically, following phagocytosis

by antigen-presenting cells, phagolysomal release of encapsulated antigens from PLGA microparticles can generate both MHC-II-directed, as well as MHC-I-directed immune response through cross-presentation [64,65]. Poly (d,l lactide-co-glycolide) MPs are therefore an excellent candidate as a carrier vehicle for vaccines utilizing encapsulated antigenic proteins or peptides along with immunomodulatory molecules such as adjuvants. Furthermore, PLGA MPs can be surface-modified to modulate activation, uptake and targeting of a key subset of antigen presenting cell, the dendritic cell. Dendritic cells (DCs) are the most efficient antigen presenting cell [66-68]. Moreover, DCs are central regulators of the immune system, processing and presenting antigen along with expression of an array of molecules (i.e., stimulatory, co-stimulatory and cytokines), directing T-cell subsets (e.g., Th1, Th2, Treg) providing either antigen-specific tolerance or immunity [69,70]. Therefore, modulation of these cells is critical, and a number of groups are investigating vaccines consisting of antigen-loaded particles targeting DCs [71-74].

Several established adjuvants exist and numerous more are under investigation. For example, molecules binding to pattern recognition receptors, such as toll-like receptors (TLRs) and c-type lectins, stimulate DC-activation [75]. Recently, Scholosser et al. demonstrated that the co-encapsulation of antigens and TLR 9 ligand, CpG oligonucleotide, or TLR 3 ligand, polyI:C, encapsulated in PLGA MPs provided DC activation and generated potent cytotoxic T-lymphocyte responses [76]. Similarly, Elamanchili et al. reported that PLGA nanoparticles encapsulated with TLR 4 ligand, mono-phosphoryl lipid A, resulted in increased expression of stimulatory and co-stimulatory molecules on DCs and resulted in a robust Th1 type response [77,78].

Additionally, antisense oligonucleotides specific for either co-stimulatory molecules or IL-10, loaded into PLGA MPs have been shown to be able to either induce immune suppression or direct specific Th-1 helper-type response respectively [79,80]. Finally, in addition to directly loading antigenic proteins or peptides into particles, it has been demonstrated that delivery of DNA encoding for antigenic protein via PLGA MPs is a viable immunotherapeutic option [81]. While results have been promising, translation into new effective vaccines has stalled. We believe the problem lies in the fact that although there are now scores of known antigenic epitopes and adjuvants, there has not emerged a platform for the systematic examination of immune cell responses in a high-throughput manner. The lack of an efficient means to test numerous combinations represents a significant blockade on the development of new vaccines. In order to overcome this barrier, we set out to develop a system to efficiently evaluate a large number of multi-parameter combinations of particle-based vaccine formulations simultaneously. Miniarraying technology has revolutionized the fields of genomics and proteomics. The success of high-throughput arrays of DNA and other biomolecules fabricated on substrates through contact pin printing has led the way to the recent development of cell-based arrays [82]. For instance, arrays have been constructed consisting of various types of stem cells adherent on combinations of printed extracellular matrix proteins, cell adhesion molecules and growth factors, in order to systematically investigate the effects of molecular microenvironment on stem cell differentiation [83-85].

Miniaturization would have the added benefit of requiring minimal patient sample, allowing the use of patient-isolated DCs to be screened for responses to thousands of

DC-targeting MP-vaccine formulations on a single chip. Patient-optimized MP-vaccine formulations could then be administered to the patient. This work describes construction of a new class of microarray – arrays of co-localized particles and cells. Utilizing standard miniarraying equipment in conjunction with surface chemistry derivatization techniques, we have generated arrays of PLGA MPs co-localized with DCs onto adhesive islands against a non-fouling background. Our intention is to employ this platform as a high-throughput technique to test multi-parameter combinations of microparticle-based vaccines targeting DCs.

Dendritic Cell Arrays for Biological Evaluation of Vaccine Particles

The large number of antigen/adjuvant strategies available in the design of new vaccines, selection of an optimal antigen/adjuvant approach has become a challenge further complicated by patient-specific responses. Combinatorial approaches of delivering multiple immuno-modulatory signals to improve the vaccine efficacy will likely be required to overcome this problem. Therefore we have developed a system to efficiently evaluate a large number of multi-parameter combinations of particle-based vaccine formulations simultaneously. This high-throughput small-volume method consequently provides multiple advantages over traditional trial-and-error methods to test efficacy and effectiveness of vaccine formulations. Additionally, with a minimal patient sample required, optimization through a small-volume high-throughput screening technique may lead toward developing personalized vaccines. Micro-arraying technology has revolutionized the fields of genomics and proteomics [85-87]. The success of these high-throughput arrays of complimentary DNA and other biomolecules on glass using contact pin printing and analyzing them by fluorescent probes, has led the way to the recent development of cell-based arrays. For instance, stem cell arrays

have been constructed by culturing various types of stem cells adherent on different combinations of printed extracellular matrix proteins, cell adhesion molecules and morphogens/growth factors, in order to systematically investigate the effects of molecular microenvironment on stem cell differentiation [88]. In this work, we describe the construction of a co-localized particle/cell array. Utilizing standard microarraying equipment in conjunction with surface chemistry derivatization techniques, we have generated microarrays of PLGA MPs co-localized with DCs onto adhesive islands against a non-fouling background. Our intention is to employ this platform as a high-throughput technique to test multi-parameter combinations of microparticle-based vaccines for immunotherapies targeting DCs.

Parallel Vaccine Particle Production

Currently, standard methodology for the generation of polymeric particles consists of single-batch processing using the double-emulsion/solvent-evaporation method. This process can take 4-5 hours and skilled hands used to handling multiple samples may be limited to producing less than a dozen MP formulations in one day. As a result of our development of high-throughput approaches for the design and optimization of particle-based vaccines, we have identified a unique, critical need to generate large numbers (hundreds to thousands) of different MPs formulated with multi-parameter combinations of immunomodulatory molecules. To meet this need, we have developed a parallel particle production technology, utilizing solid-pin miniarraying equipment for the robotic loading of pre-particle solutions with combinatorial formulations into 384-well plate wells as loading/particle-generation chambers.

CHAPTER 2
ADHESIVE SUBSTRATE-MODULATION OF ADAPTIVE IMMUNE RESPONSES IN C57BL6/J MICE

Introduction

Dendritic Cells (DC) are key regulators of the innate and adaptive immune system hence, modulation of DC responses resulting from interactions with biomaterials is critical. Additionally, interactions of DCs with biomaterials have been demonstrated to modulate DC functions. Since, C57BL6/j (B-6) mice represent the wild type mice; it is physiologically relevant to assess the immune response from DCs isolated from B-6 mice. Dendritic cells may interact with the proteins adsorbed onto the implanted biomaterials and generate an adaptive immune response. Furthermore, DCs reside in connective tissues and interact with the extracellular matrix for the majority of their lifetime. Despite its significance, modulation of innate and adaptive immune responses by DCs upon adhesion to extracellular matrix proteins has only been begun to be characterized. In the present study, DCs were cultured on extracellular matrix proteins and substrate-mediated modulation of DC maturation and DC-directed adaptive immune responses (T-cell proliferation and T-helper responses) were quantified.

Generation of Murine Bone Marrow-Derived DCs

Immature bone marrow-derived DCs were generated from 7-week-old female C57BL6/j mice in accordance with protocol approved by the University of Florida (protocol number E751) using a modified 10-day protocol. Briefly, femur and tibia from mice were isolated and kept in wash media composed of DMEM/F-12 (1:1) with L-glutamine (Cellgro, Herndon, VA) and 10% fetal bovine serum (Bio-Whittaker). The ends of the bones were cut and bone marrow was flushed out with 10 ml wash media using a 25 G needle and mixed to make a homogeneous suspension. The suspension

was then strained using 70 μm cell strainers (Becton Dickinson) and cells were collected by centrifugation at 330xg for 6 min. Precursor cells were isolated by centrifuging NycoPrep gradient (10 ml) and cell suspension (25 ml) at 670xg for 20 min at 22 ^{0}C. Leukocytes were isolated by pipetting out the layer of cells that forms at the interface of wash media and gradient. The precursor cell suspension was then washed twice with wash media and re-suspended in DMEM/F-12 with L-glutamine (Cellgro, Herndon, VA), 10% fetal bovine serum, 1% sodium pyruvate (Lonza, Walkersville, MD), 1% non-essential amino acids (Lonza, Walkersville, MD), 1% penicillin–streptomycin (Hyclone) and 20 ng/ml GM-CSF (R&D systems) (DC media). This cell suspension was then seeded in a tissue culture treated T-flask (day 0). After 48 h (day 2), floating cells were collected, re-suspended in fresh media and seeded on low attachment plates for 6 additional days. Half of the media was changed every alternate day. At the end of 6 days (day 8), cells were lifted from the low attachment wells by gentle pipetting, re-suspended and seeded on tissue culture-treated polystyrene plates for 2 more days. Cells were then lifted (at day 10) using 5 mM Na2EDTA solution in phosphate-buffered saline (PBS, Hyclone) and used for all the experiments. Purity, yield and immaturity of DCs ($CD11c^{+}$ and MHC-II) were verified via immunofluorescence staining and flow cytometry, whereas cell viability (>99% viable) was determined using Trypan blue. Marrow derived DC stimulatory capacity in terms of up-regulation of cell-surface markers MHC-II, CD80 and CD86, when cultured in the presence of LPS, was verified in comparison to immature DCs. Dendritic cells were isolated from at least 3 separate mice for each type of experiment.

Isolation of T-Cells

Spleens were isolated from 6–10-week-old BALB/cbyj mice. Single cell suspensions were prepared by mincing the spleen through a cell strainer. The effluent was centrifuged for 10 min at 300xg. This suspension was then strained again using cell strainer to separate debris and cells were counted using a hemocytometer. The cells were then spun down at 300xg for 10 min and the pellet was re-suspended in 4 ml of buffer (0.5% BSA and 2 mM EDTA in PBS) per million cells. Negative selection of $CD4^+$ T-cells was performed. A biotin-labeled antibody cocktail (CD8a (Ly-2) (rat IgG2a), CD11b (Mac-1) (rat IgG2b), CD45R (B220) (rat IgG2a), DX5 (rat IgM) and Ter-119 (rat IgG2b); Miltenyi) was added (10 ml per 10 million cells) and incubated for 10 min at 4^0C. Buffer (30 μl) and anti-biotin microbeads (20 μl) were added to the mixture per 10 million cells. After 15 min incubation at 4 ^{0}C, cells were centrifuged at 300xg for 10 min and re-suspended in 500 μl of buffer per 100 million cells. A MiniMACS magnetic column was pre-washed with 500 μl of buffer solution. Cell suspension was added to the column and the effluent comprised of $CD4^+$ T-cells was collected. The column was then washed thrice with buffer solution and the effluents were mixed. The $CD4^+$ T-cells were centrifuged at 300xg for 10 min and used in mixed lymphocyte reaction.

Protein Coating and DC Culture

Extracellular matrix proteins were coated onto 12-well tissue culture-treated polystyrene plates by overnight incubation of 20 μg/ml protein solution in PBS (**Figure 2-1**). For these single-component coating conditions, substrates are expected to be fully saturated with respect to protein surface densities. The wells were then washed with 1 M PBS with calcium and magnesium. Immature DCs were seeded (1 x 10^6 cells/well)

with or without lipopolysaccharide (1 mg/ml LPS; maturation signal) on the following protein-coated substrates: human plasma-derived fibronectin (FN) (BD Bioscience), Engelbreth–Holm–Swarm mouse tumor-derived laminin (LN) (BD Bioscience), bovine dermis-derived collagen type I (COL) (BD Bioscience), human plasma-derived vitronectin (VN) (BD Bioscience) and bovine plasma fibrinogen (FG) (Mp Biomedicals). Bovine serum albumin (BSA) (Fisher Bioreagents) and fetal bovine serum (SER) (Hyclone) protein-coated substrates were included as reference substrates. Species-specific protein sequence homologies, as compared to murine, are as follows: FN – 92%, COL – 89%, VN – 76%, FG – 81% and BSA – 70%; determined by HomoloGene, an online resource made available through the National Center for Biotechnology Information. Note that the SER substrate represents a standard culture condition, as quite often, DCs are cultured on tissue-culture polystyrene which has no pre-coated protein, but which allows uncontrolled protein adsorption from the serum-containing culture medium. One million DCs were cultured on each substrate for 24 h, supernatants were collected for cytokine analysis and cells were lifted using Na2EDTA and immunofluorescently stained for maturation markers. Dendritic cells used for positive (+LPS) and negative (iDCs) controls remained in the plates in which they were generated and were not reseeded onto new plates. Dendritic cell viability was tested using Trypan blue staining. Phase-contrast microscopy images were taken at 100X magnification. In order to assess the amount of endotoxin present on the adsorbed substrates, the chromo-Limulus Amebocyte Lysate (chromo-LAL) assay was performed as per the manufacturer's instructions (Cape Cod) using a 50 ml reaction volume per substrate with a 20 min incubation time.

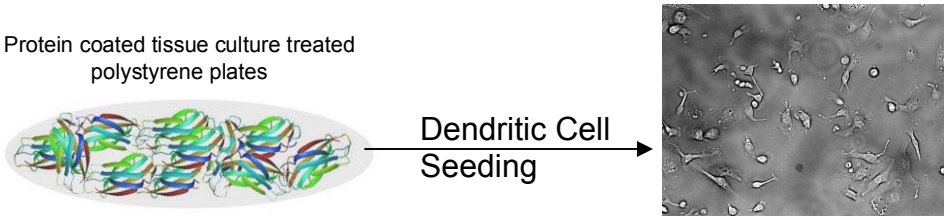

Figure 2-1. Schematic of adsorption of proteins on tissue culture treated polystyrene surfaces and culturing DCs on the modified surfaces.

Dendritic Cell Adhesion and Proliferation

Dendritic cells were seeded on adhesive substrates for 2 h. Dendritic cells were then washed once with 1x PBS, fixed with 3.7% paraformaldehyde (USB Corp.) and nuclei were stained with Hoechst (Invitrogen) according to the manufacturer's directions. The number of DCs was counted using Axiovision software 4.6.3 (Carl Zeiss Imaging Solution). Immature DCs and DCs +LPS were included as controls, where cells were re-plated onto tissue culture polystyrene without pre-coating. Additionally, DC proliferation on adhesive substrates was quantified. Dendritic cells were cultured on protein substrates for 24 h, and bromodeoxyuridine (BrdU) (kit from Beckton Dickinson) was added to the culture for the last 16 h. Dendritic cells were then immunofluorescently stained for BrdU according to manufacturer's specifications. Fluorescence output was quantified in a fluorescence plate reader (Perkin–Elmer).

Quantification of DC Surface Maturation Markers

Dendritic cell maturation was quantified by measuring cell-surface marker levels by flow cytometry. Briefly, DCs were lifted by incubating with 5 mM Na2EDTA solution in 1 M PBS solution at 37 ^{0}C for 20 min. Dendritic cells were then washed with 1% fetal bovine serum in PBS and incubated with antibodies against CD16/CD32 (Fcg III/II Receptor) (clone 2.4G2, IgG2b,k (BD Pharmingen)) for 40 min at 4^{0}C to block Fcg receptors on DCs. Cells were washed and then stained with antibodies against CD80

(clone 16-10A1, IgG2, k), CD86 (clone GL1, IgG2a, k), I-A/I-E (clone M5/114.15.2 IgG2b, k), CD11c (clone HL3, IgG1, l2) (BD Pharmingen) for 40 min at 4 ^{0}C. Appropriate isotypes were used for each antibody species as negative controls. Data acquisition was performed using (FACScalibur, Becton Dickinson) flow cytometry and the geometric fluorescent intensities determined. More than 20,000 events were acquired for each sample and data analysis was performed using FCS Express version 3 (De Novo Software, Los Angeles, CA).

Quantification of DC Cytokine Production

Cell culture supernatants were collected after 24 h of cell culture, centrifuged to remove any cell debris and stored at 20 ^{0}C until analysis. The IL-12 cytokine subunit, IL-12p40, and IL-10 cytokine production was analyzed using sandwich enzyme-linked immunosorbant assay (ELISA) kits (Becton Dickinson) according to manufacturer's directions.

Mixed Lymphocyte Reaction

Immature C57BL6/j murine bone marrow-derived DCs (40,000 cells/well) were cultured on protein-coated (adsorbed overnight, 20 μg/ml coating concentration) U-bottom tissue culture-treated 96 well plates for 24 h. $CD4^{+}$ T-cells purified from spleen of BALB/cbyj mice in the ratio of 1:6 were then added to the wells and co-cultured with adherent DCs for an additional 48 or 96 h. BrdU (Beckton Dickinson) (final concentration 10 mM) was added to the co-culture along with protein transport inhibitor (0.7 μl for every 1 ml of media) (Beckton Dickinson) 5 h before labeling T-cells with CD4 fluorescently tagged antibodies. At the end of 48 or 96 h, T-cells were immunofluorescently stained for BrdU (BD Pharmingen) to quantify proliferation rates.

Additionally, cells were immunofluorescently stained for cell-surface markers CD4 (BD Pharmingen) and intracellular cytokine staining of IFN-γ (BD Pharmingen) and IL-4 (BD Pharmingen). Flow cytometry was utilized for data acquisition of 20,000 cells. Analysis was performed on $CD4^+$ gated cells and was further classified for the presence of IFN-γ, IL-4 and BrdU. T-cells were stimulated with phorbol 12-myristate 13-acetate/Ionomycin (10 ng/ml for 2 days) to verify T-cell proliferation potential (data not shown), while a mixed lymphocyte reaction conducted with iDCs without pre-culturing on adhesive substrates comprised the negative control.

Statistical Analysis

Statistical analyses were performed using general linear nested model ANOVA, linear regression analysis and/or Pearson's correlation, as appropriate, using Systat (Version 12, Systat Software, Inc., San Jose, CA). Pair-wise comparisons were made, with p-values of less than or equal to 0.05 considered to be significant.

Results

Dendritic Cell Morphology and Adhesion

Quantification of endotoxin levels by chromo-LAL revealed that the substrate preparation yielded negligible endotoxin levels (<0.050 endotoxin units/ml). Immature DCs were seeded on substrates, cultured for 24 h and phase-contrast microscopy images were acquired. Different stages in maturation of pure DC cultures have been described as having characteristic morphologies. For example, the presence of dendritic processes is widely considered to represent a mature state. Likewise, the formation of clusters of rounded cells, likely mediated through E-cadherin, has also been attributed to a mature state. Morphological differences in B6-derived DCs were demonstrated to

be modulated by the adhesive substrate (**Figure 2-2**).

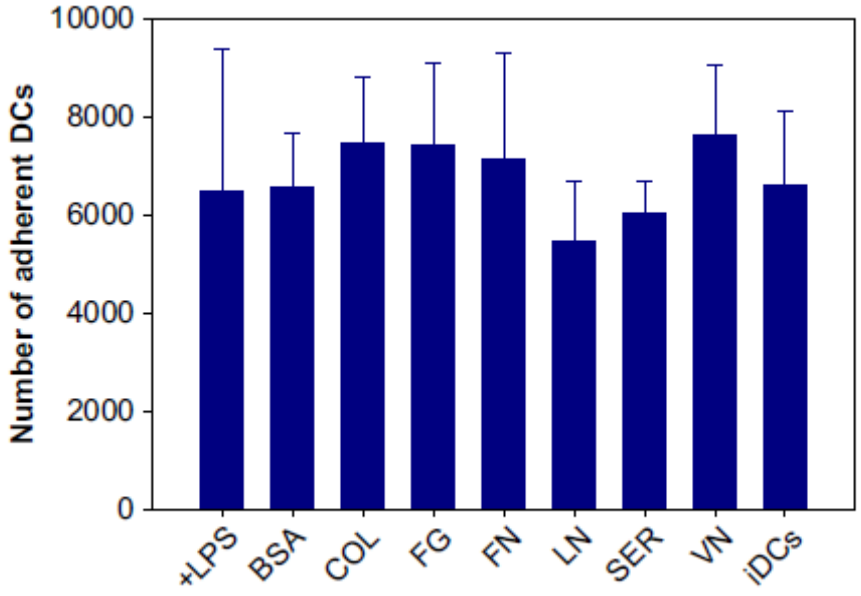

Figure 2-2. Initial adhesion of DCs is statistically not different for different adhesive substrates with an overall ANOVA p-value of less than 1. Data represents average and standard error of at least 6 data points (replicates).

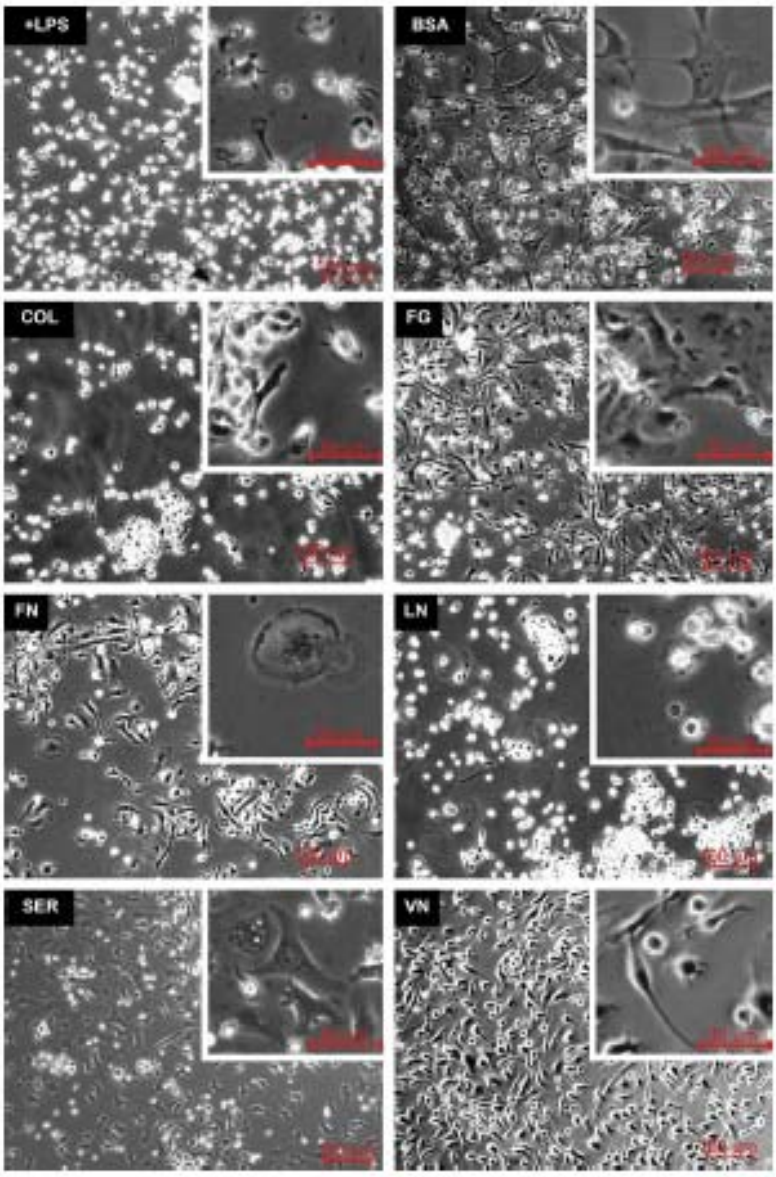

Figure 2-3. Murine C57BL6/j dendritic cell (DC) morphology is modulated by adhesive substrate. Inset micrographs represent a typical zoomed-in morphology of DCs on the given substrate.

Dendritic cells cultured on COL and LN substrates, and in the presence of LPS, evidenced both dendritic processes and clusters of rounded cells. In contrast, DCs cultured on substrates pre-coated with VN formed dendritic processes but not clusters, while DCs cultured on substrates pre-coated with FG formed clusters but very few well-formed dendritic processes. In contrast, DCs cultured on substrates pre-coated with FN

or SER demonstrated neither the presence of dendritic processes nor clusters. Interestingly, DCs cultured on BSA and FG substrates showed fibroblast-like morphology. Overall, these data demonstrate differential modulation of DC morphologies in a substrate dependent manner. In terms of a traditional view of DC morphology, COL, LN, VN and FG substrates potentially support increased levels of DC maturation, whereas DCs cultured on FN and SER demonstrate potentially lower levels of maturation. However, although there has been some tradition in linking DC morphology to maturation state, this is clearly not a sufficient indicator of maturation and further investigation was carried out. Additionally, in order to determine if substrate modulated DC adhesion, we quantified the number of adherent DCs at 2 h (**Figure 2-3**) 24 h (data not shown) and found an equivalent number of DCs adherent to all substrates.

Dendritic Cell Phenotype

In order to more clearly define substrate-dependent maturation of DC expression levels of surface molecules (stimulatory: MHC-II; co-stimulatory: CD80, CD86) and secreted cytokines (IL-10, IL-12p40) were quantified. Collectively, these metrics are descriptive of the extent and quality of maturation. DC expression of stimulatory and co-stimulatory molecules was quantified by flow cytometry and data were pooled for statistical analysis. Results were plotted as bar graphs (**Figure 2-4, Figure 2-5**), with representative density plots included (**Figure 2-6**). The percentage of DCs expressing MHC-II molecule (~80% of LPS-stimulated cultures/positive control) was equivalent across the substrate, indicating a degree of maturation on all substrates (**Figure 2-4A - € – all other conditions; £ – all conditions except VN.**). A much lower percentage of

iDCs expressed stimulatory molecule MHC-II (negative control). Overall significance was determined by ANOVA, p-value < $1x10^{-10}$. The trend in significant pairs is summarized by the inequality expression: +LPS >LN=COL=FG=FN =SER= BSA=VN> iDCs. These results indicate that all the substrates induced equivalent levels of MHC-II positive DCs, in a substrate-independent manner. It is important to note we found that when iDCs were lifted and re-plated onto clean tissue culture polystyrene, they demonstrated only a small increase in the level of phenotypic maturation at 24 h, compared to non-lifted iDCs (~8% increase in MHC-II positive cells, ~3% increase in CD86 positive cells and no increase in CD80 positive cells), thus indicating that the DC maturation observed is indeed attributable to substrate-dependent signals. Furthermore, the level of MHC-II expression was quantified by calculating the geometric mean fluorescence intensity (gMFI) (**Figure 2-4B - £ – all other conditions; € – SER.**).

Dendritic cells cultured on different adhesive substrates expressed equivalent level of MHC-II (2–5-fold less than positive control, +LPS). Overall significance was determined by ANOVA, p-value < $1x10^{-10}$. The trend in significant pairs is summarized by the inequality expressions: +LPS >BSA=COL= FG= FN= LN= SER=VN, and SER>iDCs. These results indicate that all the substrates are capable of supporting DC maturation.

In order to investigate the combined effects of adhesive substrates with a soluble maturation signal, we also quantified DC responses in the presence of LPS. With the addition of LPS to the culture, DC MHC-II expression levels were found to be slightly elevated for all substrates (**Figure 2-4B**). MHC-II levels of LPS-stimulated DCs cultured on BSA, FG and VN was relatively lower as compared to LPS-stimulated DCs cultured on COL, LN and SER. Although LPS-stimulated DCs cultured on FN had higher MHC-II

levels than iDCs, these values were not significantly different from the other substrates. Overall significance was determined by ANOVA, p-value < 1 x 10^{-10}. In the presence of LPS, the trend in salient significant pairs is summarized by: SER = LN = COL > BSA = FG = VN > iDCs. These results indicate that MHC-II expression was slightly elevated for DCs cultured on SER, LN and COL substrates in the presence of LPS compared to DCs cultured on BSA, FG and VN substrates.

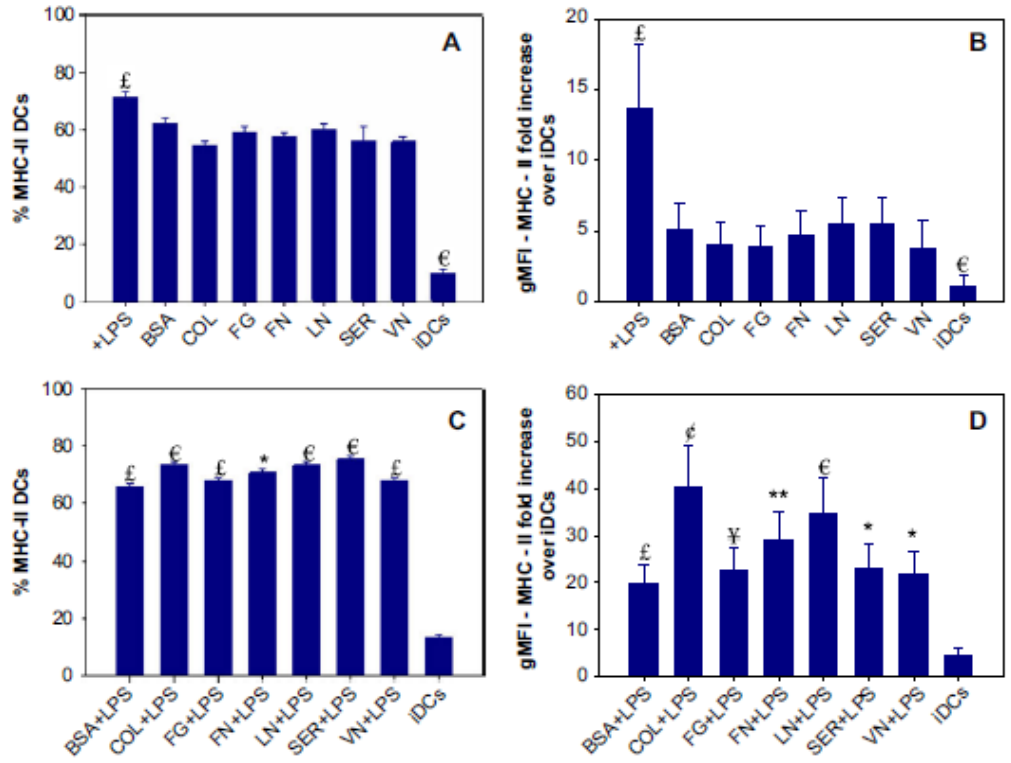

Figure 2-4. Adhesive substrates activate murine C57BL6/j bone marrow-derived dendritic cells (DCs) as evidenced through phenotypic surface presentation of major histocompatibility (MHC). Data represent average and standard error of at least 6 data points (replicates). DCs were obtained from at least 3 separate mice and each mouse handled as an independent experiment repeat. **A)** Dendritic cells positive for surface expression of MHC-II. **B)** Dendritic cells surface expression of MHC-II. **C)** Dendritic cells positive for surface expression of MHC-II when cultured in the presence of LPS. **D)** Dendritic cells surface expression of MHC-II when cultured in the presence of LPS. The significant pair symbols are described in the text.

Similar levels of co-stimulatory surface molecule, CD80, were found on DCs cultured on all substrates, comparable to the LPS-stimulated cultures and significantly higher than iDCs (overall ANOVA, p-value < 1 x 10^{-10}), suggesting a degree of maturation (**Figure 2-4C - £ – COL + LPS, LN + LPS, +LPS, iDCs; € – BSA + LPS, FG + LPS, VN + LPS, iDCs; * – iDCs.**). DC expression of co-stimulatory surface molecule, CD80, was not remarkably elevated in the presence of LPS (**Figure 2-4D - £ – COL + LPS, FN + LPS, LN + LPS, iDCs; € – SER + LPS, VN + LPS and iDCs; ¥ – LN + LPS and iDCs; ¢ – FG + LPS, FN + LPS, SER + LPS, VN + LPS and iDCs; * – iDCs; ** – VN + LPS and iDCs.**) as compared to DCs cultured on proteins alone. However, DCs cultured in the presence of LPS on COL, FN, LN and SER substrates had slightly higher (~10%) expression of CD80 as compared to DCs cultured on BSA and VN (**Figure 2-4D**). Overall significance was determined by ANOVA, p-value < 1 x 10^{-10}. In the presence of LPS, the trend in salient significant pairs is summarized by: COL = FN = LN = SER > BSA = VN > iDCs. Finally, the expression of the co-stimulatory surface molecule, CD86, was found to be elevated for DCs cultured in the presence of LPS as compared to DCs cultured on adhesive protein substrates alone (**Figure 2-5A - * – all other conditions; 2.5B - * – all other conditions; 2.5C - £ – BSA + LPS, VN + LPS and iDCs; € – COL + LPS, FN + LPS, +LPS, LN + LPS and iDCs; * – iDCs; 2.5D**

- * – with all other conditions).

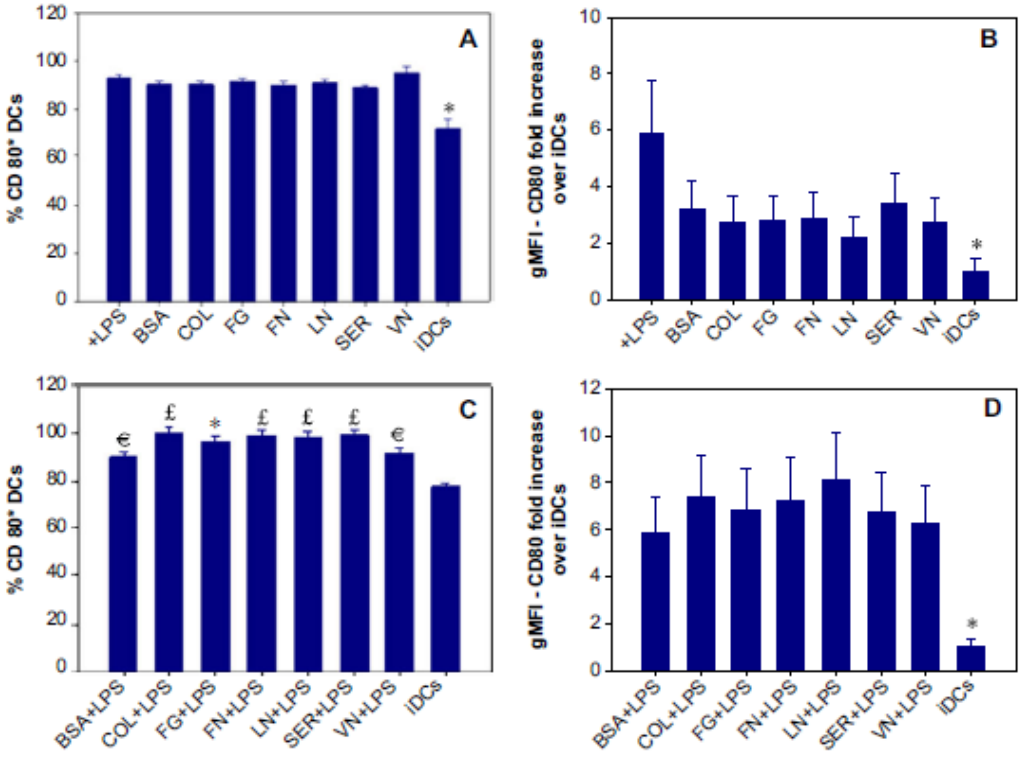

Figure 2-5. Adhesive substrates activate murine C57BL6/j bone marrow-derived dendritic cells (DCs) as evidenced through phenotypic surface presentation co-stimulatory molecules. Data represent average and standard error of at least 6 data points (replicates). DCs were obtained from at least 3 separate mice and each mouse handled as an independent experiment repeat. **A)** Dendritic cells positive for surface expression of CD86. **B)** Dendritic cells surface expression of CD86. **C)** Dendritic cells positive for surface expression of CD86 when cultured in the presence of LPS. **D)** Dendritic cells surface expression of CD86 when cultured in the presence of LPS. The significant pair symbols are described in the text.

However, statistical analysis of pooled data revealed that the expression of CD86 was statistically equivalent on DCs cultured on all substrates, with or without LPS (data not shown). Collectively, this phenotypic characterization indicates that the adhesive substrates examined support DC maturation, but do not give rise to large differences in DC expression of stimulatory (MHC-II) and co-stimulatory (CD80, CD86) molecules either in the presence or absence of LPS stimulation.

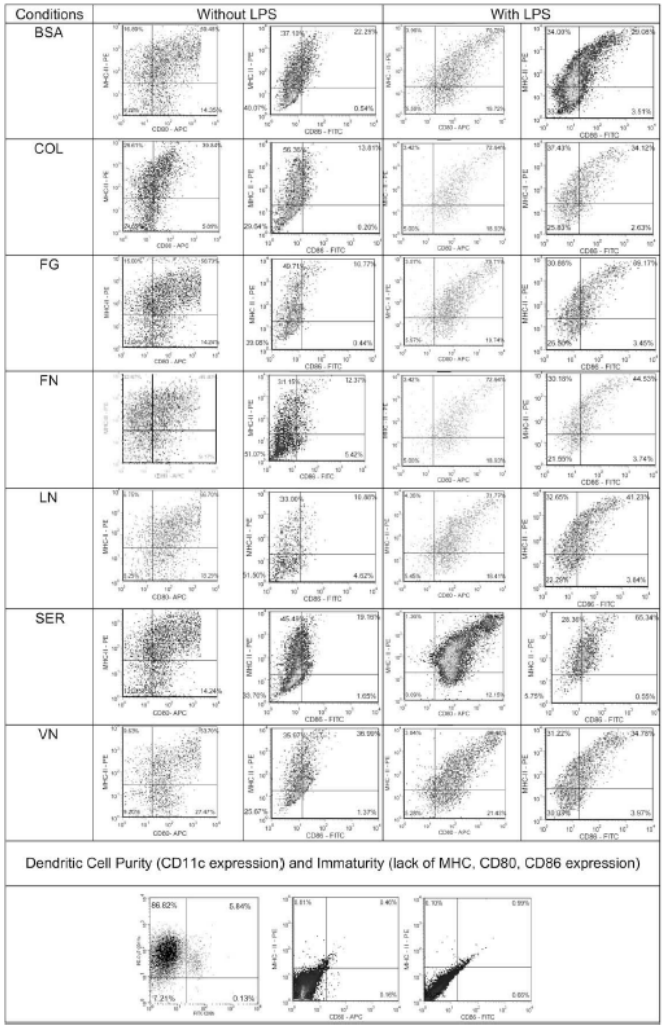

Figure 2-6. Representative phenotypic density plots of data summarized in Figs. 3 and 4 for murine C57BL6/j-derived DCs cultured on protein-coated tissue culture-treated polystyrene 24 h. Shown also are iDC purity and immaturity (lack of MHC-II, CD80 and CD86).

Dendritic Cell Cytokine Secretion

DCs cultured on adhesive substrates demonstrated a differential cytokine production profile of the pro-inflammatory cytokine, IL-12p40 (**Figure 2-7A - * – LN, COL, +LPS, VN and iDCs; ** – FN, COL, +LPS, VN and iDCs £ – BSA, FG, FN, LN, SER and iDCs; ζ – COL, +LPS and VN; € – COL, +LPS, VN and iDCs; χ – COL, FG, FN, LN, +LPS, SER and VN.**). DCs cultured on VN and COL coated substrates

secreted high levels (equivalent to positive control) of IL-12p40, compared to DCs cultured on FN, LN, FG and SER coated substrates. Notably, DC IL-12p40 secretion on VN and COL showed a greater than 2-fold increase over SER, representing standard culture conditions. The BSA coated substrate elicited intermediate levels of IL-12p40 production, lower than VN, COL, but not different from FG, FN, LN and SER coated substrates. DCs cultured on LN coated substrates also produced intermediate levels of IL-12p40, lower than COL, VN and positive control, and higher than FN coated substrates. Overall significance was determined by ANOVA, p-value < 1×10^{-10}. The trend in salient significant pairs is summarized by: +LPS = COL = VN > FG = FN = SER > iDCs. These results indicate that COL and VN induce the highest production of IL-12p40 cytokine from DCs. Interestingly, IL-12p40 cytokine trend corresponds to the presence of either the clustered or dendritic morphologies observed on these substrates, however, DCs cultured on LN did not show this trend.

We then quantified IL-12p40 production of DCs cultured on substrates in the presence of LPS. As expected, overall levels of IL-12p40 production were elevated when cultured with LPS (**Figure 2-7B - * – SER + LPS, VN + LPS, LN + LPS and iDCs; ¥ – VN + LPS and iDCs; € for FN + LPS, VN + LPS, BSA + LPS and iDCs; £ – all the other conditions.**) in comparison to substrates without LPS. LPS-stimulated DCs cultured on VN produced the highest level of IL-12p40 (~45% increase over SER+LPS, representing standard positive control culture conditions), while the other conditions induced moderate levels of IL-12p40 cytokine production. LPS-stimulated DCs cultured on BSA and FN coated substrates produced slightly higher levels of IL-12p40 than on SER and LN coated substrates. Overall significance was obtained by

ANOVA, p-value < 1 x 10^{-10}. In the presence of LPS, the trend in salient significant pairs is summarized by: VN > BSA = FN > SER = LN > iDCs. These results emphasize that adhesive substrates induce a differential pro-inflammatory IL-12p40 response in DCs in the presence of LPS, with VN inducing the elevated production of IL-12p40 cytokine.

Adhesive proteins mediated a differential DC cytokine production profile of anti-inflammatory cytokine, IL-10 (**Figure 2-7C - * – COL, FG, FN, LN, VN and iDCs.**). IL-10 cytokine production is most pronounced (equivalent to positive control, roughly 4-fold higher than all other substrates) when DCs were cultured on BSA and SER coated substrates. In contrast, levels of IL-10 production by DCs cultured on COL, FG, FN, LN and VN coated substrates were relatively low, equivalent to the negative control. Overall significance was obtained by ANOVA, p-value < 1 x 10-10. The trend in significant pairs is summarized by: +LPS = BSA = SER > COL = FG = FN = LN = VN = iDCs. These results indicate that DC culture on SER and BSA substrates results in high production levels of anti-inflammatory cytokine IL-10 compared to other substrates.

As expected, overall levels of IL-10 production were elevated when cultured with LPS (**Figure 2-7D - * – COL + LPS, FG + LPS, LN + LPS and iDCs; χ – FG + LPS, SER + LPS, BSA + LPS and iDCs; ξ – FN + LPS, VN + LPS, SER + LPS, BSA + LPS and COL + LPS; ψ – FG + LPS, LN + LPS and iDCs; ζ – FN + LPS, VN + LPS, SER + LPS and BSA + LPS; £ – SER + LPS, BSA + LPS, COL + LPS, FN + LPS and VN + LPS.**) in comparison to substrates without LPS. It is notable that DCs cultured on FG and LN substrates apparently resisted LPS stimulation, in terms of IL-10 cytokine production, with levels that were no higher than the negative control (iDC). LPS-stimulated DCs cultured on BSA, SER, FN and VN coated substrates stimulated the

highest levels of IL-10, higher than FG and LN coated substrates. LPS-stimulated DCs cultured on COL coated substrates produced intermediate levels of IL-10, less than BSA and SER and more than FG coated substrates. Overall significance was obtained by ANOVA, p-value < 1 x 10^{-10}. The trend in salient significant pairs is summarized by: BSA = FN = SER = VN > FG = LN = iDCs. These results indicate substrate-directed modulation in LPS-stimulated DC production of anti-inflammatory IL-10 cytokine.

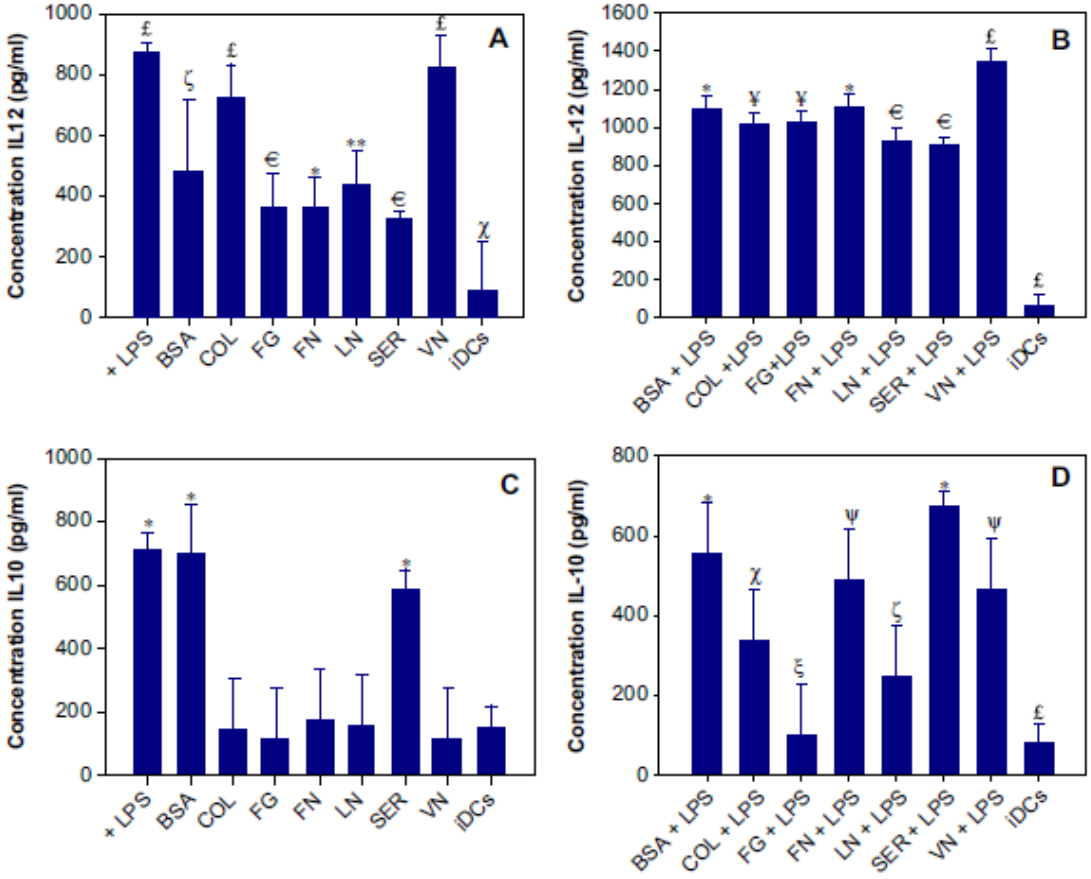

Figure 2-7. Adhesive substrates differentially modulate murine C57BL6/j bone marrow-derived dendritic cell (DC) cytokine production. Data represent average and standard error of at least 9 data points (replicates). DCs were obtained from at least 3 separate mice and each mouse handled as an independent experiment repeat. **A)** Dendritic cells production of IL-12 upon culture on adhesive substrates. **B)** Dendritic cells production of IL-12 upon culture on adhesive substrates in the presence of LPS. **C)** Dendritic cells production of IL-10 when cultured on adhesive substrates. **D)** Dendritic cells production of

IL-10 when cultured on adhesive substrates in the presence of LPS. The significant pair symbols are described in the text.

It is remarkable that DCs cultured on COL and VN adhesive substrates up-regulate IL-12p40 cytokine production while maintaining relatively low IL-10 cytokine production levels, which is skewed toward the promotion of a Th1 type response. Furthermore, it is interesting that DCs cultured on FG and LN limit production the immunomodulatory cytokine, IL-10, even after stimulating with LPS, suggesting that these substrates suppress anti-inflammatory responses. Taken together, these data indicate that adhesive substrates differentially direct DC production of cytokines known to direct specific T-helper cell type responses and can thereby skew adaptive immunity.

Mixed Lymphocyte Reaction

DC-mediated priming of T-cells is of particular interest to understand the influence of substrate-mediated modulation of immune responses. $CD4^+$ T-cell proliferation and T-helper cell type responses were examined at two different time points. Immature DCs were seeded and cultured on protein-coated substrates for 24 hours and $CD4^+$ T-cells were then subsequently co-cultured for either an additional 48 or 96 hours. T-cell proliferation was measured by the quantification of BrdU incorporation and intracellular cytokine production of IL-4 and IFN-γ by $CD4^+$ cells was quantified by flow cytometry. Adhesive substrates were found to modulate DC-directed $CD4^+$ T-cell function in a mixed lymphocyte reaction after 48 hours of co-culture (**Figure 2-8A**). The highest T-cell proliferation at 48 hours was observed in DCs cultured on BSA and LN, at levels 2–3 -fold higher than T-cells incubated with iDCs (negative control). On the other hand, DCs cultured on COL stimulated intermediate levels of T-cell proliferation, lower than BSA and LN coated substrates and higher than iDCs. All other substrates produced

relatively low T-cell proliferative responses, equivalent to iDCs. Overall significance was obtained by ANOVA, p-value < 2.2×10^{-5}. The trend in salient significant pairs is summarized by: BSA = LN > FG = FN = SER = VN = iDCs. These results indicate that BSA and LN adhesive substrates induce the highest DC-mediated T-cell proliferative response at 48 hours. Critically, $CD4^+$ T-cells cultured on adhesive substrates in the absence of DCs did not proliferate, indicating that substrate-dependent modulation of T cell function was mediated through the adherent DC culture (data not shown).

As expected, overall T-cell proliferation quantified at 96 hours was higher (~8-fold) compared to 48 hours (**Figure 2-8B**). Adhesive substrates were found to modulate DC-directed $CD4^+$ T-cell function in the mixed lymphocyte reaction after 96 hours of co-culture. T-cell proliferation at 96 hours was found to be the maximum when co-cultured with DCs seeded on VN compared to FN and LN (approximately 2-fold higher). BSA, COL, FG, and SER substrates produced intermediate levels of T-cell proliferation, indistinguishable from LN, FN, VN, and iDCs. Interestingly, at 96 hours of co-culture, DCs cultured on LN induced lower proliferation of T-cells than iDCs. Overall significance was obtained by ANOVA, p-value < 1.5×10^{-3}. The trend in salient significant pairs is summarized by: VN > FN = LN. These results demonstrate that $CD4^+$ T-cell proliferation quantified at 96 hours is adhesive substrate-dependent.

Interestingly, the mixed lymphocyte reaction demonstrated a dynamic modulation of substrate-dependent differences in T-cell proliferation over time. DCs cultured on BSA produced the highest T-cell proliferative response at 48 hours, but demonstrated only a modest ~2-fold increase in T-cell proliferation at 96 hours. Similarly, DCs cultured on LN mediated a high T-cell proliferative response at 48 hours, however, this response

was exhausted by 96 hours, producing an even lower T-cell proliferation than iDCs (**Figure 2-8A - * – COL, FG, FN, SER, VN, iDCs; £ – BSA, LN, iDCs; ** – BSA, FG, FN, SER, VN, iDCs; 2-8B - * – all other conditions except FN; ** – FN and LN.**). On the other hand, the largest increase (~10-fold) in T-cell proliferation from 48 to 96 hours was found in T-cells cultured with DCs on the VN substrate. All other substrates showed a 6–8 -fold increase in T-cell proliferation.

T-helper cell responses also demonstrated DC-directed substrate-dependent differences. Quantification of IL-4 and IFN-γ cytokine production was performed using flow cytometry, and average values of the percentage of T-cells producing either IL-4 or IFN-γ cytokines. Compared to iDCs, T-cells co-cultured with DCs on COL and LN substrates produced a balanced response, with high levels of both T_h2 (IL-4) and T_h1 type (IFN-γ) cytokines at both 48 and 96 hours. T-cells co-cultured with DCs on VN, on the other hand, produced a balanced response, with IL-4 and IFN-γ levels similar to iDCs at 48 hours, which increased to ~4-fold higher than iDCs at 96 hours. Overall, these data demonstrate that adhesive environments modulate DC-directed adaptive immune responses, inducing T-cell proliferation and specific helper T-cell responses.

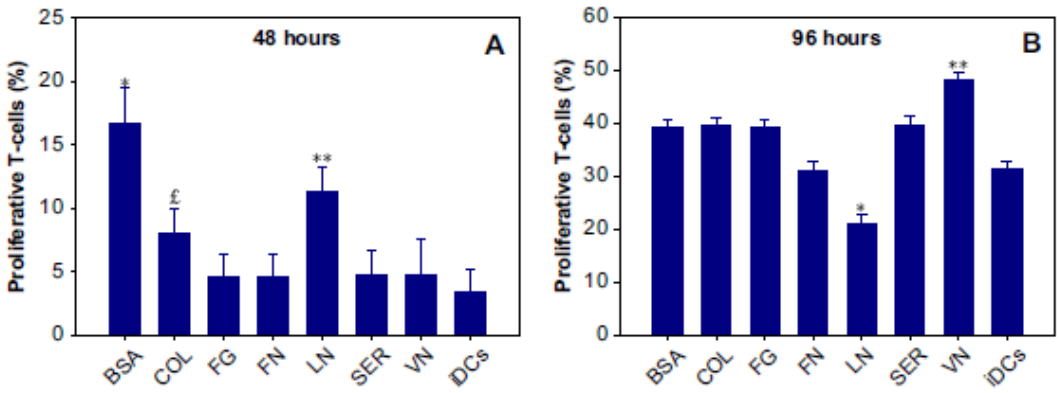

Figure 2-8. Adhesive substrates differentially modulate dendritic cell-mediated T-cell proliferation. A total of 20,000 $CD4^+$ T-cells were analyzed for each run. Each experiment was independently repeated at least 4 times (C57Bl6/j for DCs and BALB/cbyj for $CD4^+$ T-cells). **A)** T-cell proliferation at 48 h **B)** T-cell proliferation at 96 h. The significant pair symbols are described in the text. The significant pair symbols are described in the text.

Impact of the Study

We demonstrate that DC culture on extracellular matrix proteins modulates DC maturation and T-cell activation. Specifically, we found that culture on extracellular matrix proteins supported different DC morphologies, but equivalent levels of DC adhesion and phenotypic maturation, as characterized by high expression levels of stimulatory and co-stimulatory molecules. Interestingly, substrate-dependent presentation of stimulatory MHC–antigen complexes and co-stimulatory molecules, along with substrate-dependent modulation of DC cytokine production, correlates with differential T-cell proliferation. Although the cytokine IL-2 is the most notable cytokine linked to T-cell proliferation, interestingly, we found that substrate-dependent T-cell proliferative responses at 96 h correspond with the levels of IL-12p40 cytokine produced by DCs. This finding is supported by previous work that has also demonstrated correlations of IL-12 levels with Tcell proliferation. However, our data are the first to link adhesive substrate-dependent differences in DC IL-12p40 cytokine production with T-cell proliferation. For example, adhesive substrates VN (high IL-12p40) and COL (high IL-12p40) induced high T-cell proliferation, whereas LN (moderate IL-12p40) and FN (moderate IL-12p40) induced low and moderate T-cell proliferation responses, respectively, at 96 h. overall, we quantitatively demonstrate that adaptive immune responses can be directed by the adhesive substrate on which DCs are cultured. Specifically, our findings suggest that substrate-dependent modulation of DC IL-12p40

cytokine production correlates with substrate-dependent $CD4^+$ T-cell proliferation and Th1 type response in terms of IFN-g producing T-helper cells. On the contrary, our results indicate that the Th2 type response of IL-4 production does not correlate with DC-produced IL-10 cytokine, but do suggest a substrate-dependent trend. It is well-established that integrin receptors are the primary mediator of cell adhesion to extracellular matrix proteins and integrin binding to extracellular matrix proteins adsorbed onto synthetic materials has been demonstrated to direct cell adhesion and differentiation [89]. We therefore hypothesize that the substrate-mediated modulation of DC response demonstrated in this study is due to differential integrin binding to the adhesive substrates. Although it is known that DCs express multiple integrins [90,91], there are surprisingly little data on the effect of integrin binding to extracellular matrix proteins on DC response.

This work impacts the fields of biomaterials and DC-directed immunotherapy and begins the process of filling in the knowledge gap regarding the biology of DC adhesion. Critically, this work suggests plausibility for the rational design of biomaterials optimized for DC culture. Currently, DC-based immunotherapy approaches for diseases such as cancer [92] and autoimmune diseases like type-I diabetes [93-95] rely on ex vivo culture and expansion of patient-derived DCs onto tissue culture-treated polystyrene, without regard for the optimization of cell–substrate interactions. In fact, the adhesive substrate provided for DCs in this ex vivo approach is typically tissue culture-treated polystyrene presenting serum proteins adsorbed from the culture media. We therefore chose to examine serum-coated tissue culture-treated polystyrene (SER substrate) as a relevant benchmark. We found that the SER substrate elicited DC cytokine production levels that

were low in IL-12p40, high in IL-10 and produced non-optimal T-cell responses, compared to the other substrates. These findings therefore indicate that serum-coated tissue culture-treated polystyrene may not be the best choice for DC culture for immunotherapies requiring a Th1 type response, where robust T-cell proliferation and production of IFN-γ are desired (e.g., immunotherapy for HIV). Broadly, these findings stress the need to tailor adhesive culture surfaces for a given therapeutic application in order to optimize ex vivo culture and expansion for DC-based immunotherapies. Additionally, this work suggests the potential for DC adhesion based signals as a general mechanism that could prove to play a role in various phenomena such as tissue-dependent immune responses [96-98], autoimmunity and graft-versus-host disease. For example, our findings that DCs cultured on FG and LN substrates resist LPS stimulation of the anti-inflammatory cytokine IL-10 and that LPS-stimulated DCs cultured on VN substrates produced elevated levels of IL-12 are particularly interesting in this context and warrant further investigation into the role of DC adhesion in influencing tissue-dependent immune responses to danger signals.

CHAPTER 3
ADHESIVE SUBSTRATE-MODULATION OF ADAPTIVE IMMUNE RESPONSES IN NOD MICE

Introduction

Immunotherapies and biomaterial implantations involving dendritic cells (DCs) is an attractive field of research that requires effective combinations of synthetic biomaterial and biological components. Dendritic cells (DCs) are specialized antigen presenting cells that modulate both innate and adaptive immune responses. In this study, we cultured non-obese diabetic mice derived DCs on different adhesive substrates and probed modulation in surface expression of stimulatory molecule, MHC-II and co-stimulatory molecules CD80 and CD86 and, cytokine production of IL-12p40 and IL-10. Furthermore, T-cell cytokine (IL-4 and IFN-γ) production and proliferation modulated by DC cultured on different adhesive substrates was quantified. Particularly, we found that DCs cultured on vitronectin adhesive substrate induced highest IL-12p40 production whereas collagen induced highest IL-10 production from DCs. Furthermore, it was observed that DCs cultured on vitronectin induced highest population of IL-4 producing T-cells and DCs cultured on fibronectin substrate induced highest expression of IFN-γ in T-cells. This work will help in advancement of the field of adhesion based modulation of immune system and influence rational design of biomaterials and ex vivo DC-based immunotherapies for type 1 diabetes.

Generation of Murine Bone Marrow-derived DCs

Immature bone marrow-derived DCs were generated from 7-week-old female NOD mice in accordance with protocol approved by the University of Florida (protocol number E751) using a modified 10-day protocol. Same procedure was followed for isolating and culturing DCs as given in Chapter 2.

Isolation of T-Cells

Isolation of T-cells was performed using the protocols illustrated in Chapter 2.

Protein Coating and DC Culture

Extracellular matrix proteins were coated onto 12-well tissue culture-treated polystyrene plates using the same protocol as Chapter 2.

Protocols for Studying DC-Functions

Adhesion and proliferation studies of DCs were studied using the protocols mentioned in Chapter 2. Dendritic Cell maturation was quantified by measuring surface marker levels and cytokine production of IL-12p40 and IL-10, mentioned in detail in Chapter 2.

Mixed Lymphocyte Reaction

Immature NOD murine bone marrow-derived DCs (40,000 cells/well) were cultured on protein-coated (adsorbed overnight, 20 μg/ml coating concentration) U-bottom tissue culture-treated 96 well plates for 24 h. $CD4^+$ T-cells purified from spleen of BALB/cbyj mice in the ratio of 1:6 were then added to the wells and co-cultured with adherent DCs for an additional 96 h. BrdU (Beckton Dickinson) (final concentration 10 mM) was added to the co-culture along with protein transport inhibitor (0.7 ml for every 1 ml of media) (Beckton Dickinson) 5 h before labeling T-cells with CD4 fluorescently tagged antibodies. At the end of 96 h, T-cells were immunofluorescently stained for BrdU (BD Pharmingen) to quantify proliferation rates. Additionally, cells were immunofluorescently stained for cell-surface markers CD4 (BD Pharmingen) and intracellular cytokine staining of IFN-γ (BD Pharmingen) and IL-4 (BD Pharmingen). Flow cytometry was utilized for data acquisition of 20,000 cells. Analysis was performed on $CD4^+$ gated cells and was further classified for the presence of IFN-g, IL-4 and BrdU. T-cells were stimulated with phorbol 12-myristate 13-acetate/Ionomycin (10 ng/ml for 2 days) to

verify T-cell proliferation potential (data not shown), while a mixed lymphocyte reaction conducted with iDCs without pre-culturing on adhesive substrates comprised the negative control.

Statistical Analysis

Statistical analyses were performed using general linear nested model ANOVA, linear regression analysis and/or Pearson's correlation, as appropriate, using Systat (Version 12, Systat Software, Inc., San Jose, CA). Pair-wise comparisons were made, with p-values of less than or equal to 0.05 considered to be significant.

Results

Endotoxin Quantification, DC Morphology and Adhesion

Quantification of endotoxin on adhesive substrates revealed endotoxin levels below the detection limit of <0.06 endotoxin units/mL. As an initial indication of substrate influence on DC function, DC morphologies were investigated. Dendritic cells are a unique cell type, which modulate their surface morphologies to increase the surface area for antigen presentation to lymphocytes. These alterations in morphology have been linked to qualitative information in modulation of DC function. Bone marrow derived immature DCs isolated from NOD mice were cultured on tissue culture treated polystyrene pre-coated with the following adhesive proteins BSA, COL, FG, FN, LN, SER and VN and DC morphology was analyzed (**Figure 3-1**). Few DCs cultured on BSA, FG and VN adhesive substrates demonstrate dendritic morphology and formation of large clusters was not observed. Contrarily, DCs cultured on FN, SER, LN, COL and in the presence of LPS expressed both dendrites and clustering. Furthermore, many DCs cultured on SER (**inset, Figure 3-1**) demonstrated a veiled morphology while a

small number of DCs demonstrated dendritic processes.

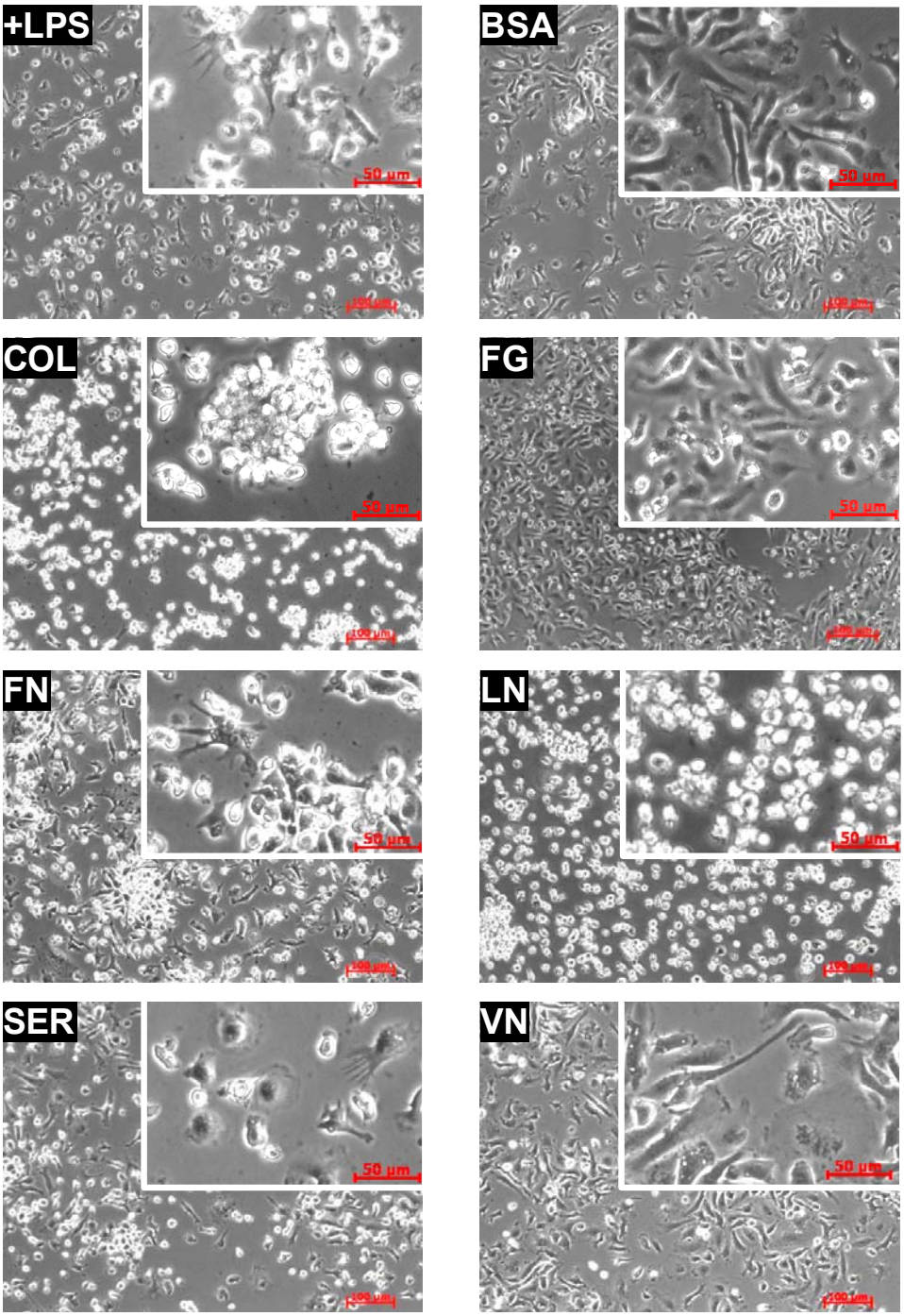

Figure 3-1. Adhesive substrates differentially modulate NOD-DC morphology. A pre-coated tissue culture treated plate was utilized to culture NOD-DCs for 24 hrs and phase contrast micrographs were acquired (scale bar =100μm). Inset micrographs are shown to clearly demonstrate morphology of DCs on the given substrate (scale bar = 50μm).

Clustering of vascular DCs was observed in atherosclerosis prone area, an indication of maturation of splenic DCs isolated from BB-DP rats and a method utilized by DCs for transferring antigens. On the other hand presentation of dendrites and a veiled morphology might be indicators of activation on DCs isolated from human peripheral blood mononuclear cells. Based on morphological characteristics, DCs cultured on COL, FN and LN adhesive substrate can be grouped together as having both homotypic clusters and dendritic processes and hence these clusters might be categorized as containing activated and matured cells. Furthermore, DCs cultured on BSA and FG substrates manifest only dendritic processes. Dendritic cells cultured onto VN uniquely falls in the group of having both dendritic processes and veil morphology without demonstrating a homotypic clustering. Interestingly, DCs cultured on SER substrate demonstrate all the three morphologies (**Figure 3-2**). It is apparent that adhesive substrates have a differential effect on morphologies of DCs cultured on different adhesive substrates. In order to ascertain the qualitative comparison of maturation states derived from morphological differences, further studies were carried out to quantify differential maturation of DCs upon culture on different adhesive substrates.

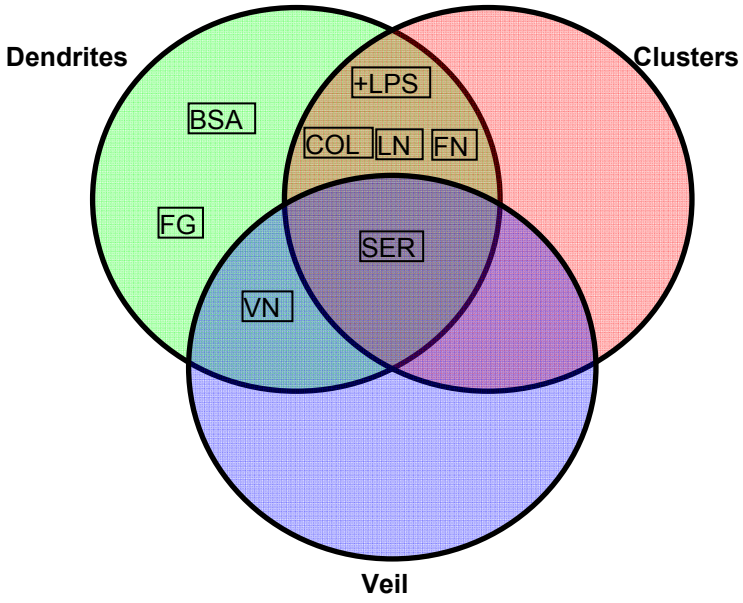

Figure 3-2. Non-obese diabetic mouse derived DCs can be divided into different groups according to the typical activated morphological manifestations of veil, dendrites and clusters is demonstrated as a Venn diagram upon culture on different adhesive protein substrates: bovine serum albumin (BSA), collagen (COL), fibrinogen (FG), fibronectin (FN), laminin (LN), serum (SER) and vitronectin (VN) while DCs cultured in the presence of lipopolysaccharide (LPS) was included as a control.

Dendritic cells isolated from bone marrow of NOD-mice show differential adhesion to different adhesive substrates (**Figure 3-3 - * - BSA, COL, FG, FN and LN; ** - +LPS, COL, FG, FN, LN, SER, VN and No Pre-coat; € - +LPS, BSA, FG, FN, SER, VN and No Pre-coat; £ - +LPS, BSA, COL, SER, VN and No Pre-coat; ¥ - +LPS, BSA, COL, SER, VN and No Pre-coat**). Dendritic cells were cultured for 24 hr on 96-well plate pre-coated with different proteins: BSA, COL, FG, FN, LN, SER, and VN. Dendritic cells cultured in the presence of LPS were also included in the analysis. Interestingly, initial adhesion of NOD-DCs to COL and LN was limited, while the largest number of DCs adhered to BSA. Dendritic cells cultured on SER and VN substrates and iDCs and in the presence of LPS demonstrated similar number of adherent cells. Overall significance was determined by ANOVA, p-value < 0.0003. The trend in significant pairs between the

number of DCs adhered onto different adhesive substrates is summarized by: BSA > +LPS = SER = VN = iDCs > FG = LN & LN = COL & FN = SER.

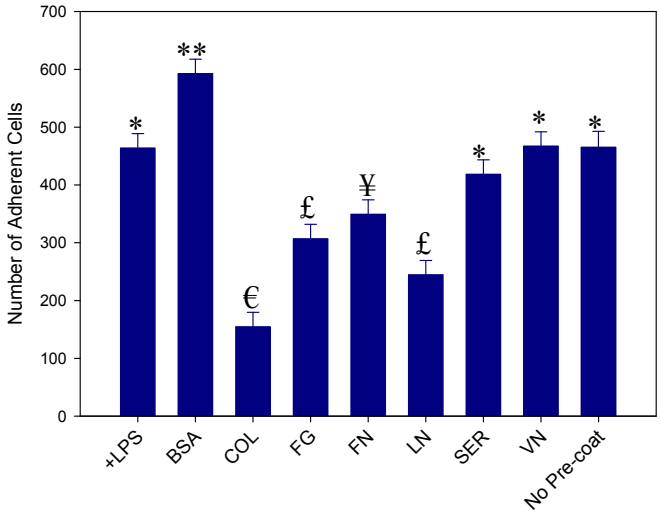

Figure 3-3. Initial-adhesion of DCs cultured on tissue culture treated 96-well plates pre-coated with following proteins: bovine serum albumin (BSA), collagen (COL), fibrinogen (FG), fibronectin (FN), laminin (LN), serum (SER) and vitronectin (VN) has a differential profile. Immature DCs (No Pre-coat) and culture with lipopolysaccharide (LPS, 1 μg/mL) were included as controls. Data represents mean and standard error of at least 12 data points (replicates) consolidated from two mice. The significant pair symbols are described in the text.

Dendritic Cell Phenotype

Morphological and adhesion differences between different adhesive substrates cultured NOD-DCs motivated us to quantify their activation upon culture on the adhesive substrates. Immature DCs were cultured on tissue culture treated 12 well polystyrene plates pre-coated with proteins: BSA, COL, FG, FN, LN, SER and VN. Immature DCs and DCs cultured in the presence of LPS were included as negative and positive control respectively. Upon 1 day of culture DCs were lifted, stained and quantified for the expression of MHC-II, a stimulatory molecule, CD86 and CD80 co-

stimulatory molecules. The DCs spread on the substrates as well as those loosely adherent were collected for phenotypic analysis.

Statistical analysis of the data revealed that adhesive substrates modulate DC-expression of both stimulatory and co-stimulatory molecules. Additionally, adhesive substrates were also able to modulate percentage population expressing MHC-II, CD86 and CD80. The data from 3 or more separate NOD-mouse bone marrow harvest was pooled together, statistically analyzed and plotted as bar graphs (**Figure 3-4, Figure 3-5, Figure 3-6**). Representative density plots are included for reference (**Figure 3-7**). Dendritic cells cultured on FN, LN, SER, COL adhesive substrates and in the presence of LPS, showed highest increase in percentage of cells expressing MHC-II as compared to iDCs. Dendritic cells cultured on BSA, FG, VN and the negative control, iDCs had similar percentage of cells expressing MHC-II. Overall significance was determined by ANOVA, p-value < 0.001. The trend in significant pairs between percentage of cells expressing MHC-II when cultured on different substrates is summarized by: +LPS = COL = FN = LN = SER > VN = iDCs & BSA = FG = VN = iDCs (**Figure 3-4A - * - FG, VN, iDCs; ** - COL, LN; $ - BSA, FG, VN, iDCs; ¥ - +LPS, COL, FN, LN and SER; ¢ - FG, VN and iDCs; $$ - BSA, FG, VN, iDCs**). Soluble LPS was added to DCs cultured on different adhesive substrates to quantify the effect of soluble maturation signal in conjunction with adhesion signaling. The percentage of DCs expressing MHC-II was the highest for the condition SER+LPS and there were no significant differences between DCs cultured on other adhesive substrates. Overall significance was determined by ANOVA, p-value < 0.001. The trend in significant pairs between percentage of cells expressing MHC-II in the presence of LPS is summarized by: SER+LPS > BSA+LPS,

COL+LPS, FG+LPS, FN+LPS, LN+LPS = VN+LPS = iDCs (**Figure 3-4C - * - BSA+LPS, FG+LPS, FN+LPS and VN+LPS**). Geometric mean fluorescence intensity (gMFI) of MHC-II was quantified form the data acquired via flow cytometery. Dendritic cells cultured on FN, VN and BSA had the highest MHC-II expression followed by DCs cultured on FG, LN and SER adhesive substrates and iDCs. Overall significance was determined by ANOVA, p-value < 0.001. The trend in significant pairs between DC-expression of MHC-II is summarized by: BSA = VN & FN > SER & BSA > FG = LN = SER = iDCs (**Figure 3-4B - ¥ - FG, LN, SER, iDCs; $l - BSA, VN; ** - SER, iDCs; * - BSA, FN, VN; ¢ - FG, LN, SER, iDCs.**). Next, MHC-II expression of DCs upon culture on adhesive substrates in the presence of LPS was quantified. Dendritic cells cultured on BSA, FG and VN adhesive substrates had highest MHC-II expression whereas DCs cultured on LN showed the least surface expression. Overall significance was determined by ANOVA, p-value < 0.001. The trend in significant pairs DC-expression of MHC-II when cultured in the presence of LPS is summarized by: BSA+LPS = VN+LPS = FG+LPS > iDCs & VN+LPS > LN+LPS & VN+LPS > SER+LPS > iDCs (**Figure 3-4D - ¢ - iDCs; ** - VN+LPS; * - VN+LPS and iDCs; ¥ - LN+LPS, SER+LPS, iDCs; $ - BSA+LPS, FG+LPS, SER+LPS, VN+LPS**). Interestingly, DCs cultured on VN, BSA and FG substrates induced the lowest percentage population of DC expressing MHC-II molecule. Next, the surface expression and percentage population expressing CD86 via flow cytomtery was quantified. The adhesive substrates modulate the surface expression as well as the percentage of population expressing CD86 – a co-stimulatory molecule. Dendritic cells cultured in the presence of LPS induced highest percentage of DCs expressing CD86. Dendritic cells cultured on FG, LN, SER and VN substrates

along with the negative control iDCs stimulate the lowest percentage of cells expressing CD86. Dendritic cells cultured on BSA, COL and FN adhesive substrates induced similar percentage of cells expressing CD86 (**Figure 3-5A - € - all other conditions; * - +LPS, FG, iDCs; ** - +LPS, FG, VN and iDCs; ¥ - +LPS, BSA, COL, FN; ¢ - +LPS; $ - +LPS, COL**). Overall significance was determined by ANOVA, p-value < 0.001. The trend in significant pairs between percentage of cells expressing CD86 when cultured on different substrates is summarized by: +LPS > COL = FN > FG = VN = iDCs & BSA > FG = iDCs & LN = SER = VN = FG = iDCs. The effect of soluble LPS as soluble maturation stimulation in the presence of adhesive substrates was quantified. It was observed that in the presence of LPS adhesive substrates modulate percentage of cells expressing CD86. Dendritic cells cultured on COL+LPS and LN+LPS induced highest percentage of cells expressing CD86. Dendritic cells cultured on FN+LPS and SER+LPS induced similar

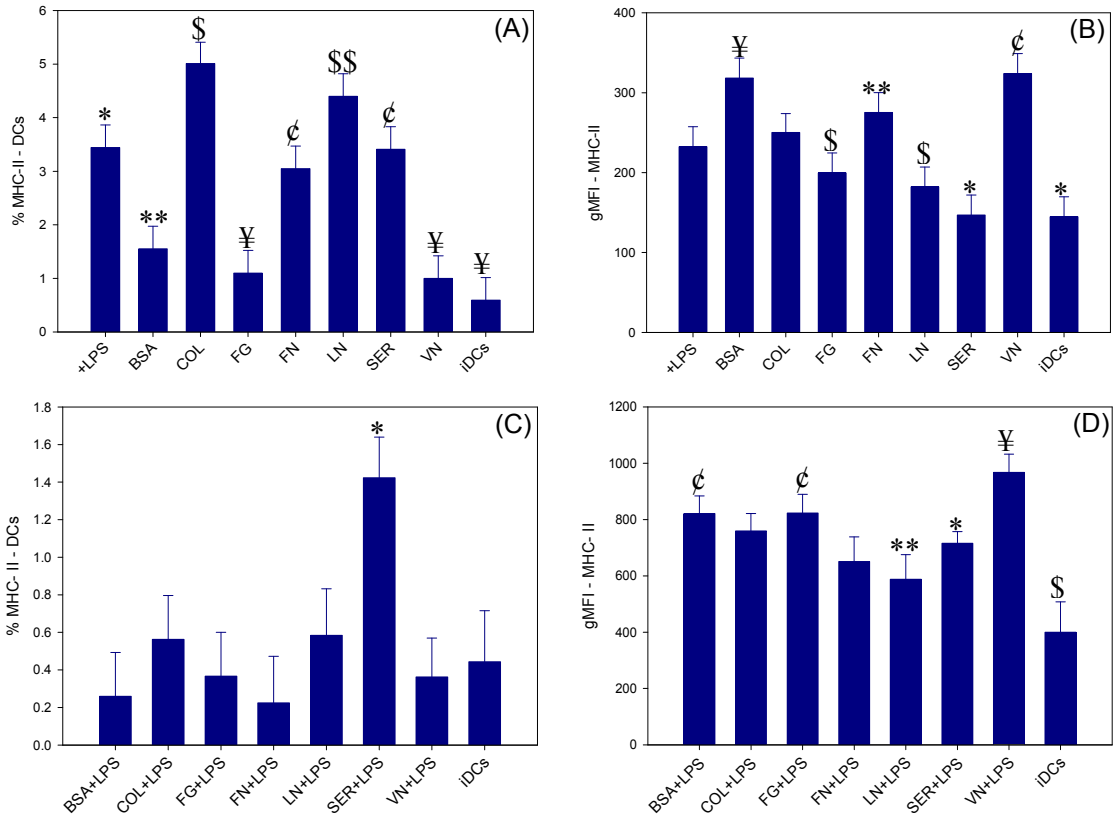

Figure 3-4. Adhesive substrates differentially activate non-obese diabetic (NOD) bone marrow derived-dendritic cells (DCs) as evidenced through surface presentation of major histocompatibility (MHC-II). Dendritic cells were isolated from at least 2 separate mice and each mouse handled as an independent experiment repeat. It is important to note that all the DCs adhered or floating were included in the analysis. . **A)** Dendritic cells positive for surface expression of MHC-II. **B)** Dendritic cells surface expression of MHC-II. **C)** Dendritic cells positive for surface expression of MHC-II when cultured in the presence of LPS. **D)** Dendritic cells surface expression of MHC-II when cultured in the presence of LPS. The significant pair symbols are described in the text.

but moderate percentage of cells expressing CD86. Dendritic cells cultured on FG+LPS, VN+LPS, BSA+LPS and the negative control iDCs had similar and lower percentage of cells expressing CD86 (**Figure 3-5C - £ - COL+LPS, FN+LPS, LN+LPS, SER+LPS; * - BSA+LPS; FG+LPS, FN+LPS, SER+LPS, VN+LPS, iDCs; € - COL+LPS, LN+LPS, SER+LPS; ¢ - BSA+LPS, COL+LPS, iDCs; ¥ - BSA+LPS, FG+LPS, SER+LPS; ** - BSA+LPS, COL+LPS, FG+LPS, LN+LPS, VN+LPS, iDCs; $**

- COL+LPS, FN+LPS ,LN+LPS, SER+LPS). Overall significance was determined by ANOVA, p-value < 1×10^{-6}. The trend in significant pairs between percentage of cells expressing CD86 when cultured on different substrates in the presence of LPS is summarized by: COL+LPS = LN+LPS = SER+LPS > FG+LPS = BSA+LPS = VN+LPS = iDCs & COL+LPS > FN+LPS > iDCs. Surface expression of CD86 cultured on adhesive substrate was quantified and statistical analysis revealed an overall ANOVA, p-value < 0.001 (**Figure 3-5B - * - COL, FG, FN, LN, SER, VN, iDCs; ** - COL, SER, VN, iDCs; £ - +LPS, BSA; ¥ - +LPS**). The trend in significant pairs between DC-expression of CD86 when cultured on different substrates is summarized by: +LPS > COL = FG = FN = LN = SER = VN = iDCs & BSA > COL = SER = VN = iDCs. Surface expression of CD86 was quantified upon DC culture on different adhesive substrate in the presence of LPS and no significant difference (**Figure 3-5D**) between DC CD86 expressions was observed. Adhesive substrates have been shown to modulate the percentage of DCs expressing CD80 co-stimulatory molecule. Interestingly the negative control (iDCs) and positive control of DCs cultured in the presence of LPS had similar levels of percentage cells positive for CD80, which was similar to DCs cultured on adhesive substrate VN and FN. Dendritic cells cultured on LN, FG and BSA demonstrated the lowest percentages of DCs positive for CD80 (**Figure 3-6A - ¥ - BSA, COL, FG, LN; * - +LPS, FN, SER, VN, iDCs; ** - +LPS, FN, LN, SER, VN, iDCs; ¢ - BSA, COL, FG, LN; £ - +LPS, COL, FN, SER, VN, iDCs; € – BSA, COL, FG, LN, VN; $ - BSA, COL, FG, LN, SER**). Overall significance was determined by ANOVA, p-value < 0.001. The trend in significant pairs between percentage of cells expressing CD80 when cultured on different substrates is summarized by: iDCs = +LPS = VN = FN & +LPS > COL = FG = BSA & COL > LN.

Surface expression of CD80 was quantified when DCs were cultured on different adhesive substrates. Dendritic cells when cultured on SER substrate induced highest expression of CD80, which was similar to DCs cultured on FG ($p = 0.052$, are significant if 90% confidence level is considered) and LN ($p = 0.085$, are significant if 90% confidence level is considered). Overall significance was determined by ANOVA, p-value < 3.4×10^{-7}. The trend in significant pairs between DC-expressing CD80 when

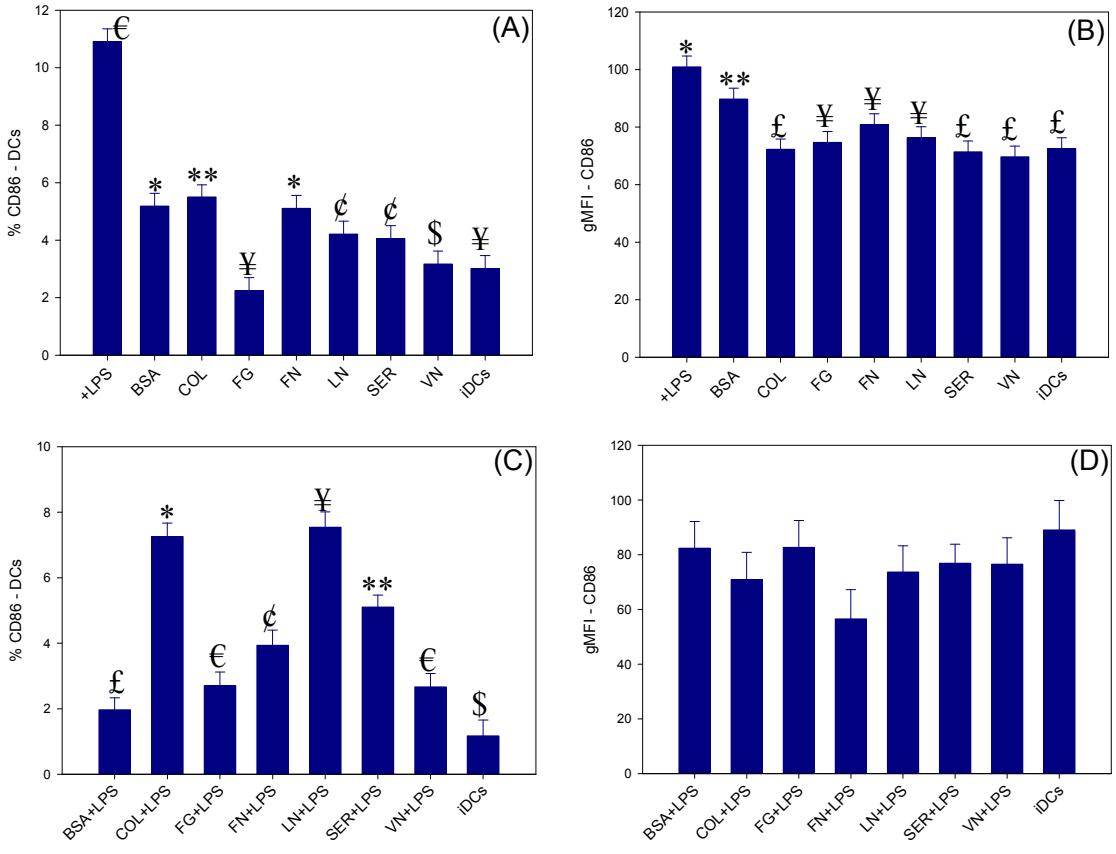

Figure 3-5. Adhesive substrates differentially activate non-obese diabetic (NOD) bone marrow derived-dendritic cells (DCs) as evidenced through surface presentation of co-stimulatory molecule, CD86. Dendritic cells were isolated from at least 2 separate mice and each mouse handled as an independent experiment repeat. It is important to note that all the DCs adhered or floating were included in the analysis. . **A)** Dendritic cells positive for surface expression of CD86. **B)** Dendritic cells surface expression of CD86. **C)** Dendritic cells positive for surface expression of CD86 when cultured in the presence of LPS. **D)** Dendritic cells surface expression of CD86 when

cultured in the presence of LPS. The significant pair symbols are described in the text.

cultured on different substrates is summarized by: SER > +LPS = COL = FN = BSA = VN = iDCs (**Figure 3-6B - * - +LPS, BSA, COL, FN, VN and iDCs**).

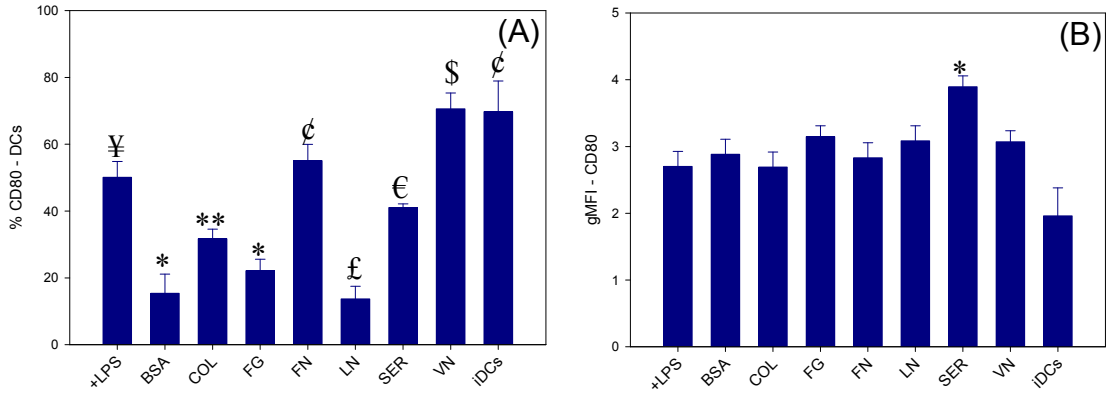

Figure 3-6. Adhesive substrates differentially activate non-obese diabetic (NOD) bone marrow derived-dendritic cells (DCs) as evidenced through surface presentation of co-stimulatory molecule, CD80. Dendritic cells were isolated from at least 2 separate mice and each mouse handled as an independent experiment repeat. It is important to note that all the DCs adhered or floating were included in the analysis. **A)** Percentage of DC population expressing CD80. **B)** Dendritic cell expression of CD80. The significant pair symbols are described in the text.

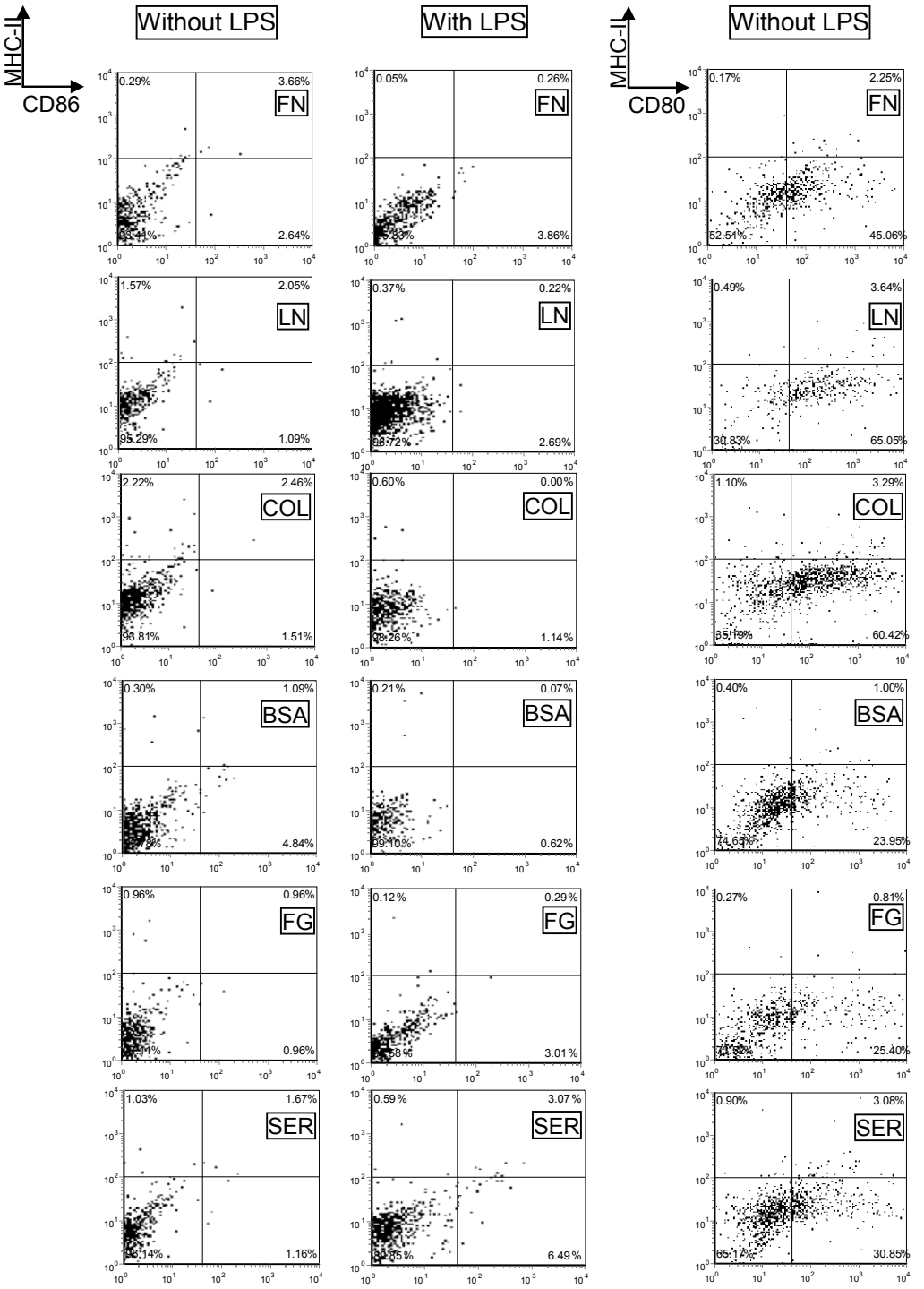
MHC-II
CD86
Without LPS
With LPS
MHC-II
CD80
Without LPS
FN
LN
COL
BSA
FG
SER
0.29%
3.66%
95.41%
2.64%
0.05%
0.26%
96.86%
3.86%
0.17%
2.25%
52.51%
45.06%
1.57%
2.05%
95.29%
1.09%
0.37%
0.22%
96.72%
2.69%
0.49%
3.64%
30.83%
65.05%
2.22%
2.46%
96.81%
1.51%
0.60%
0.00%
98.26%
1.14%
1.10%
3.29%
35.19%
60.42%
0.30%
1.09%
4.84%
0.21%
0.07%
99.10%
0.62%
0.40%
1.00%
74.65%
23.95%
0.96%
0.96%
0.12%
0.29%
96.58%
3.01%
0.27%
0.81%
25.40%
1.03%
1.67%
96.14%
1.16%
0.59%
3.07%
90.45%
6.49%
0.90%
3.08%
65.17%
30.85%

-

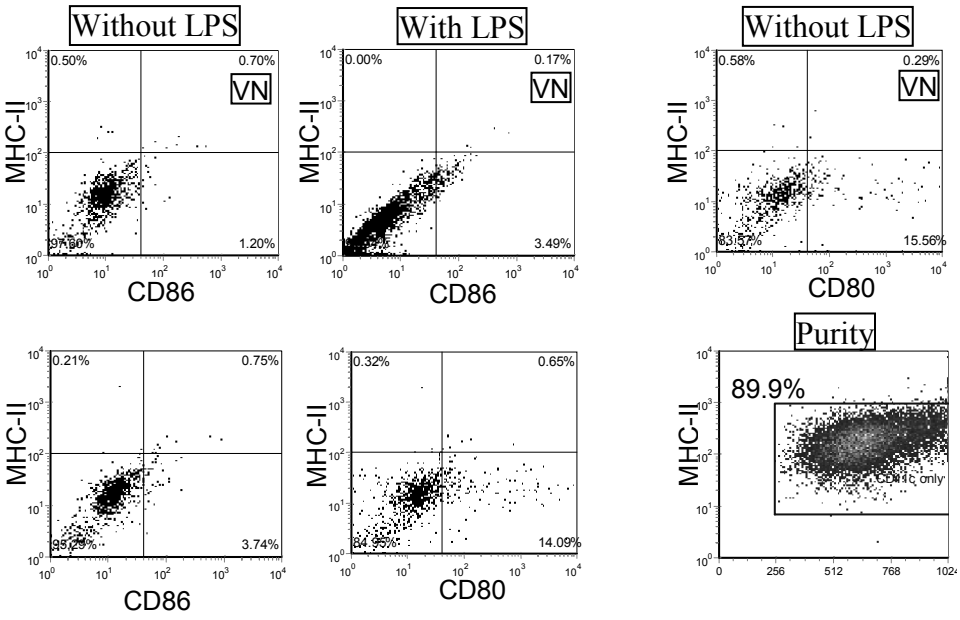

Figure 3-7. Representative phenotypic density plots of data summarized in Figure 3-5, 3-6 for murine NOD-derived DCs cultured on protein-coated tissue culture-treated polystyrene substrate for 24 h. Shown also is iDC purity and maturation markers.

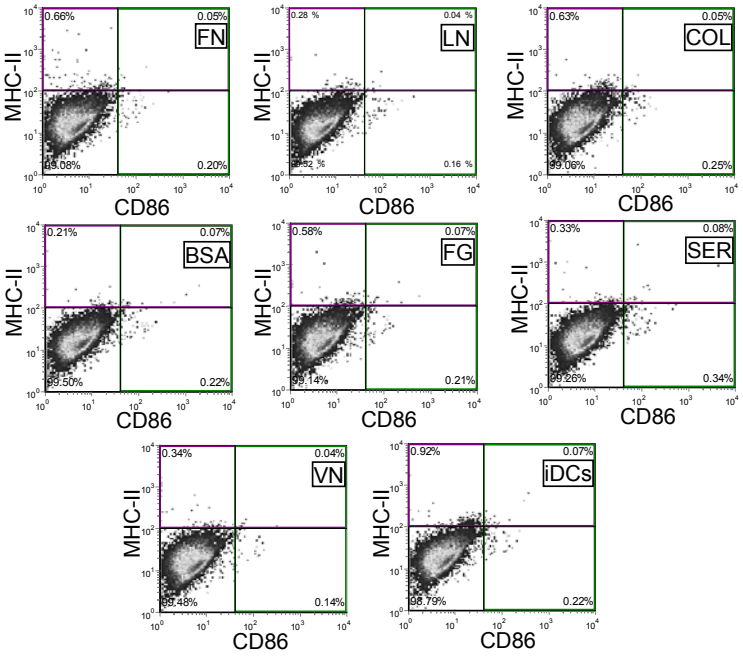

Figure 3-8. Soluble proteins do not activate DCs, quantified via percentage of cells expressing stimulatory (MHC-II) and co-stimulatory (CD86) molecules. Density plots of MHC-II vs. CD86 are generated through FCS Express version 3 software and the data was obtained using flow cytometry. The percentage of DCs positive for these molecules is reported in the insets.

Dendritic Cell Cytokine Secretion

Dendritic cells were cultured on adhesive substrates for 24 hours and the cytokine IL-12p40 – a pro-inflammatory cytokine which may induce a T_h1 type response, secreted by DCs was quantified using sandwich-ELISA. Dendritic cells spread on the substrates as well as those loosely adherent were collected for cytokine production analysis. Dendritic cells cultured in the presence of LPS induced highest amount of IL-12p40 cytokine, while DCs cultured on all the other adhesive substrates produced either low or moderate IL-12p40. Overall significance was determined by ANOVA, p-value < 1×10^{-6}. The trend in significant pairs between DC production of IL-12p40 when cultured on different substrates is summarized by: +LPS > VN > BSA > LN = SER > COL > FN > FG = iDCs (**Figure 3-9A - * - BSA, COL, FG, FN, LN, SER, VN, iDCs; ** - +LPS, COL, FG, FN, LN, SER, VN, iDCs; €€ - +LPS, BSA, FG, FN, LN, SER, VN, iDCs; £ - +LPS, BSA, COL, FN, LN, SER, VN; $ - +LPS, BSA, COL, FG, LN, SER, VN, iDCs; € - +LPS, BSA, COL, FG, FN, VN, iDCs,; $$ - +LPS, BSA, COL, FG, FN, LN, SER, iDCs**). Dendritic cells were cultured on different adhesive substrates in the presence of LPS to understand the effect of adhesive substrates on the IL-12p40 secretion by these cells. Adhesive substrates differentially modulated IL-12p40 cytokine production of DCs when cultured on adhesive substrates with a soluble maturation stimulus of LPS, however, DCs largely were resistant to induction of IL-12p40 when cultured on adhesive substrates without soluble maturation stimuli (**Figure 3-9B - ¥ - COL+LPS, FG+LPS, FN+LPS, SER+LPS, VN+LPS, iDCs; £ - BSA+LPS, FN+LPS, SER+LPS, iDCs; $ - BSA+LPS, FN+LPS, LN+LPS, SER+LPS, iDCs; ** - BSA+LPS, COL+LPS, FG+LPS, LN+LPS, SER+LPS, VN+LPS, iDCs; ¢ - FG+LPS, FN+LPS, SER+LPS, iDCs; * - BSA+LPS, COL+LPS, FG+LPS, FN+LPS, LN+LPS, VN+LPS, iDCs; € - BSA+LPS,**

FN+LPS, SER+LPS, iDCs; $$ - BSA+LPS, COL+LPS, FG+LPS, FN+LPS, LN+LPS, SER+LPS, VN+LPS). Overall significance was determined by ANOVA, p-value < 1×10^{-10}. The trend in significant pairs between DC production of IL-12p40 in the presence of LPS when cultured on different substrates is summarized by: SER+LPS > FN+LPS > BSA+LPS > COL+LPS = FG+LPS = LN+LPS = VN+LPS > iDCs.

Additionally, supernatant isolated from the culture of DCs on different adhesive substrates were quantified using sandwich-ELISA for production of IL-10 an anti-inflammatory cytokine which is traditionally considered to induce a T_h2 type response. The DCs cultured in the presence of LPS induced highest amount of IL-10 cytokine production followed by DCs cultured on COL (**Figure 3-9C - * - BSA, COL, FG, FN, LN, SER, VN, iDCs; £ - +LPS, COL, FG, VN, iDCs; ** - +LPS, BSA, FG, FN, LN, SER, VN, iDCs; € - +LPS, BSA, COL, FN, LN, SER; ¥ - +LPS, COL, FG, VN, iDCs; ψ – +LPS, COL, FG, VN and iDCs**).

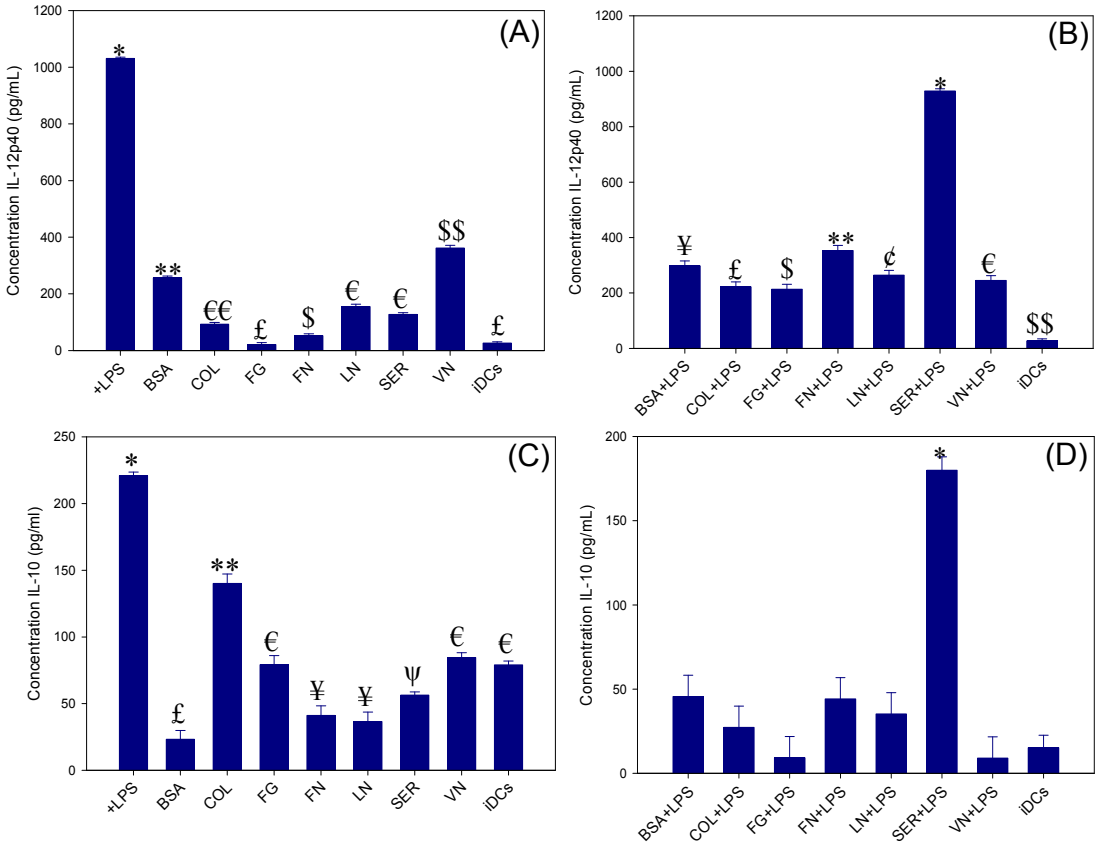

Figure 3-9. Adhesive substrate modulates non-obese diabetic (NOD) mouse dendritic cells (DCs) cytokine production. Dendritic cells were isolated from at least 3 separate mice and each mouse handled as an independent experiment repeat. It is important to note that all the DCs adhered or floating were included in the analysis. **A)** Dendritic cells production of IL-12 upon culture on adhesive substrates. **B)** Dendritic cells production of IL-12 upon culture on adhesive substrates in the presence of LPS. **C)** Dendritic cells production of IL-10 when cultured on adhesive substrates. **D)** Dendritic cells production of IL-10 when cultured on adhesive substrates in the presence of LPS. The significant pair symbols are described in the text.

Overall significance was determined by ANOVA, p-value < 1×10^{-3}. The trend in significant pairs between DC production of IL-10 when cultured on different substrates is summarized by: +LPS > COL > FG = VN = iDCs > FN = LN > BSA & FG = SER. Cytokine production by DCs when cultured on adhesive substrates in the presence of LPS was quantified and reported. The condition SER+LPS induced highest IL-10 cytokine production whereas there was no significant difference between cytokine

productions induced by other adhesive substrates (**Figure 3-9D - * - all the other conditions**). Overall significance was determined by ANOVA, p-value < 1×10^{-3}. The trend in significant pairs between DC production of IL-10 in the presence of LPS when cultured on different substrates is summarized by: SER+LPS > BSA+LPS = COL+LPS = FG+LPS = FN+LPS = LN+LPS = VN+LPS = iDCs.

Mixed Lymphocyte Reaction

Mixed lymphocyte reaction of NOD isolated DCs and BALB/cByJ $CD4^+$ T-cells was carried out to evaluate adhesive substrates modulation of DC-mediated $CD4^+$ T-cell function. The $CD4^+$ T-cell proliferation and T-helper cell type response was quantified by flow cytometery of cells obtained from the co-culture of DCs and $CD4^+$ T-cells. The $CD4^+$ T-cells were stained with intracellular cytokine IFN-γ and IL-4 which are the indicators of T_h1 and T_h2 type of response respectively.

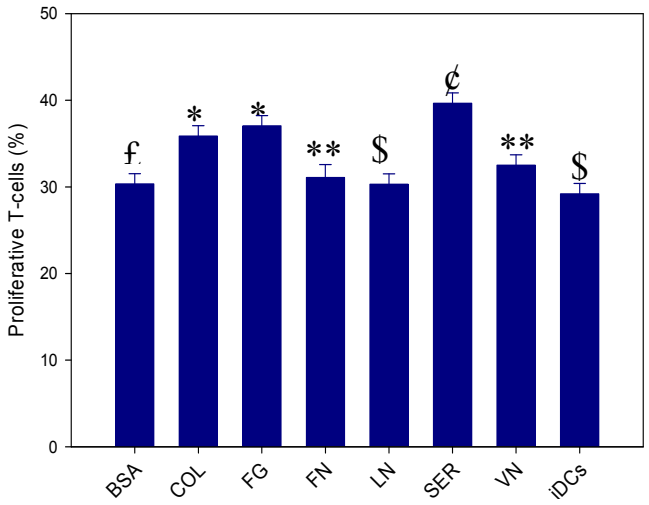

Figure 3-10. In a 96-hour mixed-lymphocyte reaction (1:6, DC to T-cell ratio) DCs modulate T-cell proliferation differentially. Immature DCs were cultured on these modified surfaces for 24 h before adding T-cells isolated from the spleen. Each experiment was independently repeated at least 3 times (NOD/LtJ for DCs and BALB/cbyj for $CD4^+$ T-cells). At least 20,000 $CD4^+$ T-cells were analyzed for each run. The significant pair symbols are described in the text.

The T-cells that were positive for CD4 surface marker were analyzed for the presence of stained BrdU for the quantification of T-cell proliferation. The T-cell proliferation was quantified at the end of 96 hours. The proliferation of T-cells was highest for DCs cultured on SER, COL and FG.

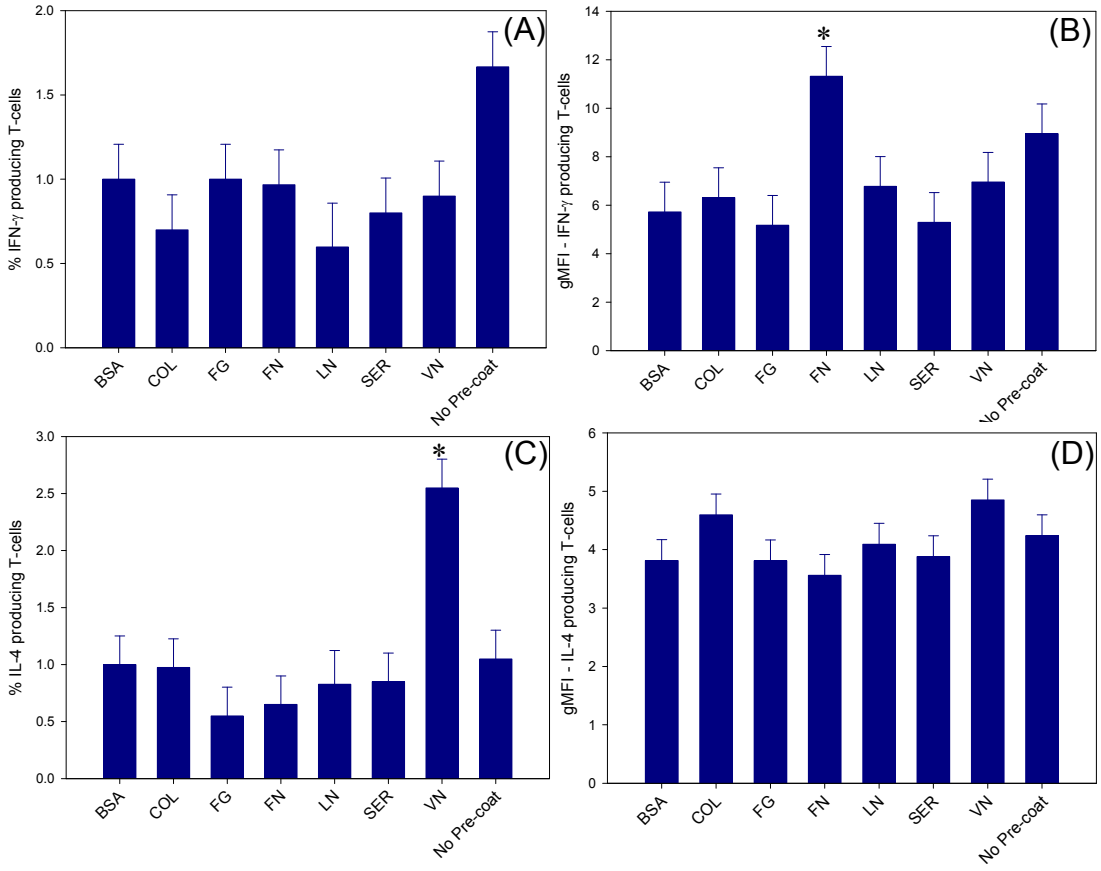

Figure 3-11. In a 96-hour mixed-lymphocyte reaction (1:6, DC to T-cell ratio) DCs modulate $CD4^+$ T-cell cytokine production and expression of these cytokines. Immature DCs were cultured on these modified surfaces for 24 h before adding T-cells isolated from the spleen. Each experiment was independently repeated at least 3 times (NOD/LtJ for DCs and BALB/cbyj for $CD4^+$ T-cells). At least 20,000 $CD4^+$ T-cells were analyzed for each run. **A)** Percentage T cells expressing IFN-γ. **B)** T cells expressing IFN-γ. **C)** Percentage T cells expressing IL-4. **D)** T cells expressing IL-4. The significant pair symbols are described in the text.

The proliferation induced by DCs cultured on FN, LN and BSA was the minimum for all the substrates. Overall significance was determined by ANOVA, p-value < 1 x 10^-

^{3}. The trend in significant pairs between $CD4^{+}$ T-cell proliferation is summarized by: SER > VN = iDCs = FN = LN = BSA & SER = COL = FG & COL = FG > LN = iDCs (**Figure 3-10 - £ - COL, FG, SER; * - BSA, LN, iDCs; ** - SER; $ - COL, FG, SER; ¢ - BSA, FN, LN, VN, iDCs**). Dendritic cells cultured on different substrate did not induce differential percentage of cells producing intra-cellular cytokine IFN-γ (**Figure 3-11A**). Overall significance was determined by ANOVA, p-value < 0.1. The data suggests (when 90% confidence level is considered) that iDCs were higher in inducing a population of T-cells positive for the IFN-γ cytokine. The geometric mean intensity (gMFI) of IFN-γ expressed by T-cells co-cultured with DCs on the adhesive substrates were quantified and reported as a bar graph. It was observed that T-cells co-cultured with DCs on FN adhesive substrates induced highest expression of IFN-γ (**Figure 3-11B - * - FG, SER**). Overall significance was determined by ANOVA, p-value < 0.03. There were no other significant differences between gMFI induced by adhesive substrates. Combining the results of gMFI and percentage T-cells expressing IFN-γ we can conclude that FN substrate might induce a T_h1 type response and all the other substrates might induce equivalent levels of T_h1 response. Similarly, the quantification of percentage of cells expressing IL-4 intracellular cytokine revealed that the co-culture on VN adhesive substrate induced highest percentage of T-cells expressing IL-4, while all the other substrates induced equivalent levels, which was less by 2.5 times the level induced by VN. Overall significance was determined by ANOVA, p-value < 0.003 (**Figure 3-11C - * - all the other conditions**). Geometric mean fluorescence intensity of T-cells expressing IL-4 was also quantified. There was no significant difference found between IL-4 expressions of T-cells induced by different substrates. Overall significance

was determined by ANOVA, p-value = 0.25 (**Figure 3-11D**). Combining the results obtained from gMFI and percentage of T-cells expressing IL-4 we can conclude that VN substrate might induce a T_h2 type response. Representative plots for percentage of $CD4^+$ T-cells expressing IL-4, IFN-γ and BrdU incorporation (for proliferation) are presented (**Figure 3-12**).

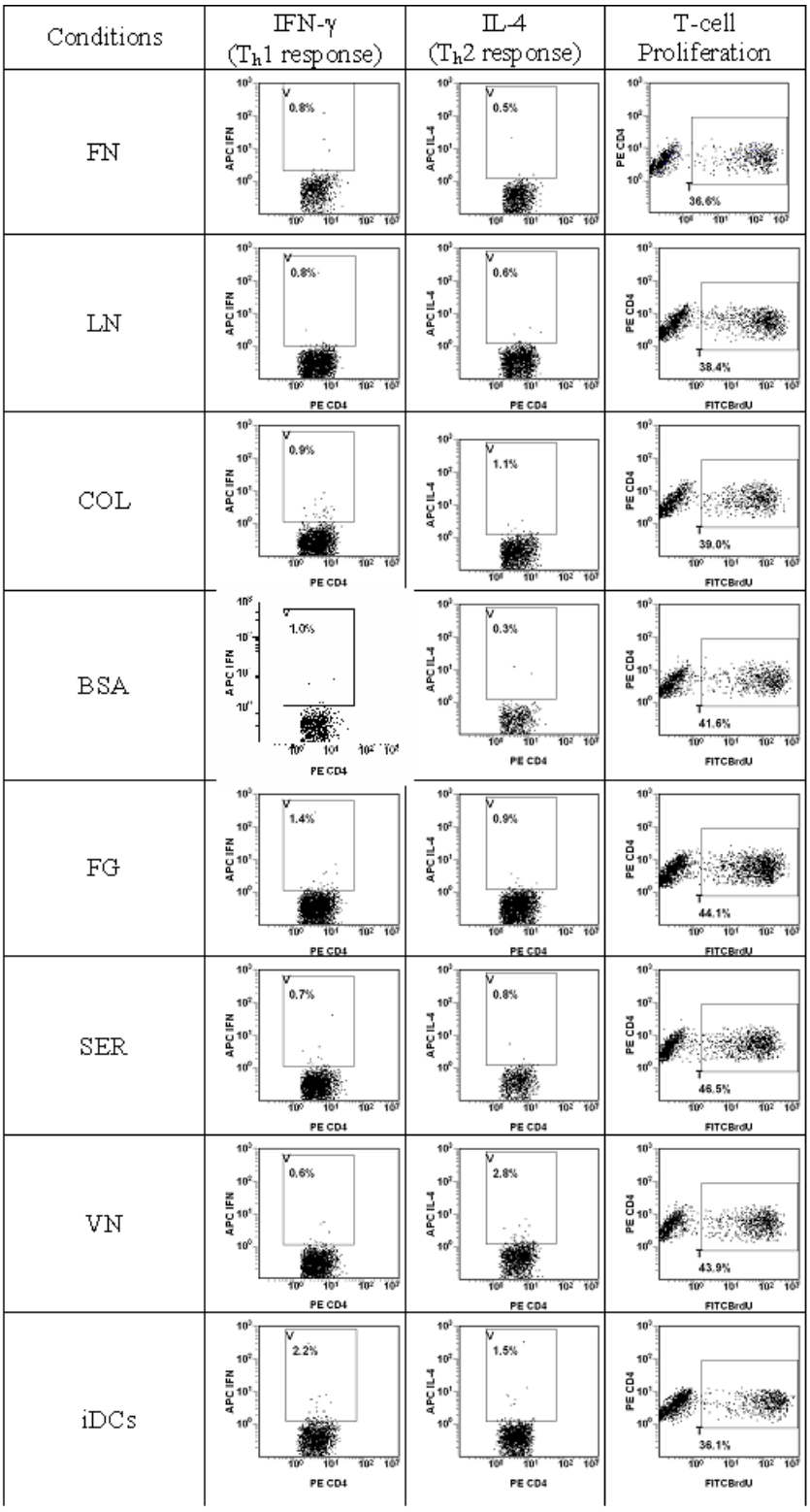

Figure 3-12. Representative phenotypic density plots of data summarized in Figure 3-10, 3-11 for murine BALB/cbyj – $CD4^+$ T-cells co-cultured with NOD-DCs on protein-coated tissue culture-treated polystyrene substrate for 96 hours.

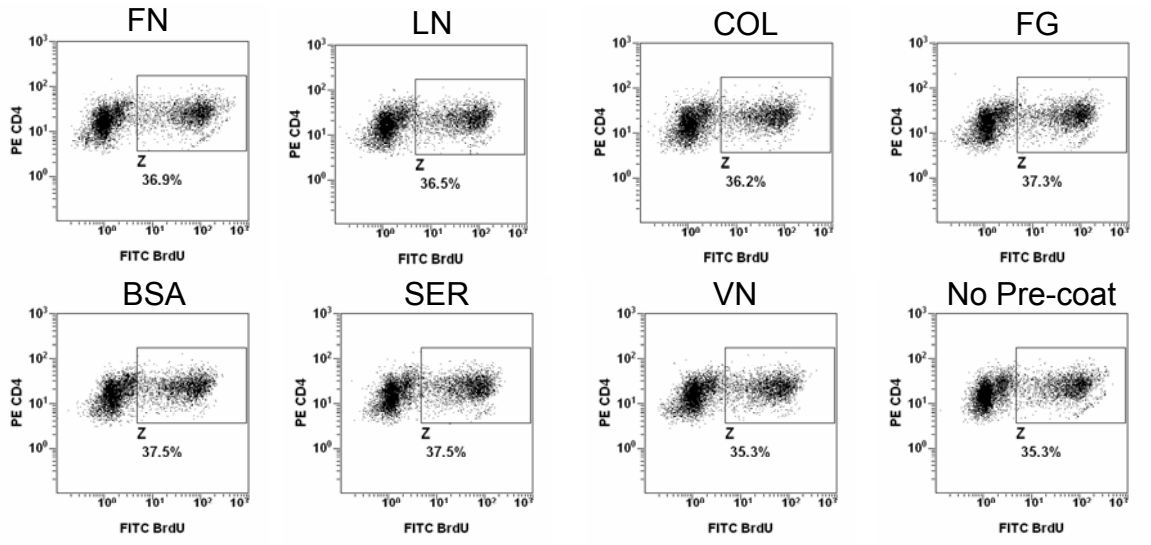

Figure 3-13. In a 96-hour mixed-lymphocyte reaction (1:6, DC to T-cell ratio) B6-DCs do not modulate T-cell proliferation differentially when cultured with soluble protein.

Impact of the Study

Type 1 diabetes (T1D) is an autoimmune disorder pathologically described by destruction of the patient's β-cell islets by T-cells via inducing apoptosis through the release of granzyme B/perforin or through the release of cytokines TNF-α/IFN-γ. Dendritic cells are said to play a central role in priming lymphocyte-based autoimmune response [99]. Dendritic cells can identify the modified microenvironment of the islets and migrate to the lymph node to prime naïve T-cells. During the migration towards lymph nodes if DCs get matured or activated they can induce an auto-reactive cytotoxic T-cell response otherwise a regulator-T-cell response is generated [100]. The migration of DCs involves transition through the pancreas-tissue and muscle capillary basement membrane to the secondary lymphoid organs. Several studies have shown that extracellular matrix (ECM) proteins, such as laminin (LN), collagen (COL) and fibronectin (FN) have abnormally high levels in the pancreas-tissue and muscle capillary basement membrane in pre-diabetic and diabetic pathology. The possibility of

involvement of ECM proteins in T1D-pathology led us to investigate the effect of ECM proteins modulation of DC-maturation and subsequent T-cell responses. Additionally, DC-maturation was evaluated in the presence of LPS to evaluate effects of adhesive substrates in the presence of a soluble maturation signal.

The differential morphological features, clearly an oversimplification of the functional differences, nonetheless point to the fact that only NOD-DCs cultured on BSA, FG and VN substrates, all of which are found in blood can be characterized as DCs that form clusters. Clustering of vascular DCs has been observed in atherosclerosis prone area [101], an indication of maturation of splenic DCs isolated from BB-DP rats [101-103] and a method utilized by DCs for transferring antigens [104]. On the other hand presentation of dendrites and a veiled morphology might be indicators of activation on DCs isolated from human peripheral blood mononuclear cells [105]. Interestingly, although among these proteins VN is found in ECM, its expression has not been shown to be up-regulated in diabetes pathology. Upon comparison of the effect of these three adhesive substrates on modulation of DC-functions we observed that a) BSA substrate induces high expression of MHC-II and CD86 whereas VN and FG substrates induced lower expression of MHC-II and CD86 and b) BSA adhesive substrates induces low but similar levels of percentage of DCs expressing CD86 and MHC-II as VN and FG adhesive substrates (**Figure 3-4, Figure 3-5**). The IL-12p40 cytokine production profile of DCs cultured on BSA and VN adhesive substrates are moderately high, whereas that of DCs cultured on FG substrate is as low as iDCs. The IL-10 cytokine production of DCs on VN and FG substrates were similar whereas DCs cultured on BSA was even lower than the negative control of iDCs. This data suggests

that DCs cultured on BSA substrates which had high expression of MHC-II and CD86 and high IL-12p40 with low IL-10 production and no cluster formation might induce Th1 type T-cells response, however, this was not apparent from the IFN-γ production from T-cells. Similarly, analyzing DCs cultured on FG, which is expected to have a moderate Th2 type response did not show higher percentages of T-cells expressing IL-4. However, DCs cultured on VN, which had moderate levels of IL-12p40 and IL-10 productions and low expression of MHC-II and CD86, with low expression of CD80 along with low percentage of DCs expressing MHC-II and CD86, high CD80 expression and not demonstrating the formation of clusters induced highest percentage of IL-4 producing T-cells (~ 2.5 times higher than all the other substrates) and low percentage of IFN-γ producing T-cells (**Figure 3-5, Figure 3-6, Figure 3-8, Figure 3-10**). These data might suggest that the defective NOD-DCs are naturally inclined toward suppressing the population of IL-4 producing T-cells, unless provided with extra-cellular signaling.

Dendritic cells are known to modulate the ECM and might cause the adsorbed proteins to become soluble. In order to validate that the NOD-DCs were not influenced by the presence of soluble proteins we cultured NOD-DCs with low concentration (10 μg/mL) of different proteins. The NOD-DCs cultured on adhesive substrates had similar levels of activation (percentage of cells expressing MHC-II and CD86) as compared to iDCs, (**Figure 3-7B**). These data suggests that adhesive cues are required for differential activation of NOD-DCs and the degradation protein products do not play a major role in modulating NOD-DC-function. Furthermore, these data also suggests that the xenogenic immune response that might be attributed to different species-derived

proteins used in different experiments here did not play a major role in activating NOD-DCs. Additionally, MLR-experiment with soluble proteins was carried out with DCs obtained from the strain of CD57BL6/j mouse (known to shown normal responses) and T-cells isolated from BALB/cByJ mouse. In this case B6-DCs induced similar levels of T-cell proliferation as iDCs on all the substrates as induced by iDCs (**Figure 3-12**). This data suggests that the soluble proteins do not have an appreciable effect on B6-DC maturation or T-cell proliferation.

Pearson's correlation was employed to further investigate, the effect of NOD-DC-cytokine on the percentages of T-cells producing either IL-4 or IFN-γand their expression. We observed that DC-produced pro-inflammatory cytokine IL-12p40 had a low and moderate but negative correlation to percentage of T-cells producing IFN-γ (Pearson's Correlation = -0.32) and expression of IFN-γ (Pearson's Correlation = -0.28) respectively. Traditionally, IFN-γ production follows similar trend to IL-12p40 however, our results do not suggest the same and hence, further stresses the defective nature of DCs (**Figure 3-14A, Figure 3-14C**). Furthermore, NOD-DC produced IL-10 had a low correlation with percentage of T-cells producing IL-4 (Pearson's Correlation = 0.22), but a high correlation with expression of IL-4 (Pearson's Correlation = 0.68). This suggests that adhesive substrate induced differential DC-production of IL-10 is a good indicator of the extent of generated Th2 type response (**Figure 3-14B, Figure 3-14D**). Furthermore, the percentage of DCs expressing stimulatory molecules MHC-II and co-stimulatory molecules CD86 and CD80 had a low and negative correlation with CD4+ T-cell proliferation, with a Pearson's correlation of -0.24, -0.14 and -0.18 respectively (**Figure 3-14E**). These data might suggest that stimulatory and co-stimulatory molecules do not

play a major role in inducing T-cell proliferation when cultured on different adhesive substrates. Upon correlating T-cell proliferation and DC-expression of stimulatory and co-stimulatory molecules, it was observed that expression of MHC-II had a low and negative Pearson's Correlation of -0.28 with T-cell proliferation; expression of CD86 had a moderate but negative Pearson's Correlation of -0.44 with T-cell proliferation and expression of CD80 had a high and positive correlation with T-cell proliferation (**Figure 3-14F**). A high correlation between T-cell proliferation and co-stimulatory molecules CD80, along with low correlation with MHC-II suggests that expression of CD80 might be the governing factor for T-cell proliferation via NOD-DCs cultured on the adhesive

substrates.

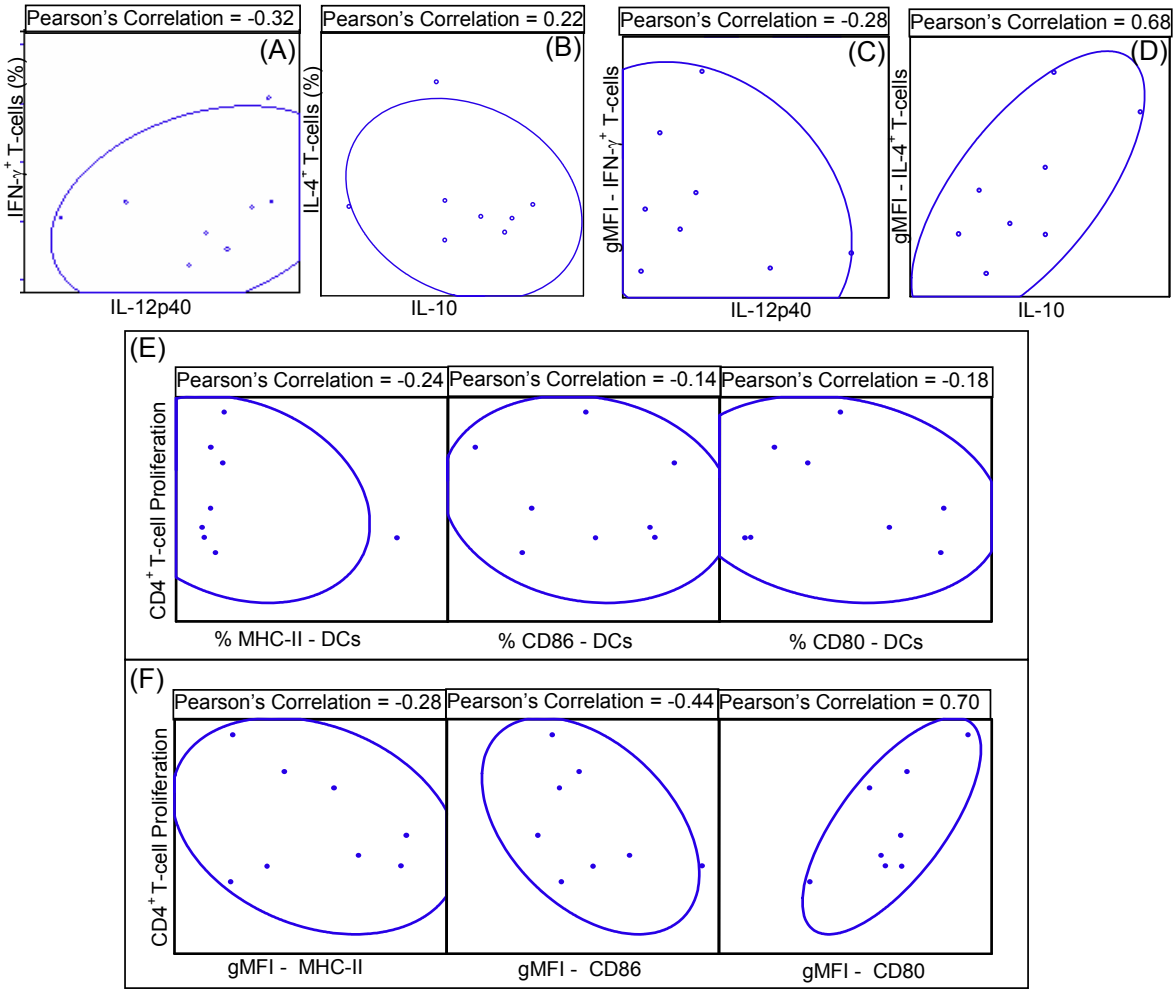

Figure 3-14. Dendritic cell surface stimulatory and co-stimulatory molecules and cytokine produced may modulate T-cell response, in a mixed lymphocyte reaction, determined using Pearson's correlation values (0.1 to 0.4 low correlation, 0.4 to 0.7 moderate correlation and 0.7 to 1.0 high correlation).

This analysis led us to compare cumulative effect of DC-cytokine production, traditionally known to direct Th-cell type response and DC-expression of CD80 on the

percentage T-cells expressing either IL-4 or IFN-γ cytokines (**Figure 3-15**).

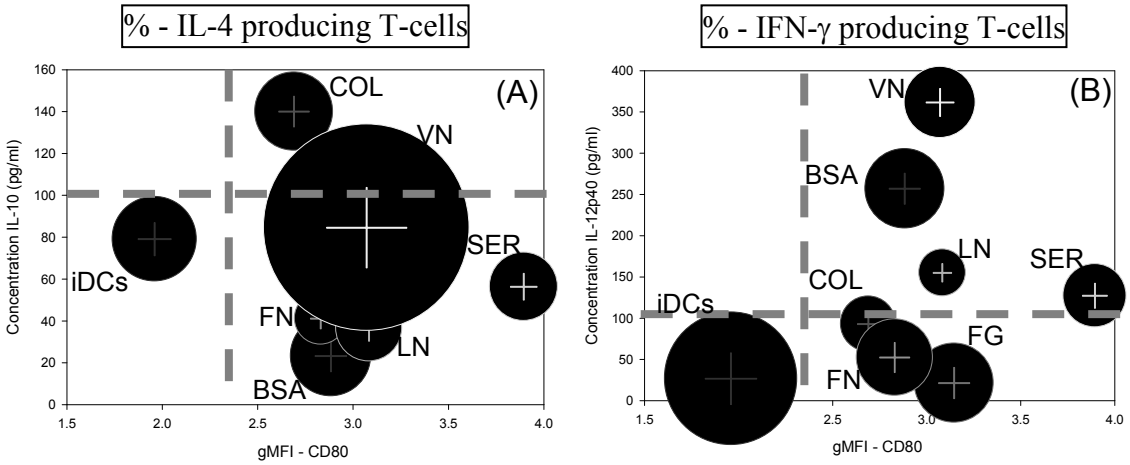

Figure 3-15. A 3-factor bubble graph between expression of CD80 by DCs (gMFI-CD80) on the x-axis and DC-cytokine production (IL-10 and IL-12p40) on the y-axis is plotted with the diameter of the bubble representing the percentage of $CD4^+$ T-cells producing IL-4 or IFN-γ. These plots have been constructed to understand the effect of cumulative effects of expression of co-stimulatory molecule and cytokine produced by DCs on T-helper type responses. **A)** Dependence of percent of T-cells producing IL-4 on DC IL-10 production and CD80 expression. **B)** Dependence of percent of T-cells producing IFN-γ on DC IL-12p40 production and CD80 expression.

A bubble graph was plotted with CD80 expression on X-axis with either IL-12p40 or IL-10 on the y-axis. The size of the bubble represents the amount of percentage cells positive for IFN-γ and IL-4 respectively. Comparing the two bubble plots (**Figure 3-15A, Figure 3-15B**) can help understand effects of different adhesive substrates on T-helper type response in a diabetic pathology. Interestingly, the no pre-coat condition of iDCs, although have low IL-12p40 production and low CD80 expression had high IFN-□ and moderate IL-4 positive T-cells, thus suggesting that iDCs might not be best suited for ex vivo immunotherapy approaches. Furthermore, DCs cultured on SER induced highest CD80-expression, with moderate IL-12p40 and IL-10 production and moderate to low IL-4 and IFN-γ responses, thus suggesting that this protein coating did not preferentially mediate the T-cell response toward tolerance (Th2-type) or inflammation (Th1-type).

Currently, several immunotherapies involve ex vivo culture of DCs [106-108]. Such cultures involve culture and expansion of DC-population on tissue-culture treated polystyrene plate which has adsorbed proteins from serum as substrate. From our studies, it is clear that culturing DCs on SER, although, produces a low Th1 type response produces a low Th2 type response as well. Another, interesting surface adsorbed protein was VN, which induced high % IL-4 producing T-cells but low % IFN-γ producing T-cells (**Figure 3-15A, Figure 3-15B**). Evidently, it is important to understand and characterize the substrate on which NOD-DCs are being cultured and choose the substrate best suited for the designed immunotherapy.

CHAPTER 4
INTEGRIN-MEDIATED PEPTIDE ADHESION BASED CONTROLLED ACTIVATION OF DENDRITIC CELLS

Introduction

Manipulating the body's immune response to boost or repair natural healing mechanisms is a powerful approach that is being explored using dendritic cell (DC) immunotherapies. We have engineered a versatile process to produce density gradients of surface-bound species for high throughput analyses of cell responses to well-characterized receptor-ligand interactions. For instance, the Arg-Gly-Asp (RGD) tripeptide sequence, which is found in a variety of extracellular matrix proteins and is recognized by a number of integrins, can be used to promote integrin-mediated adhesion in a concentration dependent manner in many cell types. In DCs, integrins are often used as markers to characterize the tissue specificity and maturation state of DC subsets. However, the functional role of DC integrins in mediating immune responses remains largely unexplored. Our goal is to engineer biomimetic cell adhesive substrates to investigate the functional interaction of integrin receptor binding and other pro-inflammatory / anti-inflammatory signals that direct DC maturation.

Chip Manufacture

The chips with RGD-peptide gradient using 'click' chemistry surface functionalization were generated by our collaborators at NIST. Briefly, "Universal Substrates" were derivitized with azo-terminated GRGDS peptide via the highly selective 1,3 Huisgen dipolar cycloaddition reaction, forming a covalent triazole linkage. This reaction proceeds under aqueous conditions with a high degree of dependability, complete specificity and using reactants that are bio-compatible (**Figure 4-1**).

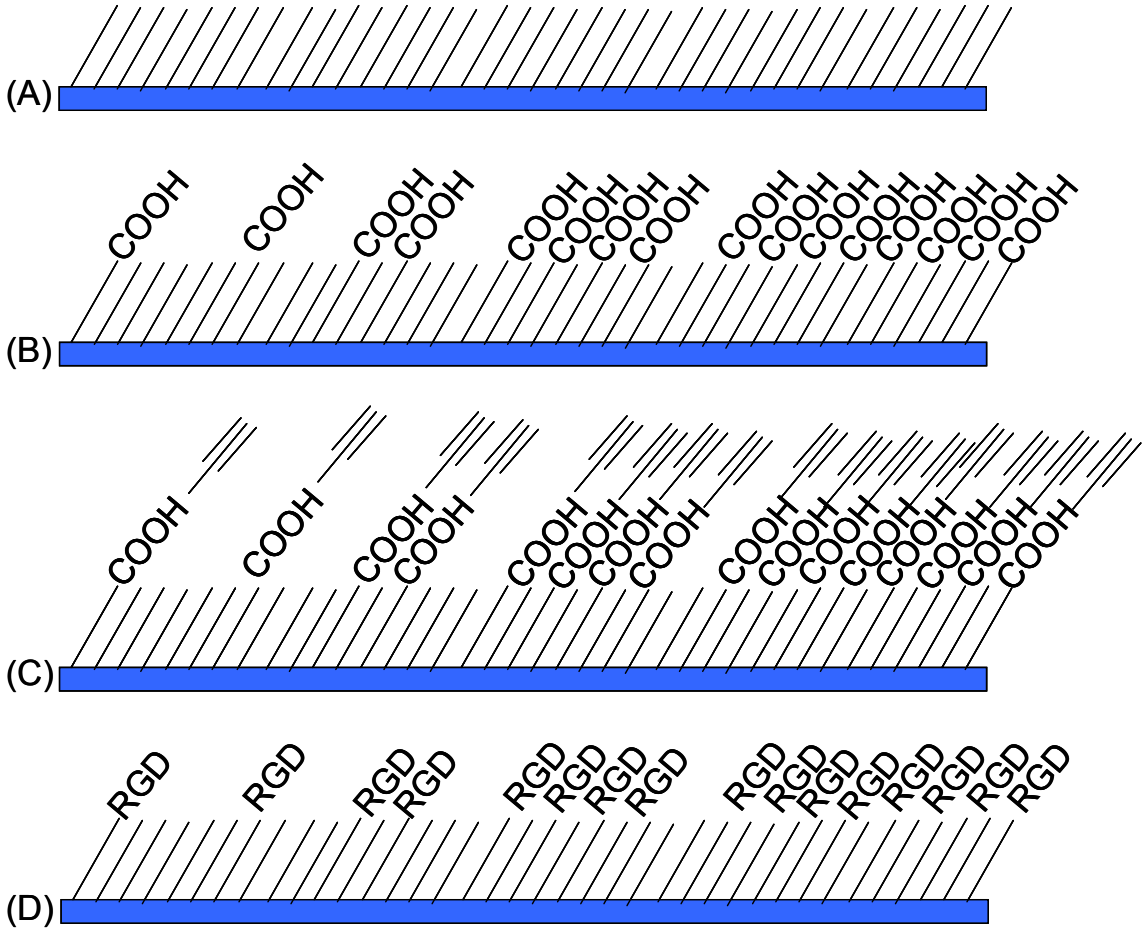

Figure 4-1. Gradient SAM substrates can be converted into biomolecule functionalized gradient surfaces with defined concentration, spatial orientation and complete chemical specificity by coupling an alkyne-terminated linker through the UV-oxidation generated carboxyl groups. The steps **A** to **D** show different process done to crosslink peptide on the substrate.

Dendritic Cell Isolation

Dendritic cells were isolated from bone marrow of 7 week old C57Bl6/j mice using a 10 day protocol. Briefly, bone marrow was isolated from femur and tibia of the mouse. Red blood cells were removed lysed by ACK lysing buffer (Whittaker) and the isolated precursor cells were incubated with DC-media consisting of 20 ng/mL of GM-CSF (R&D Systems), DMEM/F12 (1:1) with L-glutamine (Cellgro, Herndon, VA) and 10% fetal bovine serum (FBS) (Hyclone), 1% sodium pyruvate (Lonza, Walkersville, MD) and 1%

non-essential amino acid (Lonza, Walkersville, MD) for 2 days in a flask. The floating cells were collected from the flask at the end of two days and re-seeded with fresh DC-media in a 6-well low-attachment plate (Corning Inc., NY) for 6 days. After 6 days of culture the cells were re-suspended in fresh media and seeded onto tissue-culture treated 6 well plates (Corning, Inc, NY) for 2 days. After 10 day of culture DCs were lifted using 5mM solution of Na_2EDTA (Fisher Scientific) in phosphate buffer saline (PBS) (Hyclone). Dendritic cells thus isolated were then tested for immaturity ($MHC\text{-}II^+ < 6\%$ and $CD86^+ < 6\%$), purity (using flow cytometery: $CD11c^+ > 90\%$) and viability (Trypan blue staining).

Dendritic Cell Culture on Chip

The chips were washed with PBS and blocked with 1% bovine serum albumin (BSA) (Fisher Bioreagents) for 1 h. The chips were then washed with PBS before seeding the DCs. The number of cells on control chips and the sample chip were maintained the same. Dendritic cells were cultured for 24 h on the chips. The DCs were treated with monensin (BD Biosciences) for the last 5 h before staining for intra-cellular cytokines IL-12p40 and IL-10.

Immunostaining

The chips were stained for either MHC-II and CD86 or IL-10 and IL-12p40.

MHC-II and CD86

The control and the sample chips cultured with DCs were washed with PBS before blocking with 4% paraformaldehyde (USB Corporation) for 10 min. The chips were then blocked with 10% FBS in PBS for 1 h. Antibodies against major histocompatibility complex (MHC-II) and CD-86 cross-linked with phycoerythrin (PE) and fluorescein isothiocyanate (FITC) (Santa Cruz Biotechnology Inc.) respectively were diluted 1:100

in 1% FBS and utilized to stain the DCs on the same chip. The chips were then washed with PBS and mounted using 4',6-diamidino-2-phenylindole (DAPI) (Santa Cruz Biotechnology Inc.) containing mounting gel.

IL-10 and IL-12p40

The DC-cultured chips were washed with PBS and stained with IL-10 and IL-12p40 antibodies (Santa Cruz Biotechnology Inc.). The chips were incubated with cytoperm and cytofix buffers (BD Pharmingen) for 30 min. Then the chips were incubated in 10% goat serum for 1 hour for blocking, upon which the cells were stained with primary antibodies IL-10 and IL-12p40. The chips were washed with wash buffer (BD Pharmingen) and stained with respective secondary antibodies for IL-10 and IL-12p40.

αV Staining

The DCs were stained for integrin using crosslinking-extraction process. The DC-cultured chips were washed 3X with PBS to remove all the media. The chips were then incubated with 1mM solution of sulfo-BSOCOES (Bioworld) made in PBS for 15 min to crosslink the cells to the chips. The chips were then washed with 1M tris-buffer (Fisher Scientific) twice. The cells were then extracted from off the chip by incubating the chip in 0.1% SDS solution (Fisher Scientific) made in PBS for 10 min. The chips were then blocked with 0.1% BSA solution for 1 hr. The chips were stained with primary αV antibody (Santa Cruz Biotechnology Inc.) for 1 hr, followed by biotinylated secondary antibody (Santa Cruz Biotechnology Inc.) for 1 hr. The chips were then incubated in streptavidin conjugated to alkaline phosphatase for 15 min. The chips were then incubated in ELF97 substrate (Invitrogen) prepared using the manufacture's protocol for

8 min. The chips were washed in the wash buffer provided by the manufacturer and mounted on a microscope glass slide for image analysis.

Imaging and Analysis

The chips were imaged from 12.55 mm from the edge with minimum concentration of -RGD peptide or –COOH terminated groups to the maximum concentration. Chips were imaged at 12-bit using FITC, DAPI and Rhodamine (RHOD) filters using Axiovert 200M Carl Zeiss inverted fluorescent microscope. The images were analyzed using Axiovision 4.0 software. A mask was generated using DAPI channel, by selecting the region with intensity from the edge of the nucleus to 4 μm away from the nucleus. This mask was used for images obtained using both FITC and Rhodamine filters and the sum fluorescence intensity was calculated for individual DC. Similarly, the mask was utilized to quantify mean background intensity (**Figure 4-2**). The following formula was used to quantify the corrected fluorescence intensity per DC.

*Corrected Intensity / DC = (Sum fluorescence Intensity – Mean Background intensity) / {Number of DC} * {Mean Background intensity}*.

Corrected intensity of individual DC was averaged over every 500 μm (breadth) x 100 μm (length) area and plotted against the increasing length which corresponds to the increasing concentration of the RGD gradient. A total of 150,000 – 450,000 DCs were analyzed per chip. The entire length of the chip was analyzed, omitting 12.5 mm from each of the length-ends and 3 mm from breadth-ends to compensate for the edge-effects and mounting-artifacts.

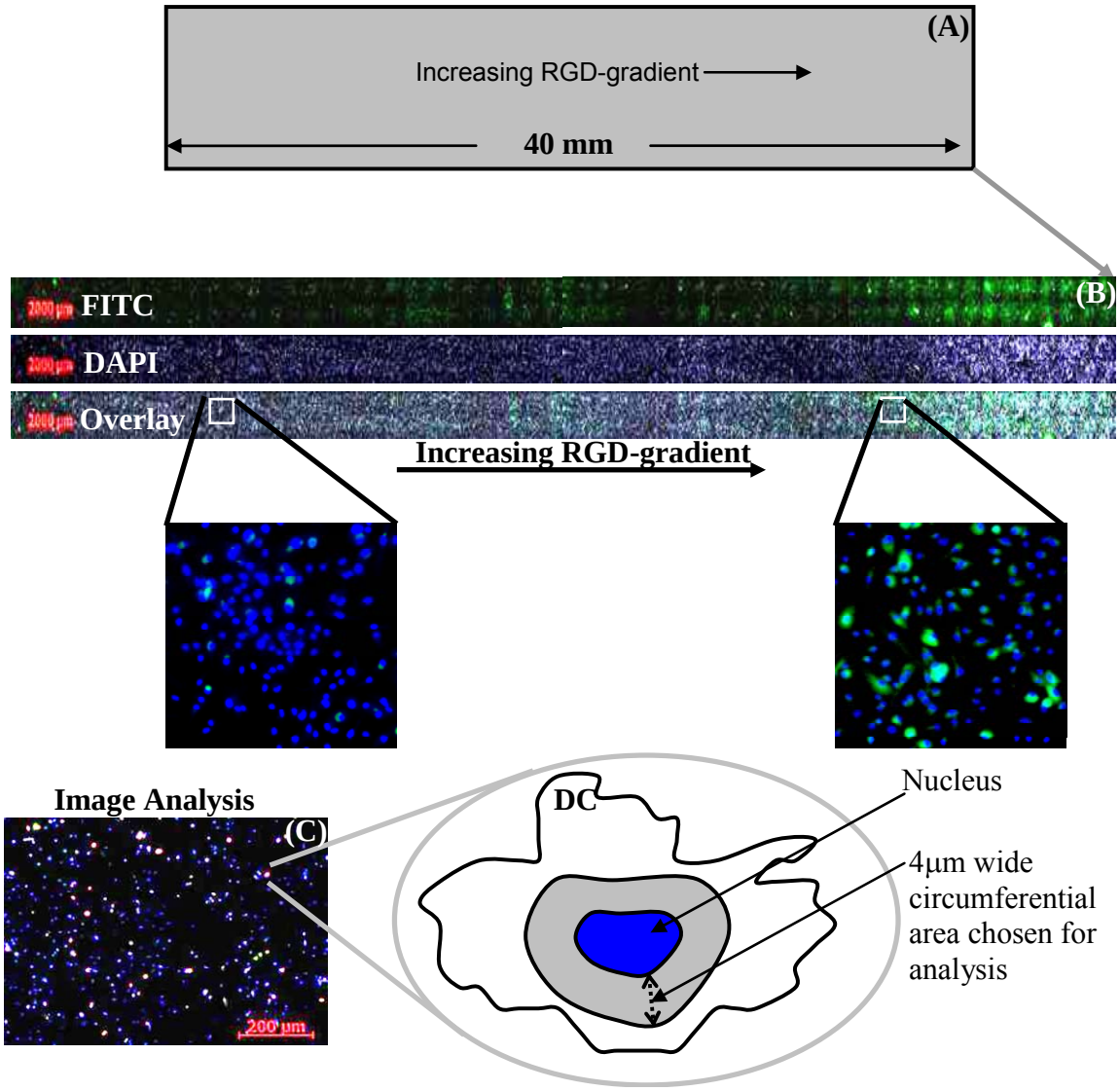

Figure 4-2. Dendritic cells cultured and immunofluorescence stained on the RGD-gradient can be quantified for the expression of surface molecules such as MHC-II- stimulatory molecule; CD86-co-stimulatory molecule and intra-cellular anti-inflammatory cytokine IL-10; pro-inflammatory cytokine IL-12p40. **A)** The schematic of the chip utilized for making the RGD-gradient is shown. **B)** A representative micrograph of a chip obtained using fluorescent microscope is shown with increasing gradient of RGD from left to right and DCs stained for surface expression of CD86 with FITC (shown in green) and nuclei with DAPI (shown in blue). **C)** Image analysis was performed on the micrographs of stained DCs for nuclei and surface markers or intracellular cytokine.

Statistical Analysis

The least mean square values and standard error were obtained using two-way ANOVA via General Linear Model program, SYSTAT 12, with independent variables as the number of runs and the RGD-peptide surface density. Additionally, Pearson's Correlation between the fluorescence intensity and the length of the chip corresponding to surface density of RGD-peptide was quantified.

Results

The DCs were cultured on the chips with RGD-gradient, control chips without RGD and chips in the presence of LPS. Upon 24 h of culture, cells were immunofluorescently stained with either the cell surface molecules or intra-cellular cytokines. The numbers of cells on the chips were quantified via nuclear staining assuming one nucleus per cell. It was observed that the number of cells over 500 μm (breadth) x 100 μm (length) block of the chip / gradient remained the same with a representative coefficient of determination of $R^2 = 0.04$ for the RGD-gradient chip and $R^2 = 0.2$ for the control chip (**Figure 4-3**). Dendritic cells were cultured on the RGD-gradient chip and CD86 cell surface expression was quantified by acquiring images using a fluorescent microscope and image analysis. The background corrected fluorescence intensity was plotted against increasing surface density of the RGD-peptide. It was observed that there is a general trend of increasing cell surface expression of CD86 with increasing surface density of RGD peptide. Two-way ANOVA revealed a coefficient of determination, $R^2 = 0.94$ and a p-value < 1.8E-12. Furthermore, DCs cultured on the highest analyzed RGD surface density have ~5 times more CD86 cell surface expression as compared to the lowest analyzed RGD surface density (**Figure 4-4A**).

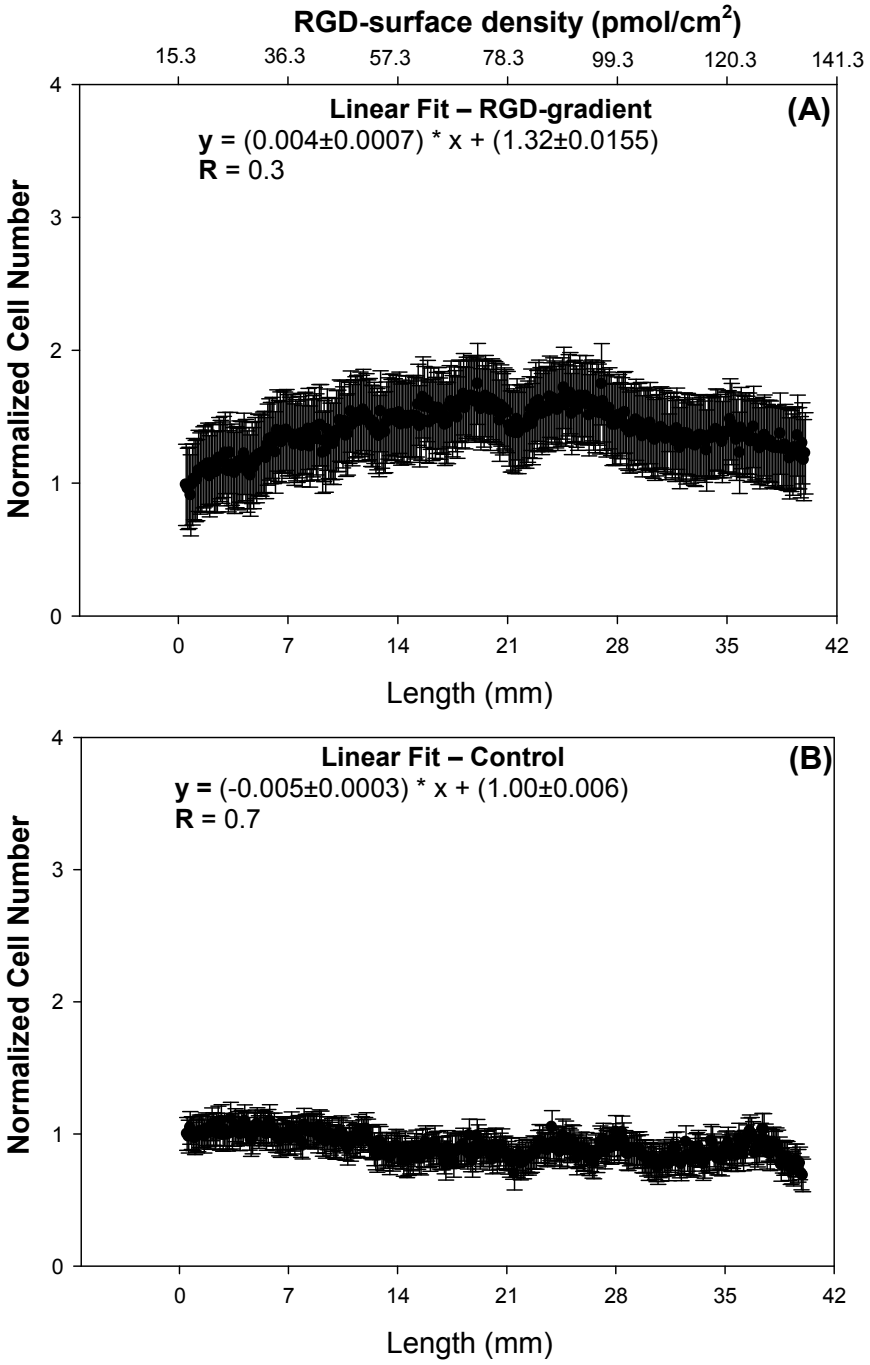

Figure 4-3. Dendritic cells cultured on RGD-gradient chips demonstrate that the number of DCs adhering does not have a correlation with the RGD-gradient or control gradient. **A)** Number of DCs on RGD gradient **B)** Number of DCs on control gradient.

Dendritic cells were cultured on the control chip and CD86 cell surface expression was quantified. The background corrected fluorescence intensity was plotted against

increasing surface density of the RGD-peptide that corresponds to the same distance from the 0mm in both RGD-gradient chip and control chip. It was observed that the CD86 expression remains constant throughout the length of the control chip. Dendritic cells cultured on the RGD-gradient chip, at the lowest RGD surface density have 10-20 times more CD86 expression and at the highest RGD surface density 50-100 times more CD86 expression of the DCs cultured on the control chip. Two-way ANOVA revealed a coefficient of determination, $R^2 = 0.65$ and a p-value < 0.0003. Dendritic cells were cultured in the presence of LPS and CD86 cell surface expression was quantified. The background corrected fluorescence intensity was plotted on the same plot as the RGD-gradient chip and control-chip plot as a positive control. It was observed that DCs cultured at the highest concentration of the RGD surface density had CD86 expression comparable to the DC expression of CD86 when cultured in the presence of LPS. The standard error of the CD86 expression of DCs is shown as dashed line where as the solid line represents the least square mean value (**Figure 4-4A**).

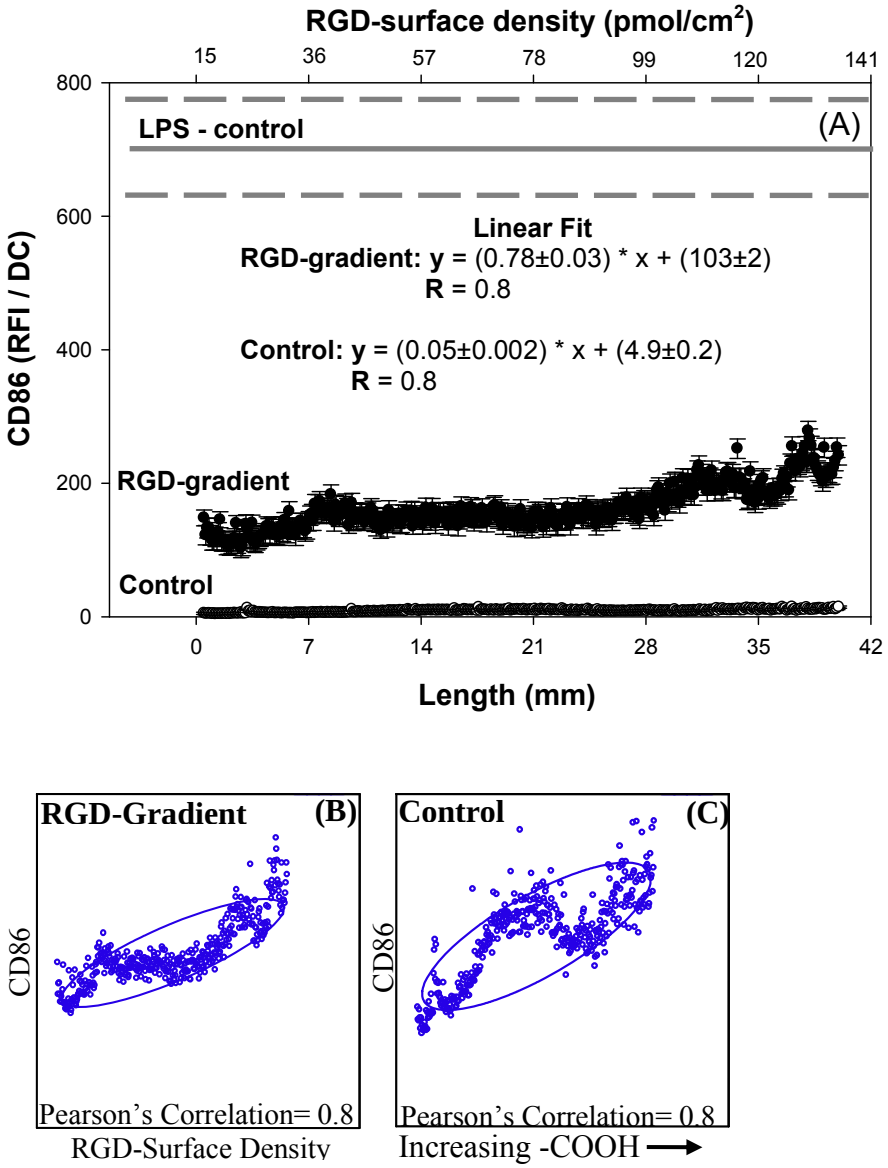

Figure 4-4. Dendritic cells cultured on RGD-gradient chips demonstrate that surface expression of CD86 co-stimulatory molecule is proportional to the RGD-gradient. **A)** CD86 expression by DCs cultured on RGD gradient and control gradient. **B)** Pearsons's Correlation coefficient for DCs cultured on RGD gradient. **C)** Pearsons's Correlation coefficient for DCs cultured on control gradient.

Dendritic cells were cultured on the RGD-gradient chip and MHC-II cell surface expression was quantified by acquiring images using a fluorescent microscope and image analysis. The background corrected fluorescence intensity was plotted against

increasing surface density of the RGD-peptide. It was observed that there is a general trend of increasing cell surface expression of MHC-II with increasing surface density of RGD peptide. Two-way ANOVA revealed a coefficient of determination, R^2 = 0.97 and a p-value < 2.5E-12. Furthermore, DCs cultured on the highest analyzed RGD surface density have ~6 times more MHC-II cell surface expression as compared to the lowest analyzed RGD surface density (**Figure 4-5A**). Dendritic cells were cultured on the control chip and MHC-II cell surface expression was quantified. The background corrected fluorescence intensity was plotted against increasing surface density of the RGD-peptide that corresponds to the same distance from the 0mm in both RGD-gradient chip and control chip. It was observed that the MHC-II expression remains constant throughout the length of the control chip. Dendritic cells cultured on the RGD-gradient chip, at the lowest RGD surface density have 6-25 times more MHC-II expression and at the highest RGD surface density 40-150 times more MHC-II expression of the DCs cultured on the control chip. Two-way ANOVA revealed a coefficient of determination, R^2 = 0.62 and a p-value < 0.02. Dendritic cells were cultured in the presence of LPS and MHC-II cell surface expression was quantified. The background corrected fluorescence intensity was plotted on the same plot as the RGD-gradient chip and control-chip plot as a positive control. It was observed that DCs cultured at the highest concentration of the RGD surface density had MHC-II expression higher than DC expression of MHC-II when cultured in the presence of LPS. The standard error of the MHC-II expression of DCs is shown as dashed line where as the solid line represents the least square mean value (**Figure 4-5A**).

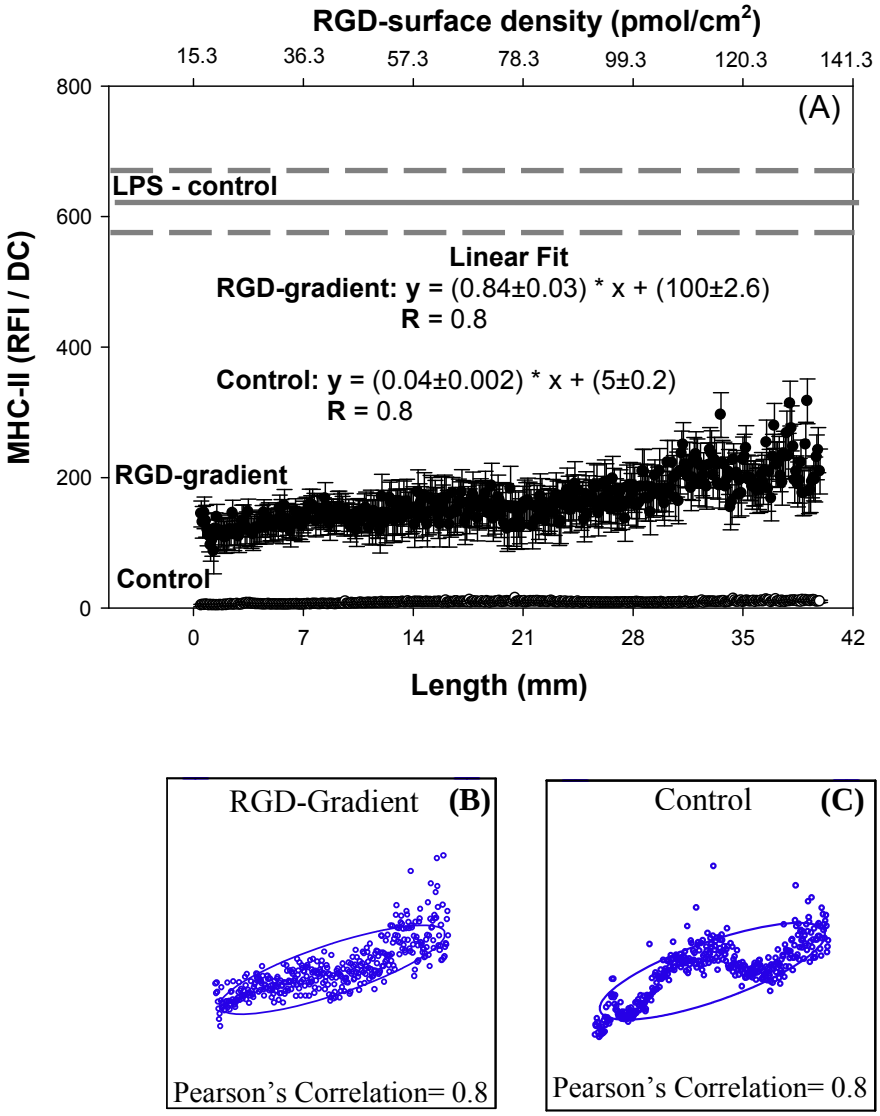

Figure 4-5. Dendritic cells cultured on RGD-gradient chips demonstrate that surface expression of MHC-II stimulatory molecule is proportional to the RGD-gradient. **A)** MHC-II expression by DCs cultured on RGD gradient and control gradient. **B)** Pearsons's Correlation coefficient for DCs cultured on RGD gradient. **C)** Pearsons's Correlation coefficient for DCs cultured on control gradient.

Dendritic cells were cultured on the RGD-gradient chip and IL-10 intracellular cytokine production was quantified by acquiring images using a fluorescent microscope and image analysis. The background corrected fluorescence intensity was plotted against increasing surface density of the RGD-peptide. It was observed that there is a

general trend of constant IL-10 cytokine production with variable surface density of RGD peptide. Two-way ANOVA revealed a coefficient of determination, R^2 = 0.01 and a p-value > 0.99 (**Figure 4-6A**). Dendritic cells were cultured on the control chip and intracellular cytokine IL-10 production was quantified.

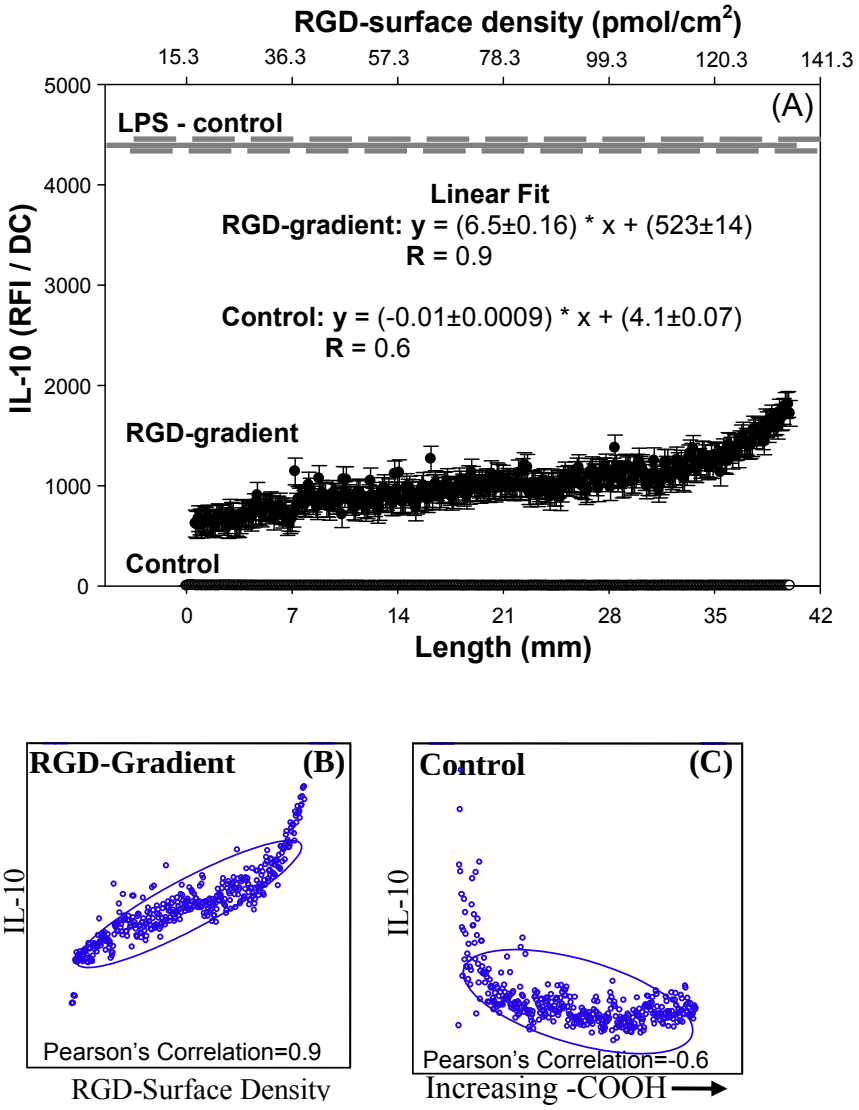

Figure 4-6. Dendritic cells cultured on the RGD-gradient chips and the control chips for 24 h, were stained for the intracellular cytokine IL-10 using immunofluorescence staining and image analysis was performed to quantify the fluorescence intensity at varying RGD surface density present on the chip. **A)** IL-10 expression by DCs cultured on RGD gradient and control gradient.

B) Pearsons's Correlation coefficient for DCs cultured on RGD gradient. **C)** Pearsons's Correlation coefficient for DCs cultured on control gradient.

The background corrected fluorescence intensity was plotted against increasing surface density of the RGD-peptide that corresponds to the same distance from the 0mm in both RGD-gradient chip and control chip. It was observed that the IL-10 expression remains constant throughout the length of the control chip. Two-way ANOVA revealed a coefficient of determination, $R^2 = 0.55$ and a p-value > 0.99. Dendritic cells were cultured in the presence of LPS and IL-10 cell surface expression was quantified. The background corrected fluorescence intensity was plotted on the same plot as the RGD-gradient chip and control-chip plot as a positive control. It was observed that DCs cultured at the highest concentration of the RGD surface density had IL-10 expression lower by 7-9 than DC expression of IL-10 when cultured in the presence of LPS. The standard error of the IL-10 expression of DCs is shown as dashed line where as the solid line represents the least square mean value (**Figure 4-6A**).

Dendritic cells were cultured on the RGD-gradient chip and IL-12p40 intracellular cytokine production was quantified by acquiring images using a fluorescent microscope and image analysis. The background corrected fluorescence intensity was plotted against increasing surface density of the RGD-peptide. It was observed that there is a general trend of increasing of IL-12p40 production with increasing surface density of RGD peptide. Two-way ANOVA revealed a coefficient of determination, $R^2 = 0.76$ and a p-value < 7.25E-12. Furthermore, DCs cultured on the highest analyzed RGD surface density have ~3 times more IL-12p40 cytokine production as compared to the lowest analyzed RGD surface density (**Figure 4-7A**). Dendritic cells were cultured on the

control chip and IL-12p40 cytokine production was quantified. The background corrected fluorescence intensity was plotted against increasing surface density of the RGD-peptide that corresponds to the same distance from the 0mm in both RGD-gradient chip and control chip. It was observed that the IL-12p40 cytokine production remains constant throughout the length of the control chip. Dendritic cells cultured on the RGD-gradient chip, at the lowest RGD surface density have similar IL-12p40 expression and at the highest RGD surface density ~6 times more IL-12p40 cytokine production of the DCs cultured on the control chip. Two-way ANOVA revealed a coefficient of determination, $R^2 = 0.55$ and a p-value < 0.0001.

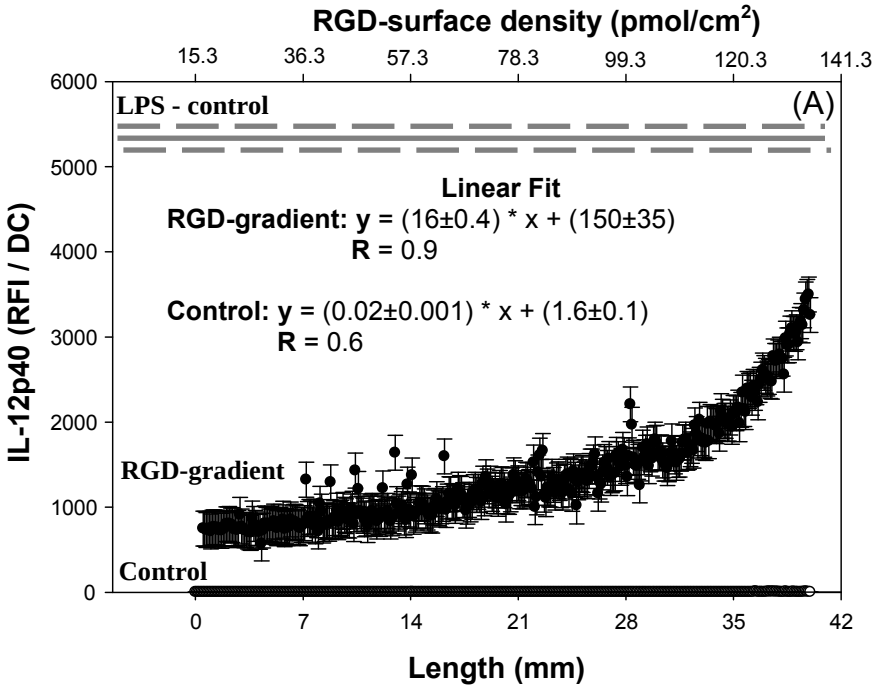

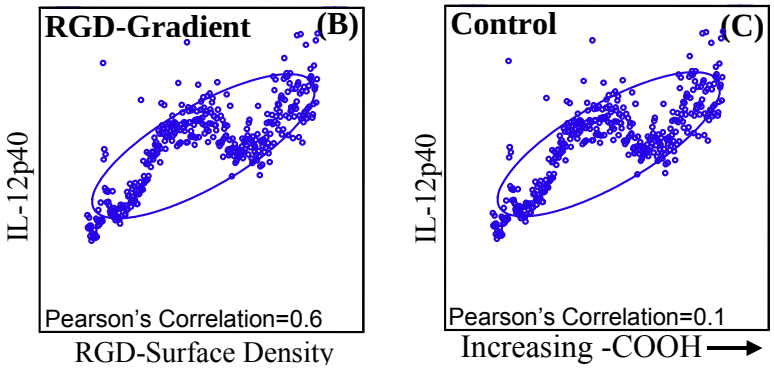

Figure 4-7. Dendritic cells cultured on RGD-gradient chips demonstrate that intracellular pro-inflammatory cytokine IL-12p40 is proportional to the RGD-gradient. **A)** IL-12p40 expression by DCs cultured on RGD gradient and control gradient. **B)** Pearsons's Correlation coefficient for DCs cultured on RGD gradient. **C)** Pearsons's Correlation coefficient for DCs cultured on control gradient.

Dendritic cells were cultured in the presence of LPS and IL-12p40 cell surface expression was quantified. The background corrected fluorescence intensity was plotted on the same plot as the RGD-gradient chip and control-chip plot as a positive control. It was observed that DCs cultured at the highest concentration of the RGD surface density had IL-12p40 expression 3-5 times lower than DC production of IL-12p40 when cultured in the presence of LPS. The standard error of the IL-12p40 production by DCs is shown as dashed line where as the solid line represents the least square mean value (**Figure 4-7A**).

Dendritic cells were cultured on the RGD-gradient chip and surface expression of αV integrin was quantified by acquiring images using a fluorescent microscope and image analysis. The background corrected fluorescence intensity was plotted against increasing surface density of the RGD-peptide. It was observed that the αV integrin expression remains low from 20-50 pmol/cm^2 of RGD-surface density and then the expression increases linearly with the increase in RGD-surface density. Two-way ANOVA revealed a coefficient of determination, $R^2 = 0.78$ and a p-value < 3.6E-12.

Furthermore, DCs cultured on the highest analyzed RGD surface density have ~30 times more αV integrin expression as compared to the lowest analyzed RGD surface density (**Figure 4-8A**). Dendritic cells were cultured on the control chip and surface expression of αV integrin was quantified by acquiring images using a fluorescent microscope and image analysis. The background corrected fluorescence intensity was plotted against increasing surface density of the RGD-peptide that corresponds to the same distance from the 0mm in both RGD-gradient chip and control chip. It was observed that the αV integrin expression remains low throughout the RGD-surface density. Two-way ANOVA revealed a coefficient of determination, R^2 = 0.01 and a p-value > 0.7 (**Figure 4-8A**).

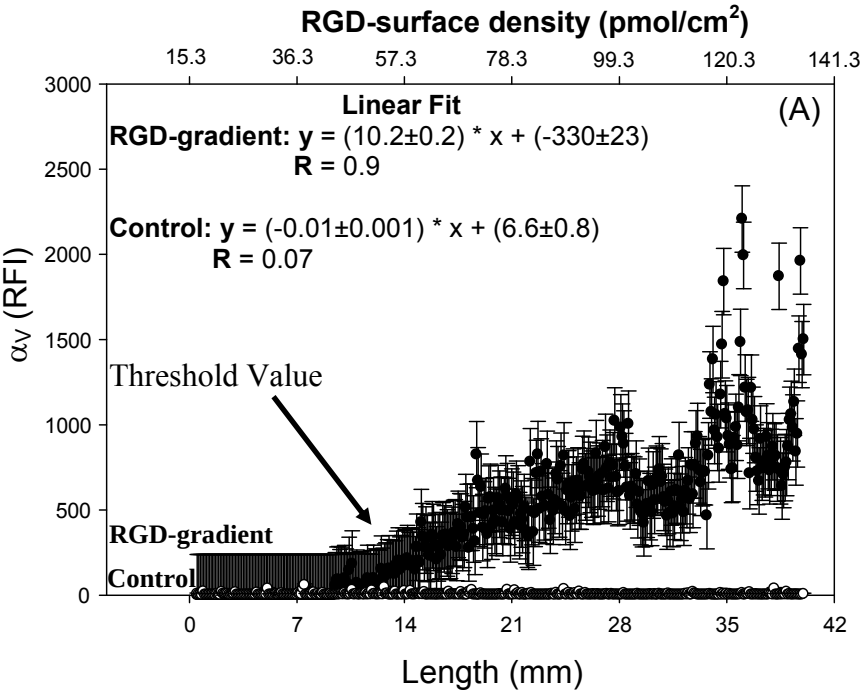

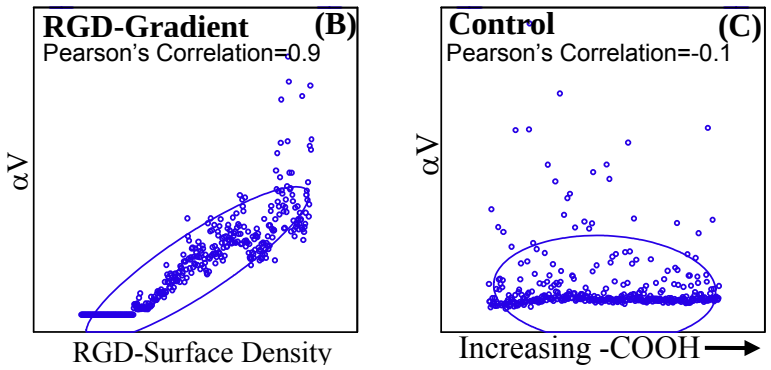

Figure 4-8. Dendritic cells demonstrate increased integrin αV expression with increase in RGD-peptide surface density. **A)** RGD bound αV integrin expression by DCs cultured on RGD gradient and control gradient. Arrow shows the threshold value upon which the RGD bound αV expression is different from the control. **B)** Pearsons's Correlation coefficient for DCs cultured on RGD gradient. **C)** Pearsons's Correlation coefficient for DCs cultured on control gradient.

Impact of the Study

Overall, this study demonstrates that the maturation of DCs based on surface density of a peptide can be predicted and controlled for *in vitro* experiments, thus, enabling us to develop systems where effects of certain immunological active components on matured DCs can be studied in a highly controlled manner. Furthermore, the results obtained through these studies can be directly correlated with the traditional immunological technique of flow cytometry, since, the basic principles behind analyzing the cells were maintained the same. This study lays groundwork to study the effects of other adhesion dependent DC-maturation and effects of immunologically relevant drugs and other immune system modulating components.

Furthermore, we have demonstrated that the DC maturation can be modulated by highly controlled adhesion cues. We have developed a system where the extent of DC maturation can be controlled and quantified by image analysis on per cell basis. We

have shown that the DC surface expression of MHC-II and CD86 is directly proportional to the surface density of RGD-peptide. Interestingly, it was observed that the increasing surface density of RGD-peptide resulted in increasing pro-inflammatory cytokine IL-12p40 production and the anti-inflammatory cytokine IL-10. This suggests that the extent of adhesion cues is an important factor in the maturation pathway of DCs and should be further studied. This work will provide incentives and tools in improving the applications of *ex vivo* culture of DCs and implanted biomaterials from immunological perspective.

CHAPTER 5
A HIGH-THROUGHPUT MICROPARTICLE MICROARRAY PLATFORM FOR DENDRITIC CELL-TARGETING VACCINES

Introduction

Immunogenomic approaches combined with advances in adjuvant immunology are guiding progress toward rational design of vaccines. Furthermore, drug delivery platforms (e.g., synthetic particles) are demonstrating promise for increasing vaccine efficacy. Currently there are scores of known antigenic epitopes and adjuvants, and numerous synthetic delivery systems accessible for formulation of vaccines for various applications. However, the lack of an efficient means to test immune cell responses to the abundant combinations available represents a significant blockade on the development of new vaccines. In order to overcome this barrier, we report fabrication of a new class of microarray consisting of antigen/adjuvant-loadable poly (d,l lactide-co-glycolide) microparticles (PLGA MPs), identified as a promising carrier for immuno-therapeutics, which are co-localized with dendritic cells (DCs), key regulators of the immune system and prime targets for vaccines. The intention is to utilize this high-throughput platform to optimize particle-based vaccines designed to target DCs *in vivo* for immune system-related disorders, such as autoimmune diseases, cancer and infection.

Preparation of PLGA Microparticles

A 50:50 polymer composition of poly(d,l lactide-co-glycolide) (PLGA) with inherent viscosity 0.55-0.75 dL/g in hexafluoroisopropanol, HFIP (Lactel, AL, USA) was used to generate microparticles. Poly-vinyl alcohol (PVA) (MW ~ 100,000 g/mol) was purchased from Fisher Science (Rochester, NY, USA) and was used as an emulsion stabilizer. Phosphate buffered saline (PBS) solution (Hyclone, UT, USA) was used as the aqueous

phase to form the emulsions while methylene chloride (Fisher Scientific, NJ, USA) was used as an organic solvent to dissolve PLGA polymer. Microparticles were formed using a standard water-oil-water solvent evaporation technique.

Briefly, the PLGA polymer was dissolved in methylene chloride at 20% concentration. Rhodamine, a red-fluorescent dye (RHOD) (Sigma-Aldrich), fluorescein isothiocyanate, green fluorescent dye (FITC) (Sigma Aldrich) or 9-anthracenecarboxylic acid, blue fluorescent dye (ACA) (Sigma-Aldrich) solution (100 μL of 5 mg/mL in PBS) was emulsified with 1000 μL of 20% PLGA solution at 26,500 rpm for 60 seconds using a tissue-miser homogenizer (Fisher Scientific, NJ, USA) to form a primary emulsion. The primary emulsion was added to 2 mL of 9% PVA solution in PBS and the homogenizing was continued at 19,500 rpm for 60 seconds to form the secondary emulsion. Then, the secondary emulsion was added to 7 mL of 9% PVA solution. The particles thus formed were agitated using a magnetic stirrer (Fisher Scientific, NJ, USA) for 3 hours to evaporate residual methylene chloride. The remaining solution was centrifuged at 10,000 x g for 10 minutes to collect MPs which were subsequently washed three times with PBS. The PBS was aspirated from the centrifuged MPs, which were then flash-frozen in liquid nitrogen and kept under vacuum in dry ice overnight. The MPs were stored at -20^{0}C until used. Bovine serum albumin (BSA) (Fisher Bioreagents) was used as a representative protein to quantify encapsulation efficiency. Bovine serum albumin was encapsulated in MPs via solvent evaporation technique by incorporating 1mg BSA in the aqueous phase of the primary emulsion.

Characterization of Microparticles

Particle Size Measurements

Particle size was characterized by dynamic light scattering technique using a Nanotrac (Microtrac Inc.) particle size analyzer. A total of 35 mg of particles were re-suspended in 50 mL of de-ionized (DI) water via sonication in a sonicating bath for 2 minutes (Branson 2510, Paragon Electronics, FL).. The laser probe was dipped in the particle suspension and the laser scattering data was collected for 3 minutes.

Scanning Electron Microscopy

Microparticle morphology was characterized by scanning electron microscope (FEG-SEM JEOL JSM – 6335F, Major Analytical Instrumentation Center, University of Florida). A particle suspension in DI water was used to print particles and dried for 16 hours at room temperature. Dried particles were then coated with 5-10 nm thickness of gold and imaged at magnifications ranging from 30x to 60,000x.

Efficiency of Protein Encapsulation

A known weight of MPs loaded with BSA was dissolved in methylene chloride. An equal amount of PBS was added to the solution and sonicated for 5 minutes. The emulsion thus obtained was then centrifuged at 10,000 x g for 10 minutes to separate the two phases. Phosphate buffered saline, containing the water-soluble BSA, was then very carefully pipetted out and saved. Equal amount of PBS was replaced in the solution and centrifuged. This process was repeated 4 times and the PBS pooled for analysis. The concentration of BSA protein in the solution was then quantified by measuring the absorbance at a wavelength of 280 nm by spectrophotometer (Nanodrop Technologies Inc., DE, USA) and comparing absorbance to a standard curve made from known concentration of BSA in PBS.

Degradation of Microparticles

The blue fluorescent dye, ACA incorporated MPs were printed into a flat bottom tissue culture treated 96-well plate (Corning Inc., NJ, USA), in an array format of 1 spot per well. Phosphate buffered saline, 1N HCl and 1M NaOH were used to make solutions of pH 4.0, 5.0, and 7.4 and 13.1 using glass pH electrode (Fisher Scientific). Microparticle arrays were incubated with these three solutions and fluorescent micrographs were taken at different times to identify the loss of fluorescence. The experimental conditions were set to minimize any photo-bleaching effect, by keeping the samples mounted on the microscope in a dark room. Intensity of the signal (here, ACA-loaded MPs) was corrected from the background fluorescence intensity by using the formula for corrected intensity: *(Signal – Background) ÷ (Background)*. The background-corrected fluorescence intensity measured at each time-point was divided by the background-corrected fluorescence intensity measured at time t = 0, and the multiplied by 100 to be expressed as a percentage. The ratio of fluorescence intensity was plotted against time and the data was fitted to the curve using Dynamic Fit Wizard – SigmaPlot.

Particle Array Fabrication

Glass coverslips (22 x 22 mm^2, Fisher scientific) were cleaned in an oxygen plasma etcher (Terra Universal, CA, USA) for 6 minutes. An array of (3-Aminopropyl) trimethoxysilane (NH_2-terminated silane) (Sigma-Aldrich) as obtained from the manufacturer was diluted in DI water. The silane solution was printed on clean coverslips using a Calligrapher Miniarrayer (BioRad) contact printer, with 400 μm diameter solid metal pin. The printed coverslips were then coated with 150 Å of titanium (Ti-99.995% pure) followed by 150 Å of gold (Au-99.999% pure) (Williams Advanced

Materials, IL, USA). Gold coated coverslips were then sonicated in 70% ethanol in DI water for 15 minutes to remove gold coating from over the printed islands exposing NH_2-terminated silane arrayed spots, while leaving the gold coating intact around the islands for further processing (**Figure 5-1A**). The coverslip was then washed with DI water without letting it dry, to ensure the lifted gold was removed. The coverslips were dried by blowing nitrogen gas on the coverslip. The coverslips were then incubated with 0.01 M, methyl-terminated alkanethiol ($CH_3(CH_2)_{11}SH$, Sigma-Aldrich) for 1 hour followed by washing with 200 proof ethyl alcohol (Fisher Scientific). Substrates were then incubated in 10% pluronic F-127 (BASF Corporation, USA) in DI water, for 4 hours to render the surface around the islands cell-resistant. The coverslip was washed with DI water and re-suspended MPs of PLGA in PBS were over-printed on the exposed islands (**Figure 5-1B**). Microparticles were printed using a pin of 100, 200 or 400 □m diameter. The MPs on the islands were allowed to dry completely by incubating them at room temperature under vacuum for 30 min. The coverslip was then rinsed with DI water. Micrographs were obtained using MosaiX module of Axiovision software (CarlZeiss). The fluorescently-labeled MPs were counted using the 'Automatic Object Measurement Program', Axiovision software. To design a printed array of a dilution of number of single fluorescent dye encapsulated MPs, we re-suspended the desired MPs in 1 mL of DI-water via combination of vortex mixing and sonication. The MP-concentration was verified by taking micrographs of fluorescent-MPs on a hemocytometer and utilizing Automatic object Measurement Program, Axiovision software. A serial 1:2 dilution of MPs in 20 μL DI-water was generated, with a starting concentration of 3.26×10^6/mL.

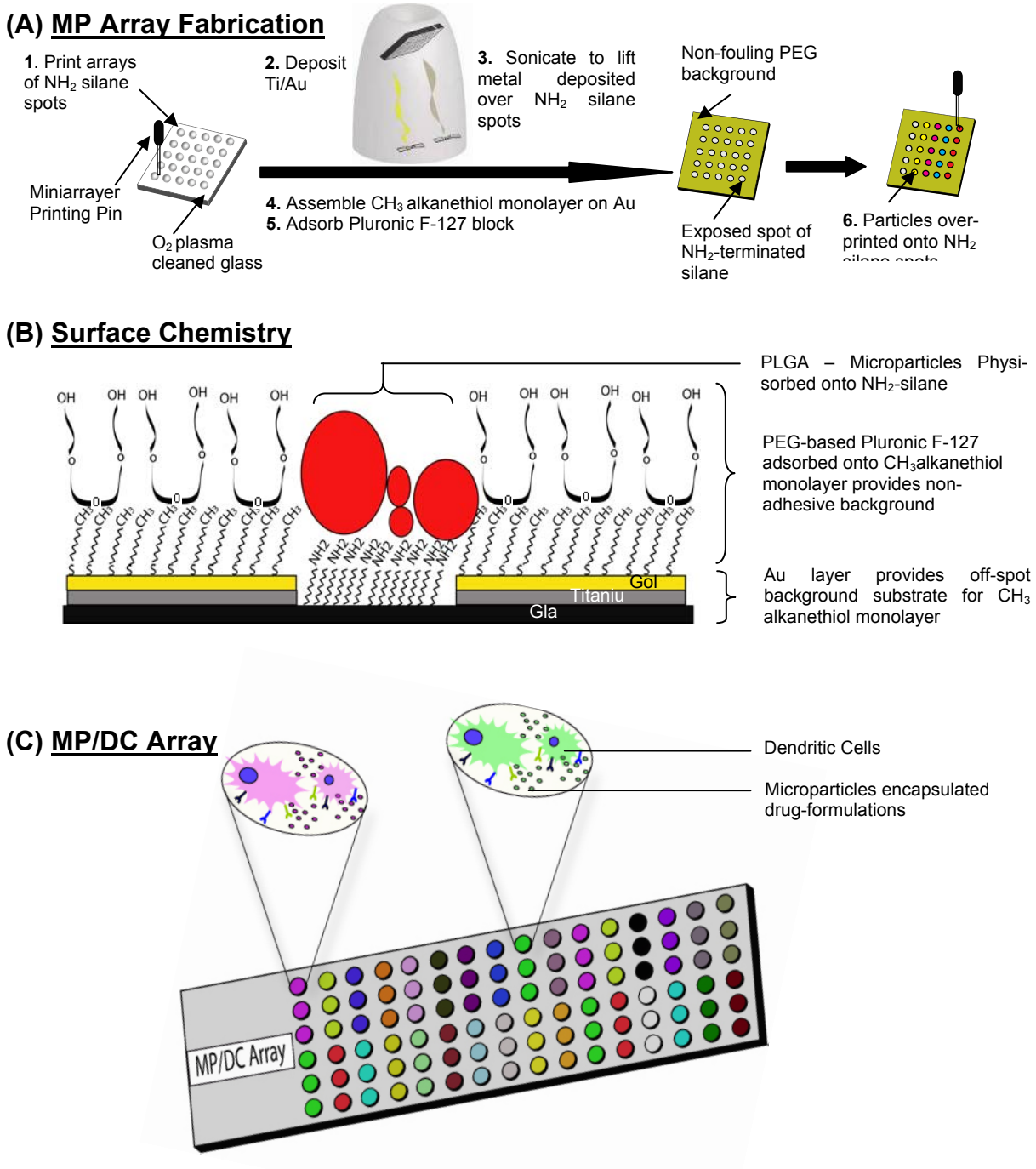

Figure 5-1. Microparticle/dendritic cell (MP/DC) array fabrication incorporates miniarraying solid pin contact printing equipment, silane and alkanethiol surface chemistry, and physisorption of MPs to provide MP/DC co-localization on isolated spots. ***A.)*** Surface-engineering MP array. ***B.)*** Cross-section of a

single spot in a MP-array illustrating physisorbed MPs on NH_2-terminated spots with a polyethylene glycol-based non-adhesive background surface chemistry (not to scale). ***C.)*** Dendritic cells are seeded on MP arrays, selectively adherent to NH_2-terminated spots providing co-localized DCs/MPs arrays.

These suspensions were added into separate wells in a 384-well plate which was used as the source plate to over-spot MPs onto the arrayed NH_2-terminated substrate. Fluorescence micrographs of the entire array were obtained and the number of MPs on each island counted using Axiovision software.

In order to generate orthogonally-overlapping dilution arrays of MPs encapsulated with different fluorescent dyes, ACA-loaded or RHOD-loaded MPs were re-suspended in DI-water separately and their individual MP-concentrations determined. Sixteen different combinatorial mixtures of RHOD-loaded and ACA-loaded MPs were generated in a 384-well source-plate using 3 different dilutions of each type of MP (final volume – 40 □L, final concentrations – RHOD: 4.5 x 10^6/mL, 8.8 x 10^6/mL and 19.7 x 10^6/mL; ACA: 4.0 x 10^6/mL, 7.9 x 10^6/mL and 15.8 x 10^6/mL). These mixed MP solutions were then over-printed onto NH_2-terminated islands. In order to minimize cross-contamination of samples, the pin was washed 3 times in a solution of 0.05 % Triton X-100 surfactant followed by washing in water and then drying under vacuum before printing each MP-spot. Fluorescence micrographs were obtained using a 10x objective for both Rhodamine and DAPI filters and AxioVision MosaiX software was utilized to align and compile individual micrographs. The number of RHOD-loaded and ACA-loaded MPs on each spot was quantified by using the AxioVision Automatic Measurement Program. A MATLAB routine was compiled to quantitatively display the resulting mean and standard deviation of 4 replicate arrays for each spot in the 4 x 4 arrays.

Dendritic Cell Culture and Staining

Dendritic cells were isolated from bone marrow of 7 week old C57Bl6/j mice using a 10 day protocol. Briefly, bone marrow was isolated from femur and tibia of the mouse. Red blood cells were removed lysed by ACK lysing buffer (Whittaker) and the isolated precursor cells were incubated with DC-media consisting of 20 ng/mL of GM-CSF (R&D Systems), DMEM/F12 (1:1) with L-glutamine (Cellgro, Herndon, VA) and 10% fetal bovine serum (Bio-Whittaker), 1% sodium pyruvate (Lonza, Walkersville, MD) and 1% non-essential amino acid (Lonza, Walkersville, MD) for 2 days in a flask. The floating cells were collected from the flask at the end of two days and re-seeded with fresh DC-media in a 6-well low-attachment plate (Corning Inc., NY) for 6 days. After 6 days of culture the cells were re-suspended in fresh media and seeded onto tissue-culture treated 6 well plates (Corning, Inc, NY) for 2 days. After 10 day of culture DCs were lifted using 5mM solution of Na_2EDTA (Fisher Scientific) in PBS. Dendritic cells thus isolated were then tested for immaturity (MHC-II^+ < 6% and $CD86^+$ < 6%), purity (using flow cytometery: $CD11c^+$ > 90%) and viability (Trypan blue staining).

A dried MP-arrayed coverslip was rinsed with PBS and re-hydrated for 30 minutes with PBS-mix containing 0.05 g/L of magnesium chloride and 0.05 g/L of calcium chloride made by mixing equal parts of PBS with magnesium and calcium and PBS without magnesium and calcium ($PBS_{50\text{-}50}$), before seeding immature DCs. Dendritic cells were seeded in a serum-free media in $PBS_{50\text{-}50}$ for 15 minutes at 37 ^{0}C. Dendritic cells were then rinsed with PBS having calcium and magnesium to wash-off non-adherent cells. Fresh DC-media was added onto the coverslip and adherent DCs were cultured for 24 hours. Dendritic cells were fixed with, 3.7% paraformaldehyde (USB Corporation, USA) for 10 minutes and then washing with PBS to remove excess fixing

agent. The nuclei of DCs were then stained with 10 mg/mL Hoechst (Invitrogen, USA) diluted to 1:10,000 times as per the manufacturer's protocol. Fluorescence and phase-contrast micrographs of adherent cells on the islands were obtained using a 10x objective and compiled using MosaiX module of Axiovision software used for stitching the acquired images. A schematic of cells cultured on the arrays is described (**Figure 5-1C**).

Statistical Analysis

Statistical analyses were performed using either a one-way ANOVA or a two-way ANOVA, using Systat (Version 12, Systat Software, Inc., San Jose, CA). Pair-wise comparisons were made using Tukey's Honestly-Significant-Difference, with p-values of less than or equal to 0.05 considered to be significant.

Results

Array Fabrication and Microparticle Characterization

The aim of constructing particle arrays was to develop an enabling platform to test and optimize MPs with multi-parameter combinatorial formulations for immunotherapies in a high-throughput format. Using a standard solid-pin miniarray contact printer, we fabricated arrays of NH_2-terminated spots with a polyethylene glycol-based non-adhesive background (**Figure 5-1**). Miniarraying NH_2-terminated silane onto clean glass allows the silane molecules to covalently bond to the glass while the drying step leaves a film spot of excess non-ligated silane. These spotted films were measured to be ~13 μm thick and ~400 μm in diameter on the surface of the glass, and prevent formation of a continuous metal coating layer during the Ti/Au deposition step. We took advantage of this surface non-uniformity and removed the Ti/Au layer deposited onto silane spots by sonication in ethanol, leaving behind the covalently-bound NH_2-terminated silane islands

surrounded by Au background. This background Au surface was then made hydrophobic by the assembly of a monolayer of CH_3-terminated alkanethiol, in preparation for the adsorption of Pluronic F-127. Pluronic F-127 is a tri-block copolymer whose central hydrophobic block facilitates adsorption to hydrophobic surfaces, while flanking blocks of polyethylene glycol provide resistance to cell adhesion. Note that altering the NH_2-terminated silane spot area may be desirable for specific applications and can be accomplished as required by using different pin diameters.

While unmodified PLGA MPs were used in the present study, this approach is generalizable to investigate other particles either of synthetic or natural origin, including viruses. Standard water-oil-water solvent evaporation technique was used to generate PLGA MPs and MP properties of particle size, surface morphology and degradation rate were investigated. Microparticle size distribution was characterized using dynamic light scattering analysis, and the average particle diameter was found to be 1.08 μm, with diameters ranging from 600 nm to 2 μm (**Figure 5-2**).

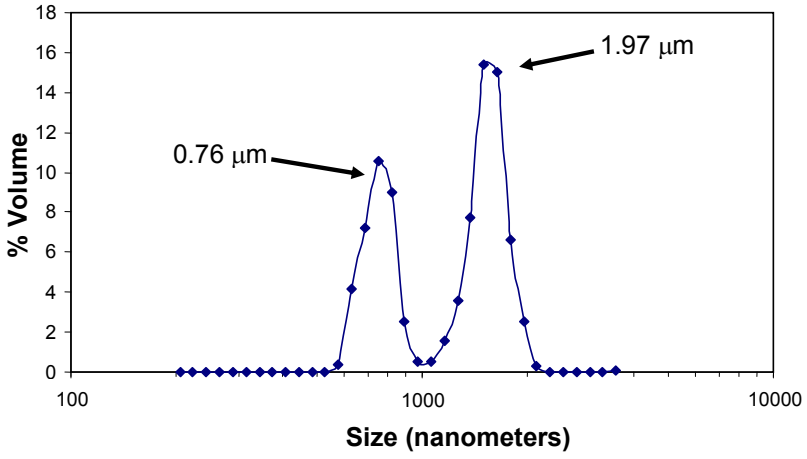

Figure 5-2. A typical size distribution curve of PLGA-microparticles quantified via dynamic light scattering analysis (based on volume estimation) demonstrates an average size of particles of 1.08 μm. A bimodal poly-dispersity in the particle size is observed; with the smaller population-set has an average

diameter of 0.76 μm, whereas the larger size population-set has 1.97 μm average diameter.

A bimodal poly-dispersity in particle size was observed, with the smaller-sized population having an average size of 0.76 μm, and the larger-sized population had an average diameter of 1.97 μm. While particle size is expected to affect cellular interactions, for the purpose of array validation, MPs were used as made without a filtering step to further restrict particle size.

Next, we investigated pH-dependent particle degradation. This is of interest because acidic degradation reflects a major mechanism by which particles can be physiologically degraded. Phagocytic cells take up particles into phagosomes which fuse with lysosomes, forming phagolysosomes where an acidic ~5 is maintained to promote degradation. Particle degradation was monitored under different pH conditions by quantifying the fluorescence of printed ACA-encapsulated MPs over a period of 12 hours. The mean and standard error of at least 5 data points are plotted (**Figure 5-3**). The acquired data was fitted to a three-parameter exponential decay equation of the form: $y = y_0 + A*e^{-B*t}$, with coefficient of determination of $R^2 > 0.94$ for all conditions over the time-frame examined. The variable t represents the time at which fluorescence intensities were quantified. The variable y represents the background-corrected fluorescence intensity measured at time t, divided by the background-corrected fluorescence intensity measured at time t = 0, multiplied by 100 to be expressed as a percentage. The parameter y_0 represents the saturation value, while the parameter A represents the difference between initial and saturation values, and the parameter B represents the decay constant. From 0–2 h, all conditions examined demonstrated similar burst-release degradation. After 2 h, pH-dependent degradation was apparent.

Specifically, at 12 h, MPs incubated at pH 7.4 (representing average physiological pH) demonstrated a degradation of 10%, whereas MPs incubated at pH 4.0 and pH 5.0 demonstrated a degradation of ~20%. Additionally, at pH 13.1 PLGA-MPs degraded completely within 5 minutes (data not shown). The degradation properties of the PLGA-MPs revealed that degradation in the acidic pH 5.0 (phagolysosomal pH ~5) is accelerated as compared to physiological extracellular pH 7.4, suggesting that DCs can degrade the MPs in the phagolysosomes and analyze MP-encapsulated immuno-modulatory molecules effectively.

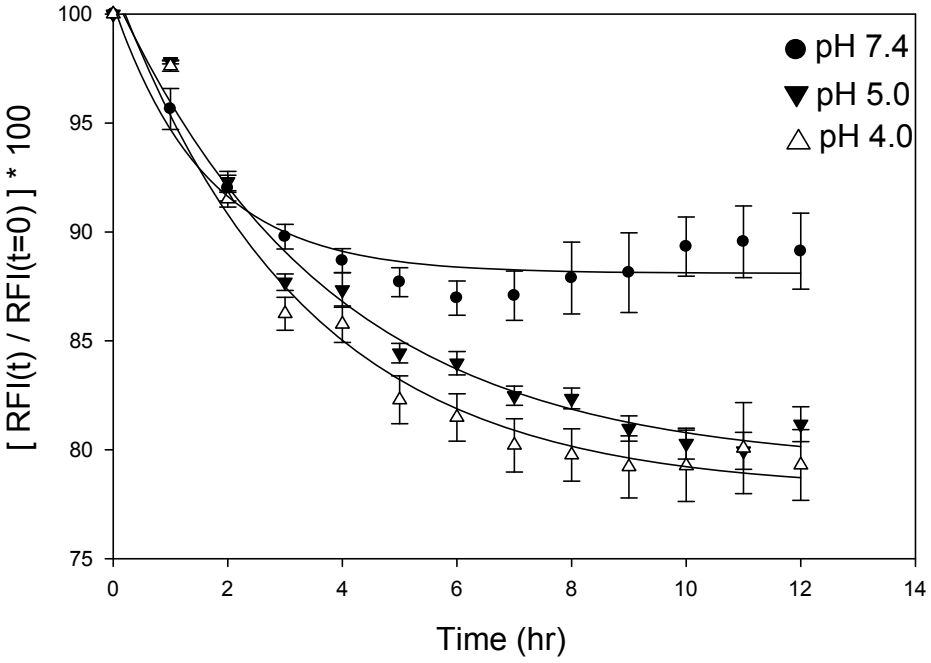

Figure 5-3. Surface-adsorbed PLGA-microparticles degrade in a pH-dependent fashion and are quantified in situ by image analysis.

Fabricated MPs were over-printed onto NH_2-terminated spots via solid-pin miniarray contact printing. Microparticle spot sizes were varied in order to present optimal co-localization with cells while providing for alignment error that can occur during over-printing. Microparticles were over-printed with different pin diameter sizes of

100, 200 and 400 □m to provide different MP spot sizes and examined by scanning electron microscope (SEM), (**Figure 5-4A)**.

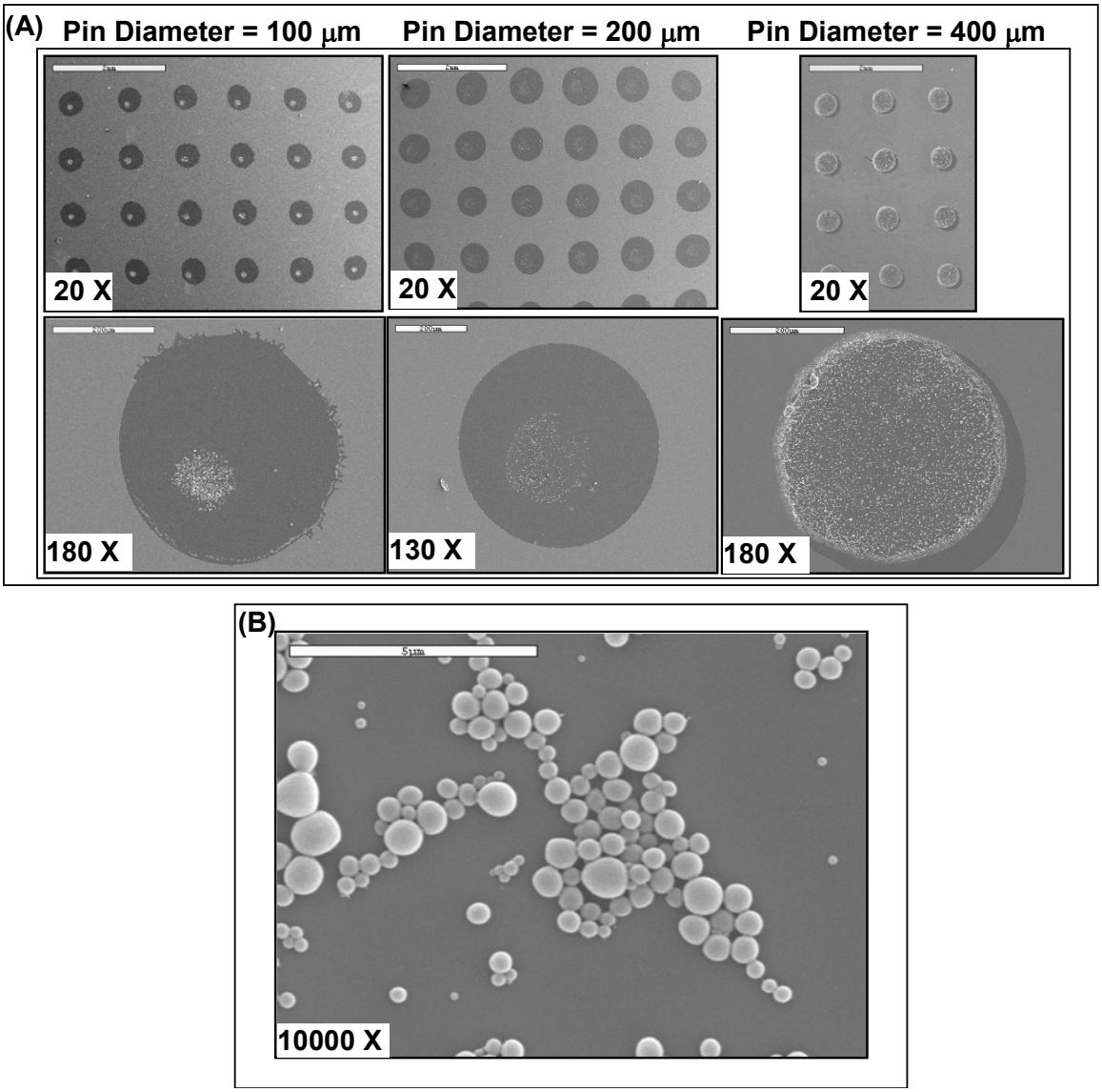

Figure 5-4. Scanning electron micrographs demonstrate constructed arrays of surface-adsorbed PLGA MPs (microparticles) on NH_2-terminated silane spots (visible as circular regions devoid of metal deposition). ***A.)*** Overspotting pin diameter is optimized for aligned delivery of MPs. ***B.)*** Representative micrograph of MPs printed on the adhesive-islands indicating MP smooth surface morphology and spherical shape (scale bar = 5 μm).

We determined that the 200 μm diameter pin provided the largest MP spot diameter that simultaneously prevented over-lapping of MPs onto the surrounding gold resulting from pin-alignment error. Generating arrays of up to 12 x 12, a maximum alignment displacement of ~20 μm was determined, while over-printing across a distance of 12 mm. Over-spot alignment error was observed to be random, without systematic misalignment, which allows construction of large high-fidelity arrays. Scanning electron microscope micrographs of MP arrays revealed that MPs were spherical in shape and had a smooth surface morphology, suggesting the array fabrication process did not adversely affect the particle morphology (**Figure 5-4B**). Furthermore, MPs were well-distributed throughout the printed spots and the Au deposited onto spots was completely removed, leaving no trace of gold flakes.

Lastly, in order to validate the PLGA MPs as a carrier vehicle, the loading of water-soluble protein, bovine serum albumin (BSA) was quantified. Bovine serum albumin was incorporated in the water phase of the primary emulsion of the solvent extraction/evaporation process. Bovine serum albumin was recovered by solvent extraction from dry PLGA-MPs and quantified by absorbance spectrophotometry. Given the initial BSA loading amount of 1 mg, an encapsulation efficiency of 62% was obtained, providing 0.2 mg of BSA per mg of PLGA polymer. These loading amounts are in good agreement with literature.

Particle Array Validation

Next, we were interested in determining the sensitivity of the delivery of MPs to the MP suspension concentration in the source plate. The number of fluorescent dye-loaded MPs arrayed onto NH_2-terminated spots was quantified by fluorescence

microscopic image analysis, and the relationship between the numbers of printed particles to the particle concentration in the source-plate was determined. To achieve this, different concentrations of RHOD-encapsulated MP suspensions were prepared by 1:2 serial dilutions using an MP starting concentration of 3.3 x 10^6/mL, and printed onto NH_2-terminated silane spots. The numbers of MPs printed onto islands from the three highest source plate concentrations were distinct from each other, as well as distinct from all other conditions. A maximum standard deviation of ± 6 MPs delivered was determined, with the highest MP source plate concentration demonstrating the lowest standard deviation of ± 1 MP. While the delivery error in the system did not allow printing MPs in distinct quantities using a source plate concentration below 0.41 x 10^6/mL, the number of printed MPs on the islands revealed a linear relationship ($y = 21.3x - 0.1$, $R^2 = 0.99$) to the concentration of the MP suspension in the source plate over the entire dilution range (**Figure 5-5 - ** - with all other conditions; † - with 3.3 x 10^6/mL, 1.6 x 10^6/mL & 0.8 x 10^6/mL**). Notably, these data demonstrate the ability to reproducibly deliver a lower limit of 7 ± 2 MPs per spot.

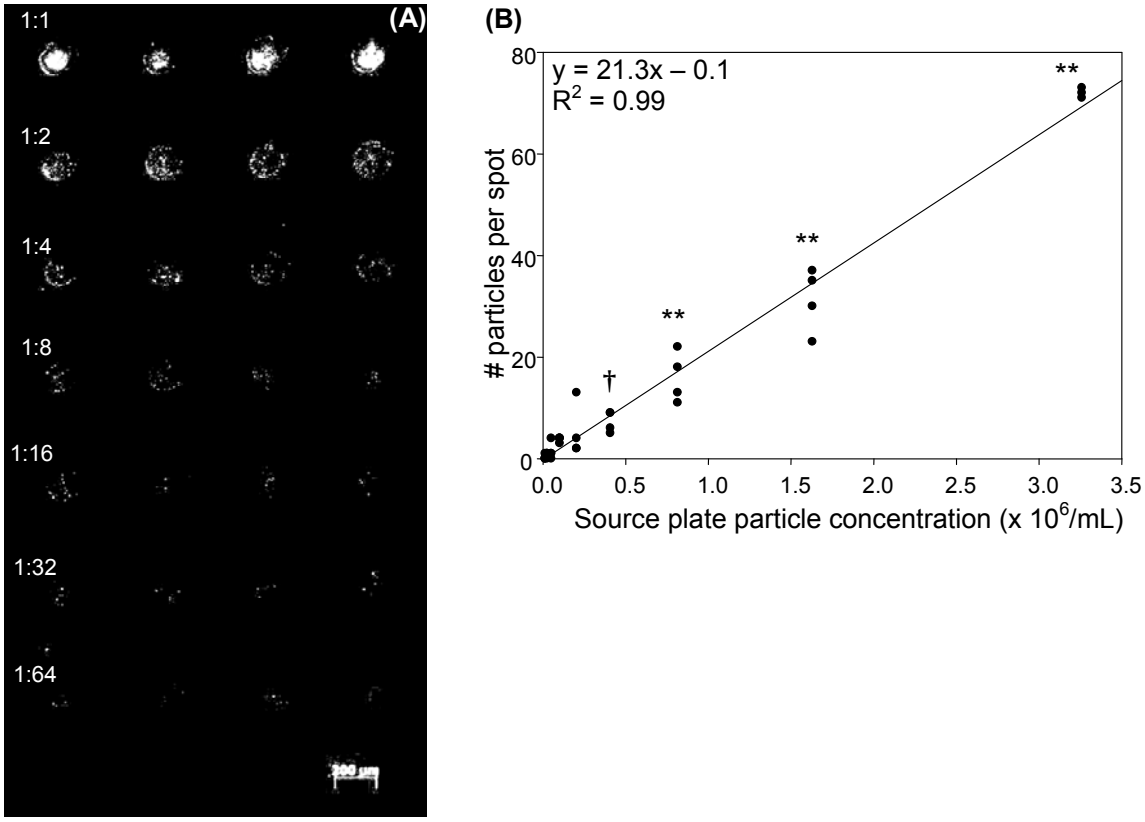

Figure 5-5. Delivery of microparticles (MPs) by solid pin microarray printing is controlled by source plate particle suspension concentration to deliver a lower limit of 16 ± 2 surface-adsorbed MPs per spot. **A.)** Representative fluorescence micrograph of serial 1:2 dilutions of rhodamine dye-loaded PLGA MPs printed in quadruplet in a 4 x 8 array format is shown (for 4 separate preparations; scale bar = 200 μm.). **B.)** Surface-adsorbed MP numbers are quantified by image analysis, average delivered MP values with standard deviations are plotted as a function of source plate concentration, and linear fit parameters are shown. The significant pair symbols are described in the text.

In order to demonstrate the utility of this system to quantitatively investigate multi-parameter MP combinations, we constructed a dosing array consisting of orthogonally-overlapping dilutions of RHOD-loaded and ACA-loaded MPs. The source plate contained 16 different MP mixtures comprising all possible combinations of 3 serial dilutions of RHOD-loaded MPs and 3 serial dilutions of ACA-loaded MPs. These combinatorial mixtures were then printed in 4 x 4 arrays, in the following configuration, where 0 represents the null dose (no MPs) and increasing integers represent increasing

MP concentration (1 – minimum, 3 – maximum), and (x,y) pairs represent (ACA, RHOD) MP loading conditions.

$$\begin{Bmatrix} 0,0 & 0,1 & 0,2 & 0,3 \\ 1,0 & 1,1 & 1,2 & 1,3 \\ 2,0 & 2,1 & 2,2 & 2,3 \\ 3,0 & 3,1 & 3,2 & 3,3 \end{Bmatrix}$$

Fluorescence micrographs were compiled of the printed arrays (**Figure 5-6**). The number of RHOD-loaded and ACA-loaded MPs on each spot was quantified, and a MATLAB routine was compiled to quantitatively display the resulting mean and standard deviation on a per spot basis from 4 replicate arrays (**Figure 5-7A, Figure 5-7B**). Additionally, the number of RHOD-loaded and ACA-loaded MPs printed on spots was plotted against the concentration of MPs in the source plate (**Figure 5-7C**). The data was then fit by linear regression and the resultant slopes for each MP formulation were compared. Potential formulation-specific differences in these slopes would reflect differences in MP delivery. For example, it is possible that differential loading of organic phase-soluble molecules (i.e., fluorescent dyes) could modulate MP surface properties, thereby affecting delivery. This is an important consideration, because our goal is to

provide precise, reproducible MP delivery, independent of formulation.

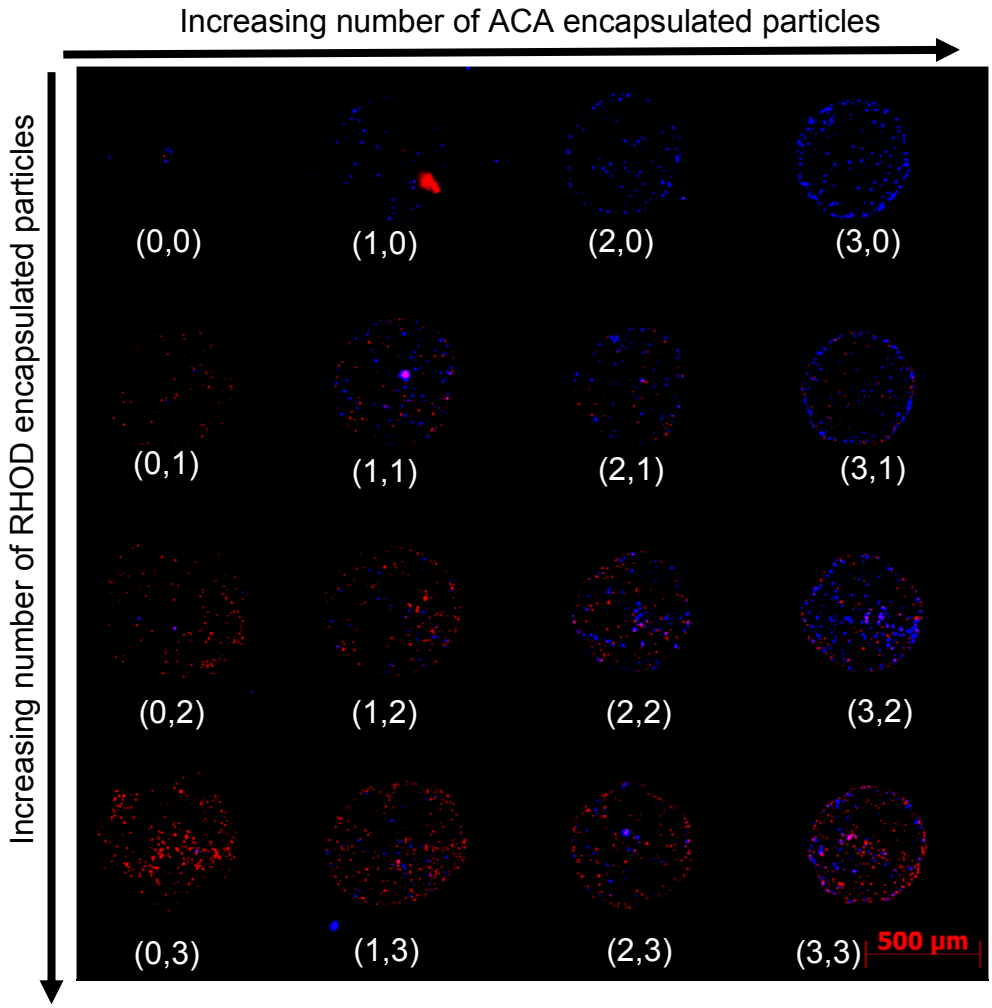

Figure 5-6. Fluorescence micrograph of different microparticle (MP) formulations quantitatively printed using solid pin contact printing in different MP-dose combinations with minimal cross-contamination.

Linear regression analysis of the raw data from 4 replicate arrays revealed average slopes of 18 ± 0.9 and 16 ± 0.9, for RHOD-loaded and ACA-loaded MPs, respectively. Statistical analysis via Student's t-test determined that these slope-data sets are statistically indistinct from each other (p-value > 0.14). This indicates that quantitative delivery of these organic phase-loaded MP formulations was achieved, independent of formulation. For PLGA MPs, it is important to note that unlike organic

phase-soluble molecules, water-soluble molecules are dispersed in submicron-sized water droplets throughout the MP polymer matrix, and would therefore be expected to alter MP surface properties to a lesser extent than oil-soluble molecules. These findings suggest broad applicability of this approach toward the investigation of a wide range of MP loading conditions.

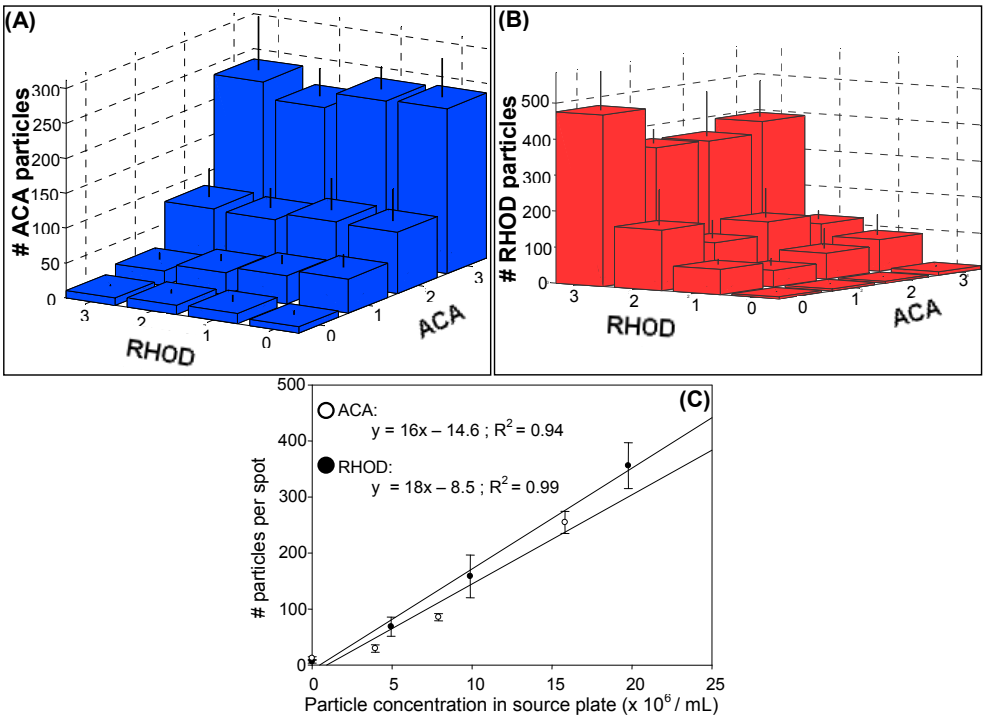

Figure 5-7. Particles encapsulating rhodamine (RHOD, red) and 9–anthracenecarboxylic acid (ACA, blue) are printed and surface-adsorbed microparticle (MP) numbers are quantified by fluorescence image analysis on a spot-by-spot basis. Data from 4 separate array preparations were pooled and average and standard deviations for each arrayed spot are presented in 3-D bar plots. Values on x- and y-axes represent the RHOD or ACA source plate MP concentration while z-axis values represent the number of surface-adsorbed MPs of either ACA (***A.***) or RHOD (***B.***). ***C.)*** Average delivered MP values with standard deviations are plotted as a function of source plate concentration, and linear fit parameters are shown.

In order to reduce cross-contamination between samples, pin-washing steps incorporating detergent/de-ionized water/drying were included before each printing step. While cross-contamination was not completely eliminated, minimal cross-contamination

of printed MPs was observed (9 ± 5 incorrectly-delivered MPs per spot, as judged by delivery to “no MP” spots, or < 3% of the highest delivered). Overall, these data demonstrate the ability to construct arrays of multi-parameter combinations of MP formulations with high precision and to quantitatively analyze delivery in situ by image analysis.

Dendritic Cell Array Fabrication

Due to our interest in DC-targeting MP-vaccines, we next fabricated co-localized MP/DC arrays by seeding DCs onto prepared MP arrays. Our intention was to construct arrays providing isolated DC populations, co-localized with physisorbed MPs of various formulations, while preventing mixing of cell populations by constraining migration via a non-adherent polyethylene glycol-based background. Toward this effort, different non-adhesive backgrounds and cell-seeding conditions were investigated. Leukocytes are well-known for their ability to adhere to numerous “non-adhesive” substrates which are capable of blocking adhesion of other cell types. For example, albumin-coated substrates have recently been shown to support DC adhesion, with an equivalent number of adherent DCs compared to adhesive proteins fibronectin, laminin, vitronectin, fibrinogen and collagen. In this work, we found that polyethylene glycol (PEG) – based Pluronic F-127 adsorbed onto a CH_3-terminated surface provided an improved and prolonged non-fouling effect compared to a self-assembled monolayer of PEG-alkanethiol ($HSC_{11}EG_3OH$) on Au. Additionally, Pluronic F-127 had the added advantage of maintaining its non-fouling properties after drying and re-hydration, as opposed to PEG-alkanethiol which did not remain non-fouling after drying and re-hydration. Furthermore, to ensure MP-stability it is imperative that printed MPs are not exposed to non-aqueous solvents such as ethanol (which is required for PEG-

alkanethiol monolayer assembly). Hence, Pluronic F-127 was determined to be clearly better-suited for this application, and was therefore utilized as the non-adhesive background.

Initial efforts to constrain DC seeding to adhesive islands focused on the use of serum-free seeding conditions. However, even after multiple washing steps, a moderate number of DCs was found to remain adherent to off-spot areas when DCs were seeded in PBS. We therefore investigated a reduction in the concentration of Ca^{++} and Mg^{++} ions in the cell seeding buffer. These divalent ions are a functional requirement for a number of cell surface receptors, including integrins. We found that reducing the Ca^{++} and Mg^{++} ion concentration by half (final concentration of 0.025 g/L for each ion) enabled efficient removal of cells from off-spot areas (which largely remained rounded), providing a favorable differential in DC adhesion between adherent and non-adherent areas. This differential adhesion was visualized by nuclear staining of fixed DCs cultured on MP-arrays for 24 h (**Figure 5-8A)**. A high density of adherent DCs (nuclei shown in blue) was preferentially located on isolated islands, co-localized with RHOD-loaded MPs (shown in red), while DCs were absent on off-spot areas. Furthermore, phase-contrast micrographs of live cells confirmed that DCs preferentially adhered and spread onto the cell-adhesive spots while adhering minimally onto the background (**Figure 5-8B**). Because soluble polyethylene glycol is known to be able to drive cellular fusion (albeit in high concentrations), cultures were inspected for multinucleated cells. Notably, no cell fusion was observed. Taken together, these data demonstrate the feasibility of constructing co-localized MP/DC arrays that can be utilized for the analysis of MP-mediated modulation of DC response.

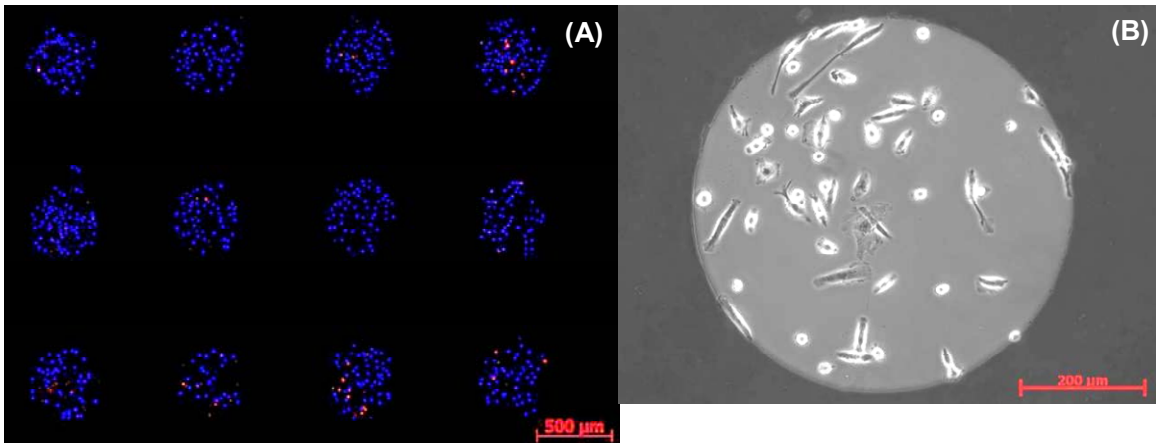

Figure 5-8. Dendritic cell (DC) adhesion is restricted to adhesive islands, and DCs are co-localized with printed microparticles (MPs) on isolated islands against a non-fouling PEG-based background. Inter-island DC migration is absent for up to at least 24 h. ***A.)*** Dendritic cells were seeded onto arrays of printed rhodamine-encapsulated MPs. Fluorescence micrograph overlay of nuclear staining, shown in blue, and MPs, shown in red, is shown (scale bar = 500 μm). ***B.)*** Representative phase-contrast micrograph of DCs cultured 24 hr on a 12 x 12 array, demonstrating that DCs are restricted to adhesive islands and are adherent and moderately spread on adhesive islands.

Impact of the Study

We report a new category of microarrays – co-localized MP/cell arrays. This method takes advantage of standard miniarraying equipment to array spots of adhesive islands against a non-adhesive background to provide co-localization of adherent cells and an adsorbed depot of MPs of desired formulations. This represents a versatile platform that can be used to probe the effects of different MP loading/modification formulations on any adherent cell type. Our overall goal was to develop a new platform enabling the screening of MP-based vaccine formulations to optimize DC response toward promoting desired immune responses. The DC, identified as the most efficient antigen presenting cell, plays a central role in immune regulation, and is therefore an ideal vaccine delivery target. The co-localization of MPs with isolated populations of DCs against a non-adhesive background in this microarray platform will permit the high-

throughput analysis of DC responses to synthetic immuno-modulating MPs targeting DCs. In this work, we have demonstrated the quantitative, reproducible printing of surface-adsorbed MPs of different formulations with minimal cross-contamination. This control over the number of printed MPs and seeded DCs allows for the modulation of MP/DC ratio. Furthermore, these results demonstrate the ability to array isolated populations of DCs on adherent islands without inter-spot migration. The miniaturization achieved by this method increases throughput and reduces the required number of cells, particles and expensive reagents by many-fold. For example, in the demonstrated configuration, a >30-fold throughput increase is achieved compared to 96-well plate, obviating need for expensive microfluidic systems. Critically, this miniaturization enables high-throughput investigation of rare cell populations, facilitating advances in personalized medicine, and in particular, personalized vaccines directed toward diseases such as cancer, autoimmune diseases and infections by *in vivo* targeting of DCs.

CHAPTER 6
DENDRITIC CELL ARRAYS FOR BIOLOGICAL EVALUATION OF VACCINE PARTICLES

Introduction

A unique core technology we have developed, involves construction of microarrays of microparticles co-localized with DCs on arrayed adhesive islands. Large numbers of these islands (>1,000) can be arrayed onto a single glass slide, with each island presenting a unique vaccine particle formulation, and providing a unique test sample. Dendritic cell function (e.g., activation, cytokine production, expression of putative tolerogenic markers), in response to co-localization and uptake of vaccine particles and in the presence of locally-delivered pro-tolerogenic biological factors is probed in situ, on arrayed chips, through immunostaining and image analysis. The working hypothesis is that rational vaccine particle design, taken to a high-throughput level will reveal unknown cross-talk among immunomodulatory agents and indicate vaccine particle formulations optimized for their ability to promote tolerogenic DC markers.

Materials and Methods

A 50:50 polymer composition of poly(d,l lactide-co-glycolide) (PLGA) with different factors encapsulated in the particles were generated using the technique described in previous chapters. Dendritic cells were isolated from C57BL6/j mice as described in previous chapters. Furthermore, co-localization of microparticles and dendritic cells on a chip was obtained as mentioned in previous chapters. Different factors that were encapsulated in the particles included lippoplysaccharide (an adjuvant), tissue growth factor-beta(TGF-beta), polyinosinic-polycytidylic acid sodium salt (Poly I:C – an immunostimulant), hemoglobin (tolerogenic factor), vitaminD_3 (tolerogenic factor) and

rapamycin (tolerogenic factor). Furthermore, particles were conjugated with different peptides using bioconjugate techniques. Briefly, 1.3 mg of EDC (1-ethyl-3-(3-dimethylaminopropyl) carbodiimide) and 0.7 mg of NHS (*N*-Hydroxysuccinimide) were dissolved in 1 mL of PBS containing 1 mg of PLGA particles for 15 minutes on a shaker rotating at 300 rpm. This made the carboxyl terminated polymer chains on the particles chemically active and ready to be crosslinked to the primary amine terminal of the peptides. 0.2 mM concentration of the peptides, CS-2 (fibronectin derived), RGD (present in different proteins), P2 (binds to CD11b cell surface molecule), PD-2 (binds to CD11c cell surface molecule) were crosslinked to the surface of the particles separately. The surface modified particles were printed in different combinations with the particles encapsulated with different factors in different concentrations on the chip. Dendritic cells were cultured on these chips and cell function such as up-regulation of cell surface molecules and intracellular cytokine production was probed in-situ using immunostaining as described in Chapter 4. Image acquisition and analysis was performed using fluorescent microscopy and Axiovision 4.0.3 software respectively.

Statistical Analysis

Statistical analyses were performed using one-way ANOVA using Systat (Version 12, Systat Software, Inc., San Jose, CA). Pair-wise comparisons were made using Tukey's Honestly-Significant-Difference, with p-values of less than or equal to 0.05 considered to be significant. Furthermore, graphs were plotted and regression analysis was performed using Sigmaplot (Version 10.0, Systat Software Inc. San Jose, CA).

Results

We show that DCs are restricted to NH_2-terminated adhesive islands, in co-localization with surface-adsorbed LPS-loaded MPs. Microparticle to DC ratio is readily

controlled and DCs are able to phagocytose surface-adsorbed MPs.

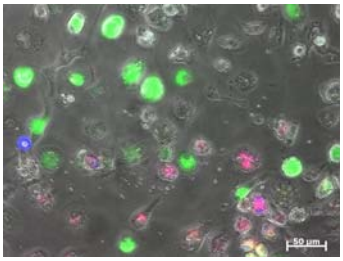

Figure 6-1. Dendritic cells can uptake MPs encapsulated with CyPher5E dye and fluoresce in the Cy5 filter thus, suggesting that the particles have been phagocytosed. Here green-cytosol, blue-particles, pink-phagocytosed MPs.

Phagocytosis of MPs is quantifiable using MPs with encapsulated pH-sensitive dye, CyPHer5E (GE Life Sciences), which increases fluorescence over 2-fold at pH 5 (in phagolysosome) compared to pH 7.4 (extracellular) (**Figure 6-1**).

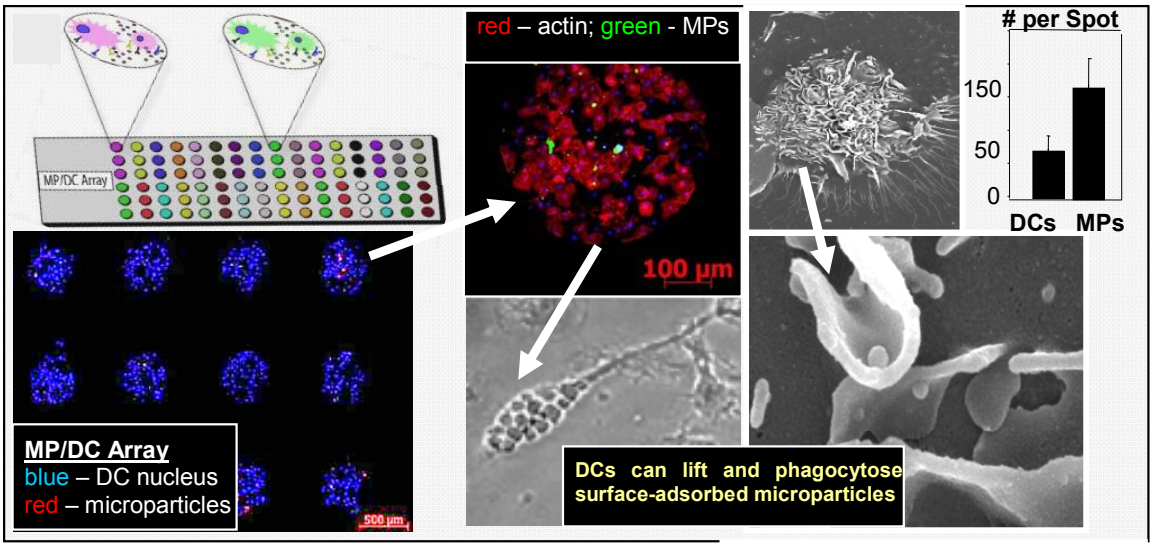

Figure 6-2. Dendritic cells selectively adhere to NH2-terminated spots (presenting adsorbed MPs) and do not adhere to the PEG background. Quantitation is obtained through image analysis (e.g., 150 MPs : 50 DCs per spot). Physi-sorbed particles are able to lifted from the substrate (seen in SEM image) and are phagocytosable (seen in DIC image and pH-sensitive dye). Phagocytosis is quantifiable using MP loading of pH-sensitive dye, CyPHer5E dye. MP to cell ratio can be optimized so all MPs are taken up in 16 h.

Studies are ongoing to optimize MP:DC ratio for efficient uptake of surface-adsorbed MPs in the test-period of 24 hr. Critically, this data demonstrates the ability to quantify DC responses in situ, on arrayed chips, amenable to high-throughput analysis (**Figure 6-2**).

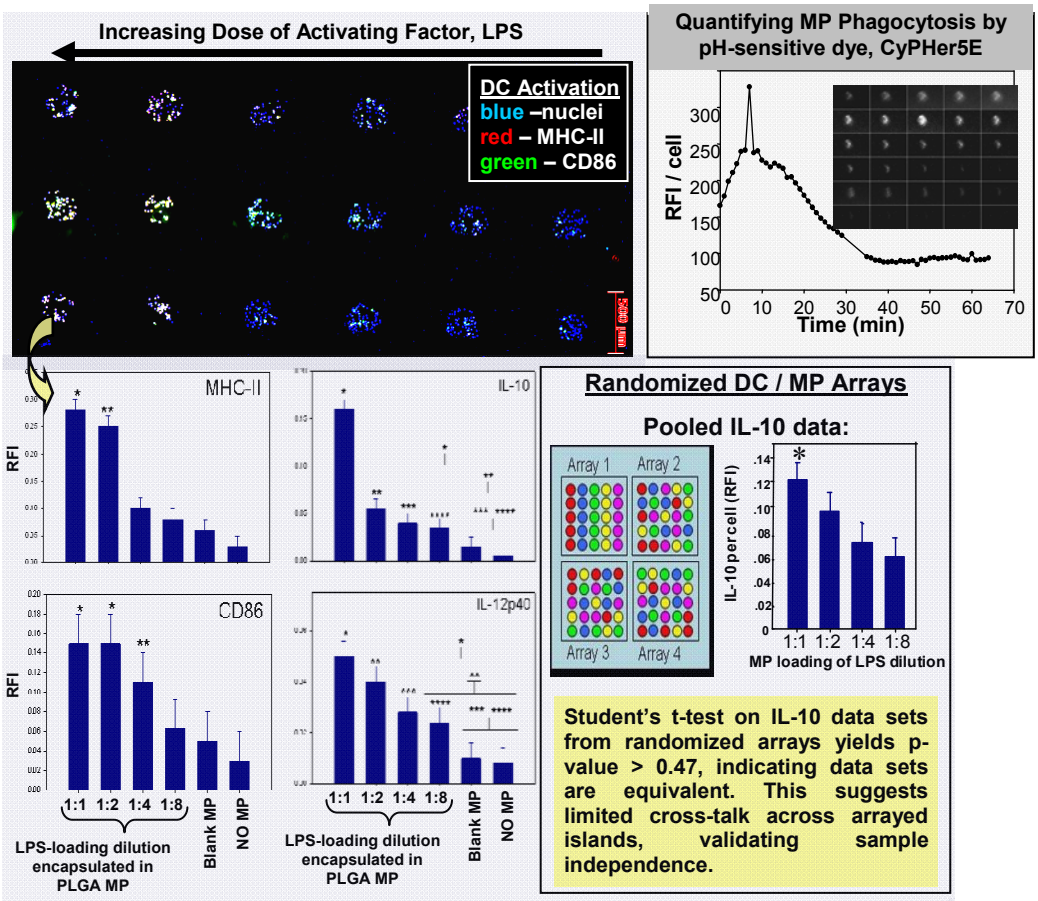

Figure 6-3. As proof-of-principle, DCs were arrayed, co-localized with MPs loaded with an increasing dose of activating factor (LPS), with equal number of particles and cells per spot. Dendritic cells were incubated 4 hrs and then immuno-stained for markers of activation, MHC-II & CD86. Quantification reveals over a 4-fold increase compared to unloaded MPs for the highest LPS dose. Furthermore, after 24 h, cytokine production of IL-10 & IL-12 was quantified in situ through "golgi-stop" treatment, followed by immuno-staining for intracellular cytokines. Comparison of pooled IL-10 data with 3 different randomized DC arrays revealed the lack of positional dependence, suggesting limited cross-talk across islands. The symbols represents that the condition is significantly different from similar symbols.

Specifically, using LPS-loaded MPs as a model MP formulation, we quantified DC production of stimulatory molecules (MHC II), co-stimulatory molecules (CD86, CD80) and cytokines (IL-10, IL-12) on DC arrays. Furthermore, we have investigated the potential for inter-island interactions due to diffusion of molecules across arrayed spots. Four array configurations (1 ordered, 3 randomized) of LPS-loaded MPs were fabricated and DC IL-10 production data sets were compared by Student's t-test. The resultant p-value >0.47 indicates data sets are equivalent, suggesting limited cross-talk across islands and validating sample independence. Pooled data for DC IL-10 production is plotted. Finally, we have begun using MP/DC arrays to investigate formulations with potential to produce tolerogenic DCs (**Figure 6-3**).

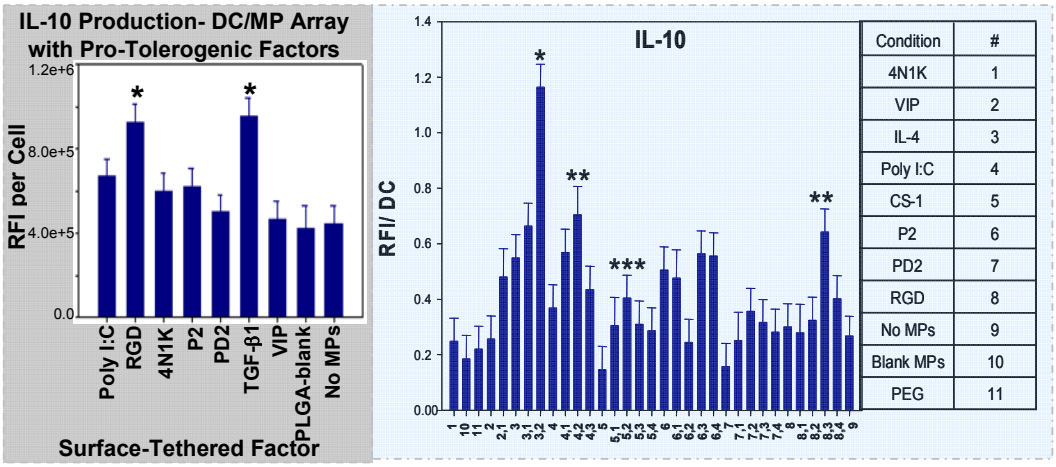

Figure 6-4. MPs (10:1 ratio MPs : DCs) with factors surface-tethered were incubated 24 h on MP/DC arrays and analyzed for production of IL-10, an anti-inflammatory cytokine. Notably, MPs with tethered TGF-β1 and RGD peptide induced elevated DC production of IL-10 compared to other factors (peptides: 4N1K, P2, P-D2, VIP), and a 2-fold increase over untreated MPs (PLGA-blank). Two-component mixtures of (1:1) MP formulations (surface-tethered: P2, PD2, 4N1K, CS-1, RGD; encapsulated: VIP, IL-4, poly I:C; surface-adsorbed: PEG-Pluronic) were investigated on MP/DC arrays for the ability to induce IL-10 cytokine.

Interestingly, we found surface tethering of factors TGF-beta and RGD peptide promote DC production of anti-inflammatory cytokine IL-10, but when two-component

mixtures of MP formulations were tested, it was the combination of tethered 4N1K peptide and encapsulated IL-4 MPs that provided synergistic IL-10 production. Furthermore, it was shown that combined delivery of particles encapsulated with VD3 and TGF-beta to DCs had a synergistic effect, where as when these factors were provided to DCs, individually, did not show a higher response (**Figure 6-4**).

Impact of the Study

We report a new category of microarrays – co-localized MP/cell arrays. This method takes advantage of standard miniarraying equipment to array spots of adhesive islands against a non-adhesive background to provide co-localization of adherent cells and an adsorbed depot of MPs of desired formulations. This represents a versatile platform that can be used to probe the effects of different MP loading/modification formulations on any adherent cell type. Our overall goal was to develop a new platform enabling the screening of MP-based vaccine formulations to optimize DC response toward promoting desired immune responses. The DC, identified as the most efficient antigen presenting cell, plays a central role in immune regulation, and is therefore an ideal vaccine delivery target. The co-localization of MPs with isolated populations of DCs against a non-adhesive background in this novel platform will permit the high-throughput analysis of DC responses to synthetic immuno-modulating MPs targeting DCs. In this work, we have demonstrated the quantitative, reproducible printing of surface-adsorbed MPs of different formulations with minimal cross-contamination. Critically, this control over the number of printed MPs and seeded DCs allows for the modulation of MP/DC ratio. Furthermore, these results demonstrate the ability to array isolated populations of DCs on adherent islands without inter-island migration. The miniaturization achieved by this method increases throughput and reduces the required

number of cells, particles and expensive reagents by many-fold. For example, in the demonstrated configuration, a >30-fold throughput increase is achieved compared to 96-well plate, obviating need for expensive microfluidic systems. Critically, this miniaturization enables high-throughput investigation of rare cell populations, facilitating advances in personalized medicine, and in particular, personalized vaccines directed toward diseases such as cancer, autoimmune diseases and infections by *in vivo* targeting of DCs.

CHAPTER 7
HIGHTHROUGHPUT PARTICLE-BASED VACCINE GENERATION

Introduction

With the advent of immunogenomic approaches combined with advances in molecular immunology, progress is now being made toward the rational design of vaccines. Several techniques are being developed to speed the process of identifying target antigens. Furthermore, the understanding of pattern recognition receptors has advanced adjuvant technology. Although, abundant publications on these topics have been produced, there has been no concomitant increase in the number of new effective vaccines developed, despite years of enormous effort. Recently, there has been an effort to develop particle based immune cell-targeting vaccines that can generate the necessary immune responses. The particle based vaccines have several advantages over traditionally administered vaccines, such as, providing stability for room-temperature storage and shipping, providing ease of administration (e.g., needle-free, single-dose), and improved ease of manufacture. Furthermore, particle based vaccines have been shown to be effective in targeting dendritic cells, an antigen presenting cell, *in vivo* and generate a T-cell based immune response. However, the number of possible combinations of the adjuvants, antigens and other immunomodulatory drugs that can be encapsulated in particle vaccines warrants a need to develop a high-throughput particle production method to produce large numbers of multi-parameter combinations of microparticle modifications and evaluate the potency of such particles. In order to meet this need we have developed a technique to synthesize particle based vaccines in a high-throughput manner. We leverage the use of standard miniarraying equipment with accurate over-spotting capabilities for both the high-throughput loading and fabrication

of large numbers of combinatorially-loaded particles in non-expensive, standard polystyrene plates using compatible organic solvent to generate poly (d,l lactide-co-glycolide) (PLGA) based particles.

Materials Utilized

A 50:50 polymer composition of poly(d,l lactide-co-glycolide) (PLGA) with inherent viscosity 0.55-0.75 dL/g in hexafluoroisopropanol, HFIP (Lactel, AL, USA) was used to generate particles. Poly-vinyl alcohol (PVA) (MW ~ 100,000 g/mol, Fisher Science, Rochester, NY, USA) was utilized as an emulsion stabilizer. Phosphate buffered saline (PBS) solution (Hyclone, UT, USA) was used as the aqueous phase to form the emulsions while propylene carbonate (PC) (Fisher Scientific, NJ, USA) was used as an organic solvent to dissolve PLGA polymer. Microparticles were formed using emulsification-diffusion technique. Fluorescent dyes, 7-diethylamino-4-methylcoumarin (Coumarin: λ_{ex} = 375nm and λ_{em} = 445nm), 1,1',3,3,3',3'-Hexamethylindodicarbocyanine iodide (Cyanine:λ_{ex} = 648nm and λ_{em} = 670nm) and rhodamine 6G (RHOD:λ_{ex} = 528nm and λ_{em} = 550nm) were encapsulated in the particles for quantification purposes. Polystyrene based 384-well plates were used as generation chambers for the particles and a Calligrapher Miniarrayer (BioRad) contact printer was used to transfer solutions in these particle generation chambers.

Parallel Particle Production

A 384-well plate was used as a source plate having 6 different dilutions of the 3 fluorescent dyes dissolved in PC. These dilutions of the dyes were then printed in a 384 well plate using the contact printer to form a 6x6x6 matrix, with all possible combinations of the 3 available dyes (Coumarin, RHOD and Cyanine), which resulted in

216 different conditions. These dyes were chosen so as to have minimum overlap of the absorption of one dye with the emission spectrums of another, in order to reduce the quenching effect. Upon printing of the dyes, 10μL PLGA dissolved in PC at a concentration of 3% was added to the wells. The plate was then sonicated in a sonicating water bath for 3 minutes. A 20μL 5% PVA solution in PBS was added to the wells and the plate was sonicated for 5 more minutes.

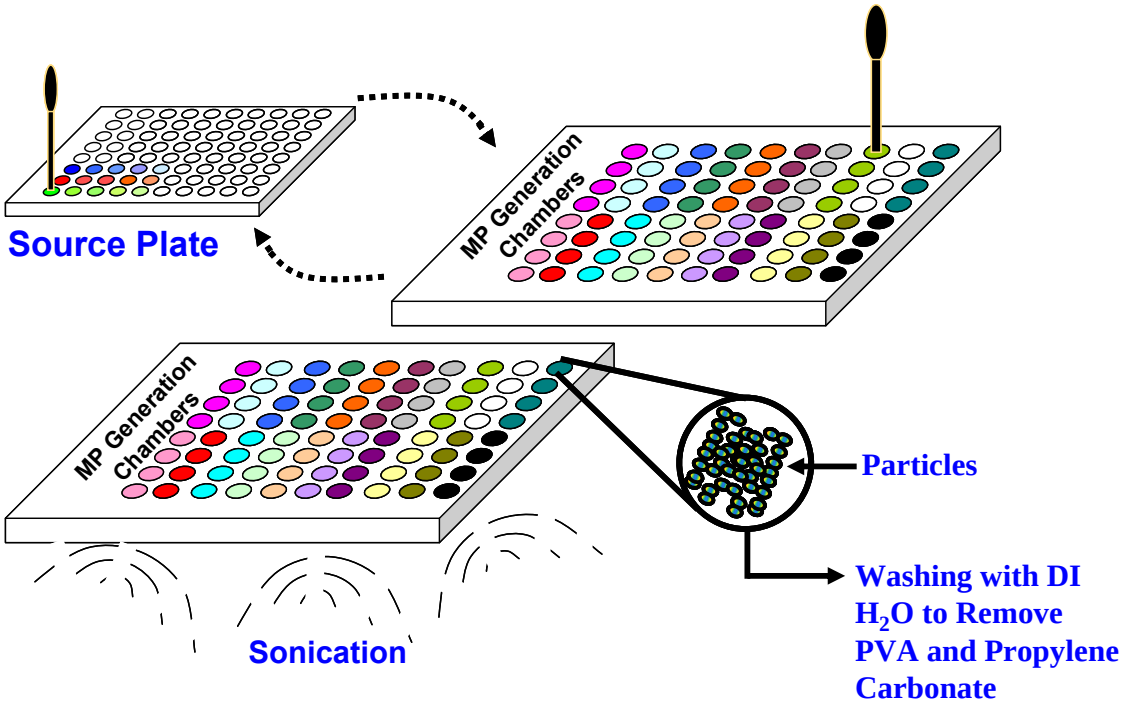

Figure 7-1. Particles were generated using a water-oil-water based emulsification–diffusion method in a multi-well polystyrene plate with multiple fluorescent dyes as representative drug formulations.

The plate was then incubated for 16 hours under a pressure of 0.2mTorr at 37^0C to evaporate PC and water. De-ionized water, 80μL, was added to each well and the plate was sonicated for 60 sec. The plate was then centrifuged at 1500 Gs for 50 minutes. The supernatant was then removed and the particles re-suspended by sonicating in 50μL/well of de-ionized water. This washing process of centrifuging,

aspirating and re-suspending was repeated 5 times to remove PVA from the particles in the well. The plate was then frozen by placing over dry ice and dried under vacuum overnight. All the particle generation steps were performed in dark to reduce photo-bleaching of the dyes (**Figure 7-1**). For analyzing, the particles were re-suspended in de-ionized water solution using a sonicating bath and printed on a plasma cleaned glass microscope slides (Fisher Scientific, NJ, USA).

Particle Analysis

The dye printed plate was analyzed using a plate reader with appropriate filters to measure fluorescence of the printed fluorescent dyes. Dyes encapsulated particles were generated and printed on a glass slide using contact pin miniarrayer. This glass slide was then scanned using Typhoon 9410 (GE Healthcare) fluorescent imager with appropriate filters for the fluorescent dyes. Furthermore, micrographs of the printed particles were obtained using Carl Zeiss 400M fluorescent microscope using the appropriate filters for each dye. Detailed image analysis of the particle spots was carried out using Axiovision software. Furthermore, the particles were printed onto microarrays using contact pin printing and then the particles were analyzed using scanning electron micrographs.

Statistical Analysis

Statistical analyses were performed using one-way ANOVA using Systat (Version 12, Systat Software, Inc., San Jose, CA). Pair-wise comparisons were made using Tukey's Honestly-Significant-Difference, with p-values of less than or equal to 0.05 considered to be significant. Furthermore, graphs were plotted and regression analysis was performed using Sigmaplot (Version 10.0, Systat Software Inc. San Jose, CA).

Results

Particles were generated via parallel particle production technique through emulsification process. The dyes, Coumarin, Rhodamine and Cyanine were printed in a 384 polystyrene plate from a source plate having 6 dilutions of the dyes. The printing was performed using standard miniarraying equipment and 6x6x6 = 216 different combinations of the dyes were generated. The relative fluorescence intensity of the dyes was measured using a plate reader. It was observed that the dyes coumarin, rhodamine and cyanine followed a linear curve with the coefficient of determination of $R^2_{Coumarin} = 0.99$; $R^2_{Rhodamine} = 0.99$ and $R^2_{Cyanine} = 0.94$, when fitted to a linear curve (**Figure 7-2**).

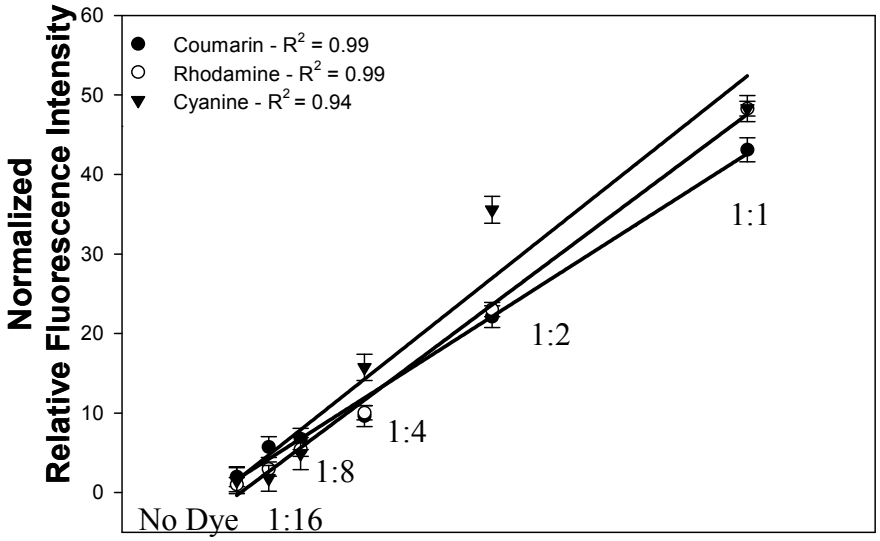

Figure 7-2. Combination of fluorescent dyes at different dilutions can be printed in the same well accurately. The coefficient of determination was obtained by simple regression analysis with the decreasing concentration of dye in the source plate: $R^2_{Coumarin} = 0.99$; $R^2_{Rhodamine} = 0.99$; $R^2_{Cyanine} = 0.94$.

A solution of PLGA in PC was added to the wells containing the dyes in different concentrations and micro-batches of particles were generated with PVA as the

emulsifier. Relative fluorescence intensity of the three dyes for each micro-batch was obtained using the plate reader and plotted against the individual condition (**Figure 7-3**).

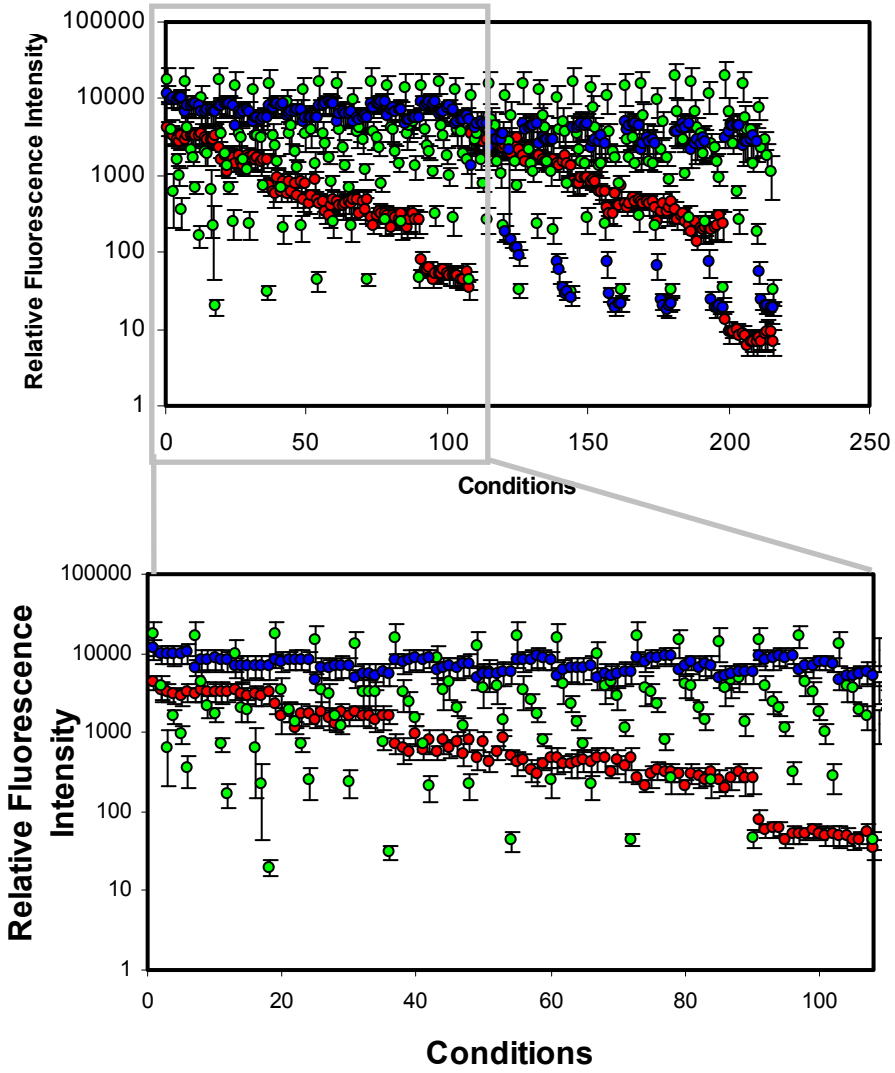

Figure 7-3. Combination of fluorescent dyes at different dilutions can be encapsulated in PLGA particles with uniform distribution of dyes within the individual population of particles.

It was observed that the relative fluorescence intensity of particles in a micro-batch follow similar trend as the printed dyes.

The particles generated using parallel particle production, were pooled together and size and shape was determined using scanning electron microscope and dynamic

light scattering technique respectively. It was observed that the particles had a smooth morphology and the average size of the particles based on volume estimation was 1.04μm (**Figure 7-4**).

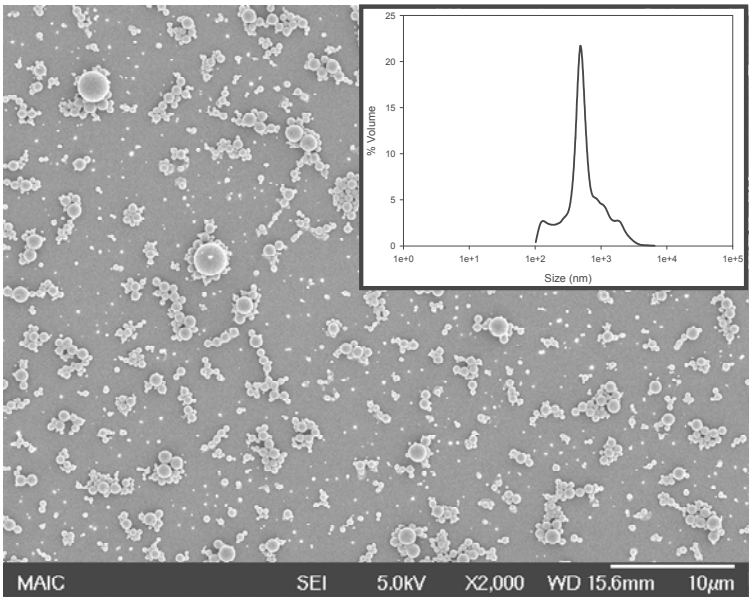

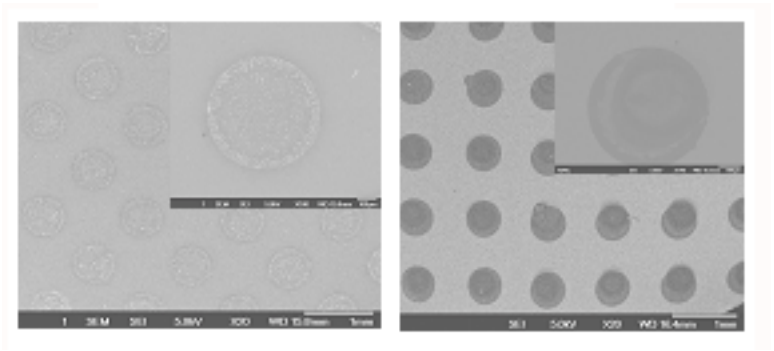

Figure 7-4. Particles were produced via parallel particle production method and the particles were analyzed using SEM and dynamic light scattering. A typical size distribution curve of PLGA-particles quantified via dynamic light scattering analysis (based on volume estimation) demonstrates an average size of particles of 1.04μm.

The particles generated using this process were then printed on glass microscope slide and were imaged using typhoon 9410 and fluorescent microscope. An overlay image was plotted (**Figure 7-5**). 3-D surface plots were plotted using ImageJ software for each of the fluorescent micrograph and the overlaid micrograph. This

method is useful for quick scanning of the amount of fluorescent dye encapsulated in the particles.

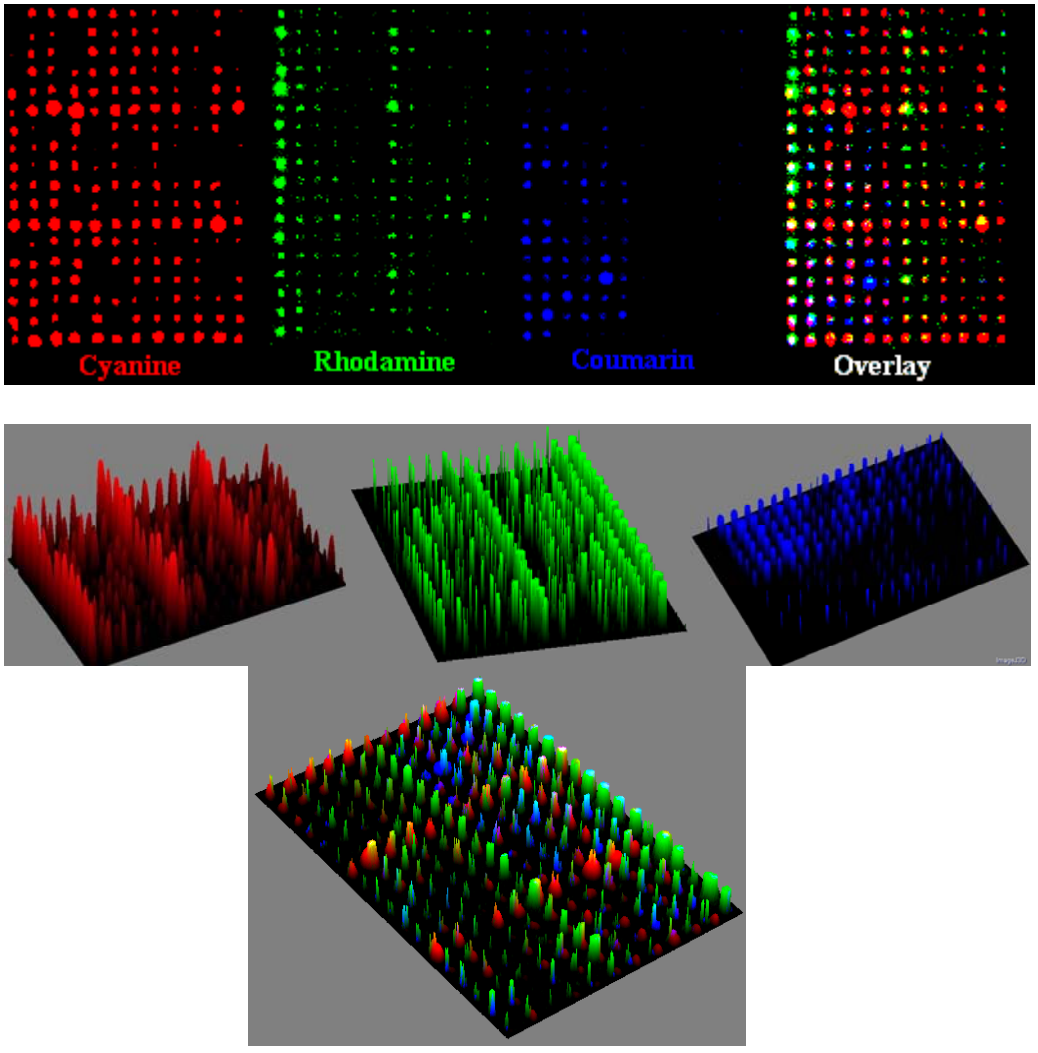

Figure 7-5. The fluorescence intensities of the particles generated via PPP method can be visualized by quick scan imaging. The particles encapsulating 3 different fluorescent dyes in 6 dilutions, thus forming 216 different combinations, were printed onto a glass slide and scanned using typhoon 9410 and fluorescent microscope. This method is useful for image quick scan and visualization of the amount encapsulated factors.

Mean fluorescent intensity (MFI) of individual particles were obtained from few of the micro-batches. These MFIs were then plotted as histograms to compare the dye

distribution within a micro-batch. It was observed that the dye was distributed uniformly among the particles of one micro-batch.

A chip was generated consisting of cell adhesive islands surrounded by non-fouling regions. Particles generated using PPP method were printed onto the cell adhesive regions. Dendritic cells were cultured onto the chip, which co-localized with the printed particles (**Figure 7-7**).

Impact of the Study

Currently, standard methodology for the generation of polymeric PLGA particles consists of single batch processing using a double-emulsion/solvent-evaporation method. This process can take 4-5 hours and even skilled hands may be limited to producing less than a dozen MP formulations in one day. As a result of our ability to assess many particle formulations at once through our high-throughput MP array approach, we have identified a unique and critical need to quickly generate large numbers (hundreds to thousands) of different MP formulations. To meet this need, we have generated a high-throughput parallel particle production technology, utilizing solid-pin miniarraying equipment for the robotic loading of component solutions into wells of a 384-well plate which then serve as particle-generation chambers.

CHAPTER 8
CONCLUSION AND FUTURE OUTLOOK

Designing biomaterials that can actively modulate the immune system is an emerging field that will help in understanding basic working of immune cell functions at a molecular level and further the field of immunomodulatory biomaterials. Biomaterials can help understand molecular and cellular processes that occur when immune cells such as antigen presenting cells interact with foreign bodies. Furthermore, design of biomaterials has to be influenced by the immunobiology of the disease. Generation of biomaterials influenced vaccines is a step forward in this direction.

Modulation of immune system using biomaterials has shown promising results in the field of cancer research. However, use of biomaterials to actively modulate the immune system for treatment of autoimmune diseases has not been extensively studied. Biomaterials in combination with biological components can be recognized by the immune system as foreign and hence get targeted by immune cells such as T-cells and B-cells. This hypothesis has been utilized in clinical trials to generate dendritic cell (DC), a specialized antigen presenting cell – targeted in vivo and ex vivo immunotherapies for autoimmune diseases. Such immunotherapies can be made more efficient with the use of biomaterials. For instance, biomaterials in the form of polymeric particles can be utilized to provide sustained release of therapeutic factors in vivo targeted to DCs. Additionally, implanted biomaterials, combination products involving biological components and synthetic materials, and ex vivo strategies can be made more effective using biomaterials based immunomodulation. Hence, looking forward, an extensive study was performed to characterize the adhesion based modulation of adaptive immune system for improving the present ex vivo strategies for generating DC

based vaccines targeting autoimmune disorder of type 1 diabetes. Furthermore, highthroughput microarraying techniques were utilized to generate and characterize particle based vaccines targeted to DCs.

Currently, the ex vivo immunotherapies involve culturing exogenously generated DCs onto tissue culture treated polystyrene plates adsorbed with serum proteins. However, this strategy has not been optimized to provide optimal surface for DC - adhesion. We have shown in this body of work that adhesion based stimuli to DCs can modulate their cell function and these DCs can subsequently modulate the adaptive immune response as quantified by T-cell responses. Furthermore, we show that NOD-mice derived DCs were differentially modulated by adhesion stimuli than the normal wild type B6 derived DCs. Furthermore, we showed that increasing integrin expression which corresponds to increasing adhesive molecules provided follows increase in expression of maturation signals of DCs. This work suggests that the mechanism of adhesion that involves integrin binding to adhesive molecules such as peptides, indeed, is a governing factor that mediates DC maturation. A peptide having RGD amino acid sequence was utilized in this study, which is present in several proteins. Looking ahead, surface modified biomaterials can be utilized to generate other known peptides / functional molecules of interest that modulate DC functions. For example, DC – T-cell synapse can be studied in great detail and critical questions such as extent of clustering of integrins required on DCs to generate such synapses can be answered.

In parallel studies were performed to design particle based vaccines that can effectively target DCs and modulate their functions to generate the needed immunotherapy. We developed highthroughput techniques to generate multicomponent

PLGA based particle vaccines. Furthermore, we developed highthroughput techniques using lab-on-a-chip format to characterize the particle vaccines cultured in the presence of DCs. Additionally, techniques were developed to screen these DCs for most effective particle vaccine formulations. In future, further, formulations will be tested on the chips and the particle vaccines selected will be tested in a mouse model for a desired immunotherapy. This work will further the field of biomaterials based vaccines.

LIST OF REFERENCES

[1] Adorini, L. and Penna, G., Dendritic cell tolerogenicity: a key mechanism in immunomodulation by vitamin D receptor agonists, Hum Immunol **70** (5) (2009), pp. 345-352.

[2] Lu, L. and Thomson, A. W., Manipulation of dendritic cells for tolerance induction in transplantation and autoimmune disease, Transplantation **73** (1 Suppl) (2002), pp. S19-S22.

[3] Miretti, M. M. and Beck, S., Immunogenomics: molecular hide and seek, Hum Genomics **2** (4) (2006), pp. 244-251.

[4] Steinman, R. M. and Nussenzweig, M. C., Dendritic cells: features and functions, Immunol Rev **53** (1980), pp. 127-147.

[5] Steinman, R. M., Dendritic cells in vivo: a key target for a new vaccine science, Immunity **29** (3) (2008), pp. 319-324.

[6] van, Duin D., Medzhitov, R., and Shaw, A. C., Triggering TLR signaling in vaccination, Trends Immunol **27** (1) (2006), pp. 49-55.

[7] http://clinicaltrials.gov/ (2009).

[8] Giannoukakis, N., Phillips, B., and Trucco, M., Toward a cure for type 1 diabetes mellitus: diabetes-suppressive dendritic cells and beyond, Pediatr Diabetes **9** (3 Pt 2) (2008), pp. 4-13.

[9] Phillips, B., Nylander, K., Harnaha, J., Machen, J., Lakomy, R., Styche, A., Gillis, K., Brown, L., Lafreniere, D., Gallo, M., Knox, J., Hogeland, K., Trucco, M., and Giannoukakis, N., A microsphere-based vaccine prevents and reverses new-onset autoimmune diabetes, Diabetes **57** (6) (2008), pp. 1544-1555.

[10] Phillips, B. E., Giannoukakis, N., and Trucco, M., Dendritic cell mediated therapy for immunoregulation of type 1 diabetes mellitus, Pediatr Endocrinol Rev **5** (4) (2008), pp. 873-879.

[11] Matzinger, P., An innate sense of danger, Ann N Y Acad Sci **961** (2002), pp. 341-342.

[12] Medzhitov, R. and Janeway, C. A., Jr., Innate immune recognition and control of adaptive immune responses, Semin Immunol **10** (5) (1998), pp. 351-353.

[13] Fernandez, N. C., Lozier, A., Flament, C., Ricciardi-Castagnoli, P., Bellet, D., Suter, M., Perricaudet, M., Tursz, T., Maraskovsky, E., and Zitvogel, L., Dendritic cells directly trigger NK cell functions: cross-talk relevant in innate anti-tumor immune responses in vivo, Nat Med **5** (4) (1999), pp. 405-411.

[14] Lambrecht, B. N., Salomon, B., Klatzmann, D., and Pauwels, R. A., Dendritic cells are required for the development of chronic eosinophilic airway inflammation in response to inhaled antigen in sensitized mice, J Immunol **160** (8) (1998), pp. 4090-4097.

[15] Shi, Y., Evans, J. E., and Rock, K. L., Molecular identification of a danger signal that alerts the immune system to dying cells, Nature **425** (6957) (2003), pp. 516-521.

[16] Nakajima, H. and Takatsu, K., Role of cytokines in allergic airway inflammation, Int Arch Allergy Immunol **142** (4) (2007), pp. 265-273.

[17] Yates, S. F., Paterson, A. M., Nolan, K. F., Cobbold, S. P., Saunders, N. J., Waldmann, H., and Fairchild, P. J., Induction of regulatory T cells and dominant tolerance by dendritic cells incapable of full activation, J Immunol **179** (2) (2007), pp. 967-976.

[18] Kijima, M., Yamaguchi, T., Ishifune, C., Maekawa, Y., Koyanagi, A., Yagita, H., Chiba, S., Kishihara, K., Shimada, M., and Yasutomo, K., Dendritic cell-mediated NK cell activation is controlled by Jagged2-Notch interaction 1, Proc Natl Acad Sci U S A 105 (19) (2008), pp. 7010-7015.

[19] Ranjit, S. and Dazhu, L., Potential role of dendritic cells for progression of atherosclerotic lesions, Postgrad Med J **82** (971) (2006), pp. 573-575.

[20] Hammad, H. and Lambrecht, B. N., Dendritic cells and epithelial cells: linking innate and adaptive immunity in asthma, Nat Rev Immunol **8** (3) (2008), pp. 193-204.

[21] Hynes, R. O., Integrins: bidirectional, allosteric signaling machines, Cell **110** (6) (2002), pp. 673-687.

[22] Anderson, J. M., Rodriguez, A., and Chang, D. T., Foreign body reaction to biomaterials, Semin Immunol **20** (2) (2008), pp. 86-100.

[23] Hunter, S. K., Kao, J. M., Wang, Y., Benda, J. A., and Rodgers, V. G., Promotion of neovascularization around hollow fiber bioartificial organs using biologically active substances, ASAIO J **45** (1) (1999), pp. 37-40.

[24] Jenney, C. R. and Anderson, J. M., Adsorbed serum proteins responsible for surface dependent human macrophage behavior, J Biomed Mater Res **49** (4) (2000), pp. 435-447.

[25] Keselowsky, B. G., Bridges, A. W., Burns, K. L., Tate, C. C., Babensee, J. E., LaPlaca, M. C., and Garcia, A. J., Role of plasma fibronectin in the foreign body response to biomaterials, Biomaterials **28** (25) (2007), pp. 3626-3631.

[26] Shen, M. and Horbett, T. A., The effects of surface chemistry and adsorbed proteins on monocyte/macrophage adhesion to chemically modified polystyrene surfaces, J Biomed Mater Res **57** (3) (2001), pp. 336-345.

[27] Tang, L. and Eaton, J. W., Fibrin(ogen) mediates acute inflammatory responses to biomaterials, J Exp Med 178 (6) (1993), pp. 2147-2156.

[28] Acharya, A. P., Dolgova, N. V., Clare-Salzler, M. J., and Keselowsky, B. G., Adhesive substrate-modulation of adaptive immune responses, Biomaterials **29** (36) (2008), pp. 4736-4750.

[29] Lo, J. and Clare-Salzler, M. J., Dendritic cell subsets and type I diabetes: focus upon DC-based therapy, Autoimmun Rev **5** (6) (2006), pp. 419-423.

[30] Nencioni, A. and Brossart, P., Cellular immunotherapy with dendritic cells in cancer: current status, Stem Cells **22** (4) (2004), pp. 501-513.

[31] Ludewig, B., Odermatt, B., Landmann, S., Hengartner, H., and Zinkernagel, R. M., Dendritic cells induce autoimmune diabetes and maintain disease via de novo formation of local lymphoid tissue, J Exp Med **188** (8) (1998), pp. 1493-1501.

[32] Morel, P. A., Vasquez, A. C., and Feili-Hariri, M., Immunobiology of DC in NOD mice, J Leukoc Biol **66** (2) (1999), pp. 276-280.

[33] Turley, S. J., Dendritic cells: inciting and inhibiting autoimmunity, Curr Opin Immunol **14** (6) (2002), pp. 765-770.

[34] Peng, R., Bathjat, K., Li, Y., and Clare-Salzler, M. J., Defective maturation of myeloid dendritic cell (DC) in NOD mice is controlled by IDD10/17/18, Ann N Y Acad Sci **1005** (2003), pp. 184-186.

[35] Siperstein, M. D., Unger, R. H., and Madison, L. L., Studies of muscle capillary basement membranes in normal subjects, diabetic, and prediabetic patients, J Clin Invest **47** (9) (1968), pp. 1973-1999.

[36] Kaur, H., Chen, S., Xin, X., Chiu, J., Khan, Z. A., and Chakrabarti, S., Diabetes-induced extracellular matrix protein expression is mediated by transcription coactivator p300, Diabetes **55** (11) (2006), pp. 3104-3111.

[37] Thomas, R. and Lipsky, P. E., Dendritic cells: origin and differentiation, Stem Cells **14** (2) (1996), pp. 196-206.

[38] Morel, P. A. and Feili-Hariri, M., How do dendritic cells prevent autoimmunity?, Trends Immunol **22** (10) (2001), pp. 546-547.

[39] Hynes, R. O., Structural biology. Changing partners, Science **300** (5620) (2003), pp. 755-756.

[40] Takagi, J., Structural basis for ligand recognition by integrins, Curr Opin Cell Biol **19** (5) (2007), pp. 557-564.

[41] Wang, Q., Klyubin, I., Wright, S., Griswold-Prenner, I., Rowan, M. J., and Anwyl, R., Alpha v integrins mediate beta-amyloid induced inhibition of long-term potentiation, Neurobiol Aging **29** (10) (2008), pp. 1485-1493.

[42] Tanabe, J., Fujita, H., Iwamatsu, A., Mohri, H., and Ohkubo, T., Fibronectin inhibits platelet aggregation independently of RGD sequence, J Biol Chem **268** (36) (1993), pp. 27143-27147.

[43] Rezania, A. and Healy, K. E., The effect of peptide surface density on mineralization of a matrix deposited by osteogenic cells, J Biomed Mater Res **52** (4) (2000), pp. 595-600.

[44] VandeVondele, S., Voros, J., and Hubbell, J. A., RGD-grafted poly-L-lysine-graft-(polyethylene glycol) copolymers block non-specific protein adsorption while promoting cell adhesion, Biotechnol Bioeng **82** (7) (2003), pp. 784-790.

[45] Benoit, J. P., Faisant, N., Venier-Julienne, M. C., and Menei, P., Development of microspheres for neurological disorders: from basics to clinical applications, J Control Release **65** (1-2) (2000), pp. 285-296.

[46] Bromberg, L., Intelligent hydrogels for the oral delivery of chemotherapeutics, Expert Opin Drug Deliv **2** (6) (2005), pp. 1003-1013.

[47] dlakha-Hutcheon, G., Bally, M. B., Shew, C. R., and Madden, T. D., Controlled destabilization of a liposomal drug delivery system enhances mitoxantrone antitumor activity, Nat Biotechnol **17** (8) (1999), pp. 775-779.

[48] Gao, Y., Gao, G., He, Y., Liu, T., and Qi, R., Recent advances of dendrimers in delivery of genes and drugs, Mini Rev Med Chem **8** (9) (2008), pp. 889-900.

[49] Reddy, S. T., Rehor, A., Schmoekel, H. G., Hubbell, J. A., and Swartz, M. A., In vivo targeting of dendritic cells in lymph nodes with poly(propylene sulfide) nanoparticles, J Control Release **112** (1) (2006), pp. 26-34.

[50] Richards Grayson, A. C., Choi, I. S., Tyler, B. M., Wang, P. P., Brem, H., Cima, M. J., and Langer, R., Multi-pulse drug delivery from a resorbable polymeric microchip device, Nat Mater **2** (11) (2003), pp. 767-772.

[51] Shi, L., Caulfield, M. J., Chern, R. T., Wilson, R. A., Sanyal, G., and Volkin, D. B., Pharmaceutical and immunological evaluation of a single-shot hepatitis B vaccine formulated with PLGA microspheres, J Pharm Sci **91** (4) (2002), pp. 1019-1035.

[52] Tamber, H., Johansen, P., Merkle, H. P., and Gander, B., Formulation aspects of biodegradable polymeric microspheres for antigen delivery, Adv Drug Deliv Rev **57** (3) (2005), pp. 357-376.

[53] Cohen, S., Yoshioka, T., Lucarelli, M., Hwang, L. H., and Langer, R., Controlled delivery systems for proteins based on poly(lactic/glycolic acid) microspheres, Pharm Res **8** (6) (1991), pp. 713-720.

[54] Elamanchili, P., Diwan, M., Cao, M., and Samuel, J., Characterization of poly(D,L-lactic-co-glycolic acid) based nanoparticulate system for enhanced delivery of antigens to dendritic cells, Vaccine **22** (19) (2004), pp. 2406-2412.

[55] Waeckerle-Men, Y. and Groettrup, M., PLGA microspheres for improved antigen delivery to dendritic cells as cellular vaccines, Adv Drug Deliv Rev **57** (3) (2005), pp. 475-482.

[56] Waeckerle-Men, Y., Allmen, E. U., Gander, B., Scandella, E., Schlosser, E., Schmidtke, G., Merkle, H. P., and Groettrup, M., Encapsulation of proteins and peptides into biodegradable poly(D,L-lactide-co-glycolide) microspheres prolongs and enhances antigen presentation by human dendritic cells, Vaccine **24** (11) (2006), pp. 1847-1857.

[57] Bonifaz, L., Bonnyay, D., Mahnke, K., Rivera, M., Nussenzweig, M. C., and Steinman, R. M., Efficient targeting of protein antigen to the dendritic cell receptor DEC-205 in the steady state leads to antigen presentation on major histocompatibility complex class I products and peripheral CD8+ T cell tolerance, J Exp Med **196** (12) (2002), pp. 1627-1638.

[58] Faraasen, S., Voros, J., Csucs, G., Textor, M., Merkle, H. P., and Walter, E., Ligand-specific targeting of microspheres to phagocytes by surface modification with poly(L-lysine)-grafted poly(ethylene glycol) conjugate, Pharm Res **20** (2) (2003), pp. 237-246.

[59] Kempf, M., Mandal, B., Jilek, S., Thiele, L., Voros, J., Textor, M., Merkle, H. P., and Walter, E., Improved stimulation of human dendritic cells by receptor engagement with surface-modified microparticles, J Drug Target **11** (1) (2003), pp. 11-18.

[60] Elamanchili, P., Diwan, M., Cao, M., and Samuel, J., Characterization of poly(D,L-lactic-co-glycolic acid) based nanoparticulate system for enhanced delivery of antigens to dendritic cells, Vaccine **22** (19) (2004), pp. 2406-2412.

[61] Reddy, S. T., Rehor, A., Schmoekel, H. G., Hubbell, J. A., and Swartz, M. A., In vivo targeting of dendritic cells in lymph nodes with poly(propylene sulfide) nanoparticles, J Control Release **112** (1) (2006), pp. 26-34.

[62] Waeckerle-Men, Y. and Groettrup, M., PLGA microspheres for improved antigen delivery to dendritic cells as cellular vaccines, Adv Drug Deliv Rev **57** (3) (2005), pp. 475-482.

[63] Yoshida, M., Mata, J., and Babensee, J. E., Effect of poly(lactic-co-glycolic acid) contact on maturation of murine bone marrow-derived dendritic cells, J Biomed Mater Res A **80** (1) (2007), pp. 7-12.

[64] Babensee, J. E., Interaction of dendritic cells with biomaterials, Semin Immunol **20** (2) (2008), pp. 101-108.

[65] Schlosser, E., Mueller, M., Fischer, S., Basta, S., Busch, D. H., Gander, B., and Groettrup, M., TLR ligands and antigen need to be coencapsulated into the same biodegradable microsphere for the generation of potent cytotoxic T lymphocyte responses, Vaccine **26** (13) (2008), pp. 1626-1637.

[66] Elamanchili, P., Lutsiak, C. M., Hamdy, S., Diwan, M., and Samuel, J., "Pathogen-mimicking" nanoparticles for vaccine delivery to dendritic cells, J Immunother **30** (4) (2007), pp. 378-395.

[67] Kasturi, S. P., Sachaphibulkij, K., and Roy, K., Covalent conjugation of polyethyleneimine on biodegradable microparticles for delivery of plasmid DNA vaccines, Biomaterials **26** (32) (2005), pp. 6375-6385.

[68] Jilek, S., Zurkaulen, H., Pavlovic, J., Merkle, H. P., and Walter, E., Transfection of a mouse dendritic cell line by plasmid DNA-loaded PLGA microparticles in vitro, Eur J Pharm Biopharm **58** (3) (2004), pp. 491-499.

[69] Schena, M., Shalon, D., Davis, R. W., and Brown, P. O., Quantitative monitoring of gene expression patterns with a complementary DNA microarray, Science **270** (5235) (1995), pp. 467-470.

[70] El-Ali, J., Sorger, P. K., and Jensen, K. F., Cells on chips, Nature **442** (7101) (2006), pp. 403-411.

[71] Flaim, C. J., Chien, S., and Bhatia, S. N., An extracellular matrix microarray for probing cellular differentiation, Nat Methods **2** (2) (2005), pp. 119-125.

[72] Soen, Y., Mori, A., Palmer, T. D., and Brown, P. O., Exploring the regulation of human neural precursor cell differentiation using arrays of signaling microenvironments, Mol Syst Biol **2** (2006), pp. 37.

[73] Schena, M., Shalon, D., Davis, R. W., and Brown, P. O., Quantitative monitoring of gene expression patterns with a complementary DNA microarray, Science **270** (5235) (1995), pp. 467-470.

[74] Soen, Y., Chen, D. S., Kraft, D. L., Davis, M. M., and Brown, P. O., Detection and characterization of cellular immune responses using peptide-MHC microarrays, PLoS Biol **1** (3) (2003), pp. E65.

[75] Flaim, C. J., Chien, S., and Bhatia, S. N., An extracellular matrix microarray for probing cellular differentiation, Nat Methods **2** (2) (2005), pp. 119-125.

[76] Keselowsky, B. G., Collard, D. M., and Garcia, A. J., Surface chemistry modulates focal adhesion composition and signaling through changes in integrin binding, Biomaterials **25** (28) (2004), pp. 5947-5954.

[77] Kempf, M., Mandal, B., Jilek, S., Thiele, L., Voros, J., Textor, M., Merkle, H. P., and Walter, E., Improved stimulation of human dendritic cells by receptor engagement with surface-modified microparticles, J Drug Target **11** (1) (2003), pp. 11-18.

[78] Xia, C. Q., Peng, R., Beato, F., and Clare-Salzler, M. J., Dexamethasone induces IL-10-producing monocyte-derived dendritic cells with durable immaturity, Scand J Immunol **62** (1) (2005), pp. 45-54.

[79] Xiao, B. G., Huang, Y. M., and Link, H., Tolerogenic dendritic cells: the ins and outs of outcome, J Immunother **29** (5) (2006), pp. 465-471.

[80] Johansson, U. and Londei, M., Ligation of CD47 during monocyte differentiation into dendritic cells results in reduced capacity for interleukin-12 production, Scand J Immunol **59** (1) (2004), pp. 50-57.

[81] Johansson, U., Higginbottom, K., and Londei, M., CD47 ligation induces a rapid caspase-independent apoptosis-like cell death in human monocytes and dendritic cells, Scand J Immunol **59** (1) (2004), pp. 40-49.

[82] Pasquali, L., Giannoukakis, N., and Trucco, M., Induction of immune tolerance to facilitate beta cell regeneration in type 1 diabetes, Adv Drug Deliv Rev **60** (2) (2008), pp. 106-113.

[83] Yuri V.Bobryshev, Dendritic cells in atherosclerosis, (2001), pp. 547-557.

[84] Lord, R. S. and Bobryshev, Y. V., Clustering of dendritic cells in athero-prone areas of the aorta, Atherosclerosis **146** (1) (1999), pp. 197-198.

[85] Delemarre, F. G., Hoogeveen, P. G., De Haan-Meulman, M., Simons, P. J., and Drexhage, H. A., Homotypic cluster formation of dendritic cells, a close correlate of their state of maturation. Defects in the biobreeding diabetes-prone rat, J Leukoc Biol **69** (3) (2001), pp. 373-380.

[86] Verdijk, P., van Veelen, P. A., de Ru, A. H., Hensbergen, P. J., Mizuno, K., Koerten, H. K., Koning, F., Tensen, C. P., and Mommaas, A. M., Morphological changes during dendritic cell maturation correlate with cofilin activation and translocation to the cell membrane, Eur J Immunol **34** (1) (2004), pp. 156-164.

[87] Xiao, B. G., Huang, Y. M., and Link, H., Tolerogenic dendritic cells: the ins and outs of outcome, J Immunother **29** (5) (2006), pp. 465-471.

BIOGRAPHICAL SKETCH

Abhinav Acharya was born in 1983 in Jhansi, India. Abhinav earned his bachelor's degree from National Institute of Technology, Tiruchirappalli in June 2005. He came to the United States of America to pursue the degree of PhD. He started his graduate studies under the guidance of Dr. Benjamin Keselowsky, and earned his Ph.D. in materials science and engineering in May 2010. Abhinav had an extensive interaction with faculty members from different departments and had a multi-disciplinary research experience. He wishes to remain in academia and is looking forward to his time as a postdoctoral researcher.